Draft Report

ALASKA MM5 MODELING FOR THE 2002 ANNUAL PERIOD TO SUPPORT VISIBILITY MODELING

Prepared for

The Western Regional Air Partnership
1515 Cleveland Place, Suite 200
Denver, CO 80202

Prepared by

Sue Kemball-Cook
Yiqin Jia
Chris Emery
Ralph Morris
ENVIRON International Corporation
101 Rowland Way, Suite 220
Novato, CA 94945-5010

Zion Wang
Gail Tonnesen
University of California at Riverside
College of Engineering
Center for Environmental Research and Technology
Riverside, CA 92507

September 2005

TABLE OF CONTENTS

TABLES

FIGURES

1.0 INTRODUCTION

In 1999, the U.S. Environmental Protection Agency (EPA) announced a major effort to improve air quality in national parks and wilderness areas. The Regional Haze Rule (RHR) calls for state and federal agencies to work together to improve visibility in 156 national parks and wilderness areas (referred to as "Class I" areas). The objective of the RHR is to achieve natural visibility conditions in these federally protected lands by the year 2064. The rule requires the states to develop and implement air quality protection plans to reduce the pollution that causes visibility impairment. The Western Regional Air Partnership (WRAP) is a consortium of federal, state, and tribal agencies charged with implementing regional planning processes to improve visibility in all western Class I areas. To meet this goal, WRAP is providing the necessary technical and policy tools to help states and tribes implement the RHR.

The WRAP has formed the Regional Modeling Center (RMC), consisting of the University of California at Riverside (UCR), ENVIRON International Corporation, and the University of North Carolina (UNC). The RMC is performing the modeling and analysis necessary to develop visibility State Implementation Plans and Tribal Implementation Plans (SIPs/TIPs).

The State of Alaska is developing a plan to protect visibility and comply with the intent of the Regional Haze Rule. Alaska poses some unique challenges for regional haze modeling. It is geographically far enough removed from the rest of the WRAP states that a unified modeling domain would be quite large and inefficient. Also, it has much lower emission densities than the other WRAP states (except during fire events) and there are longer transport distances between the various emission source regions and Class I areas. The influence of long-range (international) transport of pollutants from Eurasia may dominate regional haze events on occasion (this phenomenon is known as Arctic Haze).

There are four Class I areas in Alaska (Figure 1-1):

- Denali National Park and Preserve
- Tuxedni Wilderness
- Simeonof Wilderness
- Bering Sea Wilderness

Both the Simeonof and Bering Sea Wilderness Area are quite far away (> 500 miles) from Anchorage and Fairbanks, the two largest cities in Alaska. However, the Tuxedni Wilderness and Denali National Park are close enough so that they may be affected by emissions from, respectively, Anchorage and Fairbanks, as well as other emission sources in the region.

As part of WRAP Alaska effort, we will develop techniques for credible modeling of regional haze in Alaska and provide a preliminary initial evaluation of the potential contributions to regional haze in the Alaska Class I areas that are due to in-state emissions. The focus of this effort is namely on the Denali National Park and Tuxedni Wilderness Area Class I area, as well as the Simeonof Wilderness (due to its remoteness, the Bering Sea Wilderness will not be addressed in this initial modeling analysis). There are three main components of regional haze modeling:

- Meteorological Modeling
- Emissions Modeling
- Air Quality Modeling

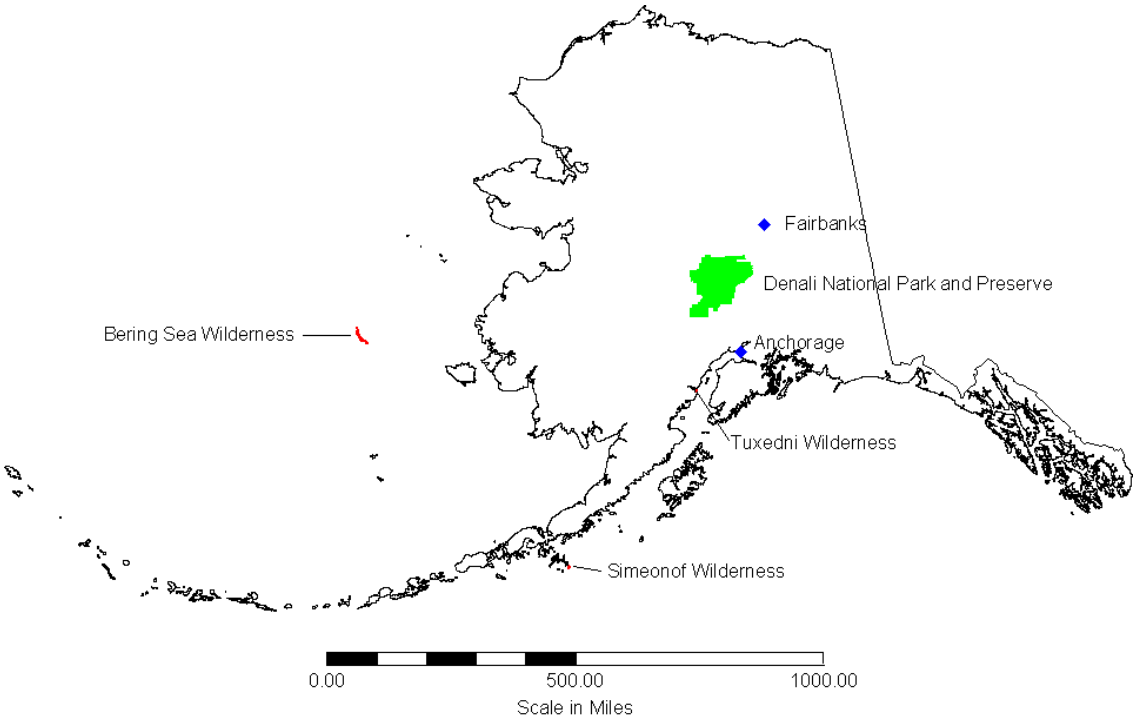

Figure 1-1. Locations of the four Class I areas in Alaska along with the two biggest Alaska cities, Anchorage and Fairbanks.

The State of Alaska is developing a statewide emissions inventory for "all" sources. However, currently the emissions inventory for Alaska is incomplete. Consequently, it is premature to perform photochemical grid modeling with a model such as CMAQ since source-oriented models require complete emission inventories. Thus, the approach in this WRAP Alaska modeling work effort is to evaluate meteorological modeling techniques to simulate the unique and complex meteorological conditions of Alaska. Then, we will perform preliminary air quality modeling using a simplified Lagrangian (trajectory) model to provide a first order assessment of the potential contributions of emissions from Anchorage and Fairbanks as well as major stationary sources on visibility at the Denali National Park and Tuxedni Wilderness. The Lagrangian model CALPUFF will be used for preliminary WRAP Alaska visibility modeling. The Fifth Generation Mesoscale Model (MM5), developed and maintained by the Pennsylvania State University and National Center for Atmospheric Research (PSU/NCAR), is used to develop hourly meteorological fields for the Alaska region for the entire year 2002. These 2002 meteorological fields are supplied to CALPUFF for the WRAP visibility modeling effort.

In this document, we evaluate the 2002 MM5 annual run performed by the WRAP RMC. In Section 2, we present an overview of the MM5 system and the modeling challenges posed by the meteorology of Alaska. Next, we describe the MM5 physical configuration used in the 2002 run. In Section 3, we describe our evaluation tools and procedures. Then, in Sections 4-6, we

evaluate the performance of the model run in replicating the evolution of observed winds, temperature, humidity, and precipitation to the extent that resources and data availability allow; this serves as an assessment of the reliability of the new WRAP run's 15-km meteorological fields in adequately characterizing the state of the atmosphere and for serving as the meteorological driver for the CALPUFF visibility modeling run that will be discussed in subsequent documents.

2.0 METEOROLOGICAL MODELING APPROACH

The CALPUFF modeling system includes the CALPUFF dispersion model and the meteorological preprocessor CALMET. CALPUFF requires inputs of three-dimensional gridded wind, temperature, humidity, cloud/precipitation, and boundary layer parameters. These fields are generated by CALMET, which can reprocess output fields from the PSU/NCAR MM5 meteorological model and supply them in a suitable format to CALPUFF. MM5 is a state-of-the-science atmosphere model that has proven useful for air quality applications and has been used extensively in past local, state, regional, and national modeling efforts. MM5 has undergone extensive peer-review, with all of its components continually undergoing development and scrutiny by the modeling community. The MM5 modeling system software is freely provided and supported by the Mesoscale Prediction Group in the Mesoscale and Microscale Meteorology Division of NCAR. For these reasons, MM5 is the most widely used public-domain prognostic model. In-depth descriptions of MM5 can be found in Dudhia (1993) and Grell et al. (1994), and at http://www.mmm.ucar.edu/mm5.

Description of MM5

The PSU/NCAR MM5 is a limited-area, terrain-following (sigma-coordinate), prognostic meteorological model. It solves the full suite of non-hydrostatic prognostic primitive equations for the three-dimensional wind, temperature, water, and pressure fields. It can be run with multiple one-way or two-way nested grids to resolve a range of atmospheric processes and circulations on spatial scales ranging from one to several thousands of kilometers. The model is highly modular, facilitating the interchange of physics and data assimilation options. Several options exist for boundary layer schemes, resolved and sub-grid cloud and precipitation treatments; soil heat budget models, and radiative transfer. The model equations are solved horizontally on an Arakawa-B grid structure defined on a number of available map projections. The polar stereographic projection is used for MM5 applications in Alaska. The vertical coordinate is a terrain-following normalized pressure coordinate, referred to as a “sigma-p”. Typically, 30-50 vertical levels are used to resolve the troposphere and lower stratosphere to an altitude of approximately 15 km (100 mb).

The model is supported by several pre- and post-processing programs, which are referred to collectively as the MM5 modeling system. The MM5 modeling system software is mostly written in Fortran, and has been developed at Penn State and NCAR as a community mesoscale model with contributions from users worldwide. The pre- and post-processing tools facilitate the development of various model inputs and the analysis of model output.

Because MM5 is a limited-area model, it requires lateral boundary conditions that define the space- and time-varying conditions at the periphery of the coarsest domain throughout the simulation. Both initial and boundary conditions are generally specified using observational analyses, and may be supplemented by additional surface or upper air observations. These data sources can be obtained from a variety of routine analysis systems, from several global analysis products to higher resolution (time and space) forecast initialization fields prepared by the National Weather Service or other entities. Most datasets are available directly from NCAR.

The model may be constrained during the simulation to relax toward observed temperature, wind and humidity observations through the use of a Newtonian nudging four dimensional data assimilation technique known as FDDA (Stauffer and Seaman 1990, 1991). In the Newtonian nudging technique, a relaxation term is added to the prognostic equations and serves to "nudge" the model solution towards objective analysis fields and/or individual observations. Application of this technique has been shown to significantly reduce drift in the solution during simulations of several days or more. Drift may be caused by (among other effects) inaccuracies in the initial conditions, the effects of discretization, and/or errors in the formulation of various parameterizations.

The Meteorology of Alaska

The meteorology of Alaska poses some unique challenges for MM5 modeling. In winter, there is little liquid water or insolation, and temperatures and specific humidities are extremely low north of the Alaska Range. There is extensive sea ice in the winter in the Bering Sea and Arctic Ocean. Interactions between sea ice and the air above have historically been difficult for models to simulate well, and the energy exchange between the sea ice and the overlying air is not well understood (Curry et al. 2001). In the dark of winter, the ice undergoes intense radiative cooling, which can produce a strong temperature inversion near the surface. This also occurs over the snow covered inland areas from the Alaska Range north. This strong inversion creates an extremely stable boundary layer that can then decouple from the flow aloft. It is therefore possible to have air masses with different origins and properties superimposed in the vertical. This can be significant in terms of air quality modeling if the overlying air mass has different chemical properties than the air below. In addition, it is difficult for an atmospheric model to handle this type of extremely stable boundary layer well, as turbulent flows in stable layers are not well understood (Mahrt 1998). These stable layers can be broken up by intermittent turbulence, sometimes arising from gravity wave generation over the Alaska Range. These events are notoriously difficult for an atmospheric model to simulate (Tilley 2004).

The MM5 modeled temperature fields are very sensitive to the cloud fields. Small errors in cloud cover can produce large errors in the temperatures. Because clouds can be a sub-grid scale phenomenon, errors in characterization of the cloud field are inevitable, and may lead to significant temperature errors, particularly in winter. For example, in a region with strong radiative cooling over sea ice, if the model places a cloud where there is none in the real world, the outgoing longwave radiation trapped by the modeled cloud and re-emitted downward will cause a spurious warming below the cloud. This will cause the model to overestimate the surface temperature and underestimate or entirely fail to produce the inversion which should be there. This may have serious implications for subsequent air quality modeling.

Further complicating the characterization of the cloud field is the fact that some Arctic clouds have unusual properties. There are clouds composed of ice crystals which can extend down to the ground, and are known as diamond dust. Multiple thin cloud decks may appear in the statically stable atmosphere, and convective plumes may appear in gaps in the sea ice (Curry et al. 2001). All of these phenomena may be difficult or impossible to capture in a model running at a minimum resolution of 15 km.

In the spring and fall, the model must account for the breakup and formation of sea ice. Sea ice has a large effect on the surface energy budget, and a mis-characterization of the extent of sea ice

will degrade MM5's simulation of the thermal structure of the overlying atmospheric column. The model must also address the possibility of snow cover. A model grid cell may be fully or partially covered with snow and/or ice, and the model must treat the radiative properties of ice and snow as well as the transfer of heat through them and the to and from the underlying soil and the air above.

In addition to the challenges of modeling Alaska, there is less data available for performance assessment than is generally the case for a modeling study done over the continental U.S. Given the low population density and harsh conditions, it is not surprising that the observing network in Alaska is sparse compared to that of the U.S. mainland. This complicates model validation, particularly in the 15 km domain, where representative observations may be very widely spaced if one or more observing sites are down (Tilley, 2004). The rugged Alaskan terrain can also cause problems in model validation. Many stations are located in regions where meso-gamma and microscale effects forced by topography can form a significant part of the signal in temperature and winds (Tilley, 2004).

Currently, there is no readily available high-resolution gridded precipitation data set for Alaska. We use the global CMAP (Climate Prediction Center Merged Analysis of Precipitation) gridded precipitation data set, which has a resolution of 2.5 x 2.5 degrees (~ 275 km). With such a large mismatch between the resolution of the observations and the model output, we are limited to doing only a qualitatative assessment of the MM5 precipitation fields.

MM5 Configuration

The WRAP MM5 modeling system configuration for the Alaska application was based on the work of the Mesoscale Modeling and Applications Group at the University of Alaska Fairbanks (UAF). The UAF Group has extensive experience with operational numerical weather prediction in high latitudes using MM5 modeling (http://knik.iarc.uaf.edu/AtmGroup). We built on their experience by incorporating some facets of their MM5 configuration for use in the present application, and then performing a series of sensitivity tests with different physics options to arrive at an optimal configuration of MM5 for our 2002 run. These tests are discussed in detail in the Modeling Protocol (ENVIRON 2004) and are summarized below.

Modeling Domain

MM5 was configured to run two grids: a large-scale grid with 45-km grid point spacing, and a smaller grid with 15-km grid point spacing focused on the two Class I areas and emission sources of primary interest (Figure 2-1). The model was run on both grids simultaneously, but in a "one-way" nesting mode. In this approach, information from the 45-km grid is transferred to the 15-km domain through boundary conditions during the simulation, but there is no feedback of the 15-km fields up-scale to the 45-km domain. Another alternative is "two-way" nesting, wherein MM5 is run for both grids simultaneously and information propagates both down and up-scale between the two. Our experience suggests that the choice of one- vs. two-way nesting does not have a significant impact on model performance on the inner grid for regional applications with coarse grid spacing.

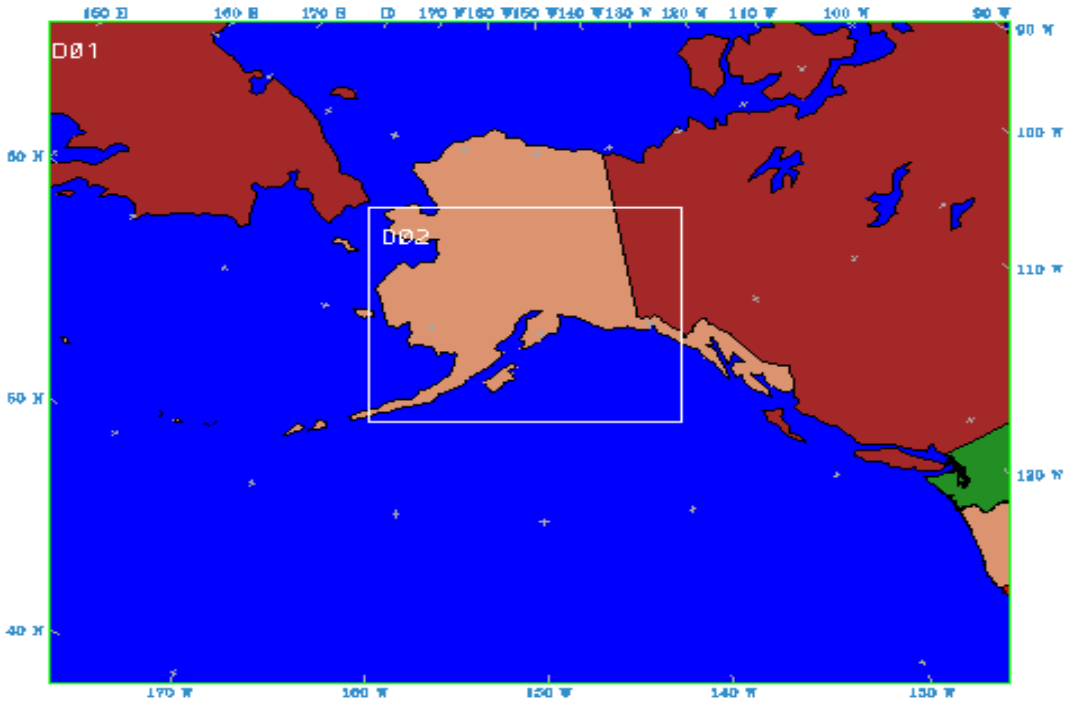

Figure 2-1. Spatial coverage of the Alaska Grid with 45 km grid point (D01) and the nested 15 km grid (D02).

The 45 km Alaska Grid is defined on a polar stereographic projection, with central latitude 59º and central longitude 151º W. The grid has 109 (east-west) by 90 (north-south) dot points, and 108 (east-west) by 89 (north-south) cross points (Figure 2-1). The 15 km grid is defined on the same polar stereographic projection, but covers the Anchorage and Fairbanks populated areas and Class I areas of primary interest with 15-km grid point spacing. The coverage of the MM5 15-km subregional grid is shown in Figure 2-1.

Vertical Grid Structure

The vertical layer structure is summarized in Table 2-1. The altitudes above sea level are estimated according to standard atmosphere assumptions used in MM5 (surface pressure of 1000 mb, model top at 50 mb, surface temperature of 275 K, and log-pressure lapse rate of 50 K/ln[p]).

Table 2-1. MM5 vertical layer structure for the Alaska 2002 application.

Level	Sigma	Pressure (mb)	Height (m)
40 – top	0.000	50	23354.9
40	0.018	67.1	21150.9
39	0.040	88.0	19097.4
38	0.060	107.0	17605.0
37	0.085	130.8	16065.0
36	0.107	151.6	14919.9
35	0.134	177.3	13708.1
34	0.158	200.1	12766.3
33	0.187	227.7	11759.0
32	0.213	252.4	10952.3
31	0.244	281.8	10085.7
30	0.272	308.4	9375.9
39	0.304	338.8	8634.5
28	0.334	367.3	7996.4
27	0.367	398.7	7348.2
26	0.398	428.1	6783.2
25	0.431	459.5	6222.2
24	0.462	488.9	5728.4
23	0.495	520.3	5233.8
22	0.526	549.7	4795.1
21	0.559	581.1	4352.8
20	0.590	610.5	3958.1
19	0.623	641.9	3558.0
18	0.654	671.3	3199.2
17	0.687	702.7	2833.9
16	0.718	732.1	2505.1
15	0.749	761.6	2189.0
14	0.778	789.1	1903.9
13	0.806	815.7	1637.9
12	0.832	840.4	1398.4
11	0.855	862.3	1192.2
10	0.878	884.1	991.1
9	0.897	902.2	828.6
8	0.917	921.2	661.0
7	0.932	935.4	537.5
6	0.949	951.6	400.0
5	0.961	963.0	303.9
4	0.975	976.2	193.5
3	0.983	983.9	131.1
2	0.992	992.4	61.4
1	0.995	995.25	38.3
0 - ground	1.000	1000	0

Physics Options and FDDA

In this section, we will discuss the rationale behind the choice of physics options and FFDA parameters made for the Alaska MM5 modeling effort. As mentioned above, the 2002 annual MM5 application was configured in many aspects according to the optimum arrangement identified by the UAF group with some input coming from additional sensitivity tests specific to this application.

When modeling a full year over the Alaska domain, it is necessary to take into account the annual cycle of sea ice. The sea ice, which forms part of the atmosphere's lower boundary condition, grows in spatial extent during fall and winter, and retreats during the spring and early summer. MM5 has an option whereby the sea ice fraction in a grid cell is diagnosed using the sea surface temperature, and this flag must be used during the winter months to ensure an adequate treatment of the atmosphere's lower boundary condition. Use of the sea ice option limits the available physics options in MM5, as it requires the use of the 5-layer land surface model (LSM). This entails running the model in two different physics configurations: one for summer and one for winter, each having a different sea ice and LSM parameterization.

The switch over from the summer to the winter configuration and back again is necessarily arbitrary, and there is no clear indicator to determine the date for the switch. To set the date for the sea ice switch on and off, we used sea ice concentration data to estimate the spatial coverage of sea ice within the domain. This data came from NASA's Goddard Space Flight Center National Snow and Ice Data Center, and was gathered by passive microwave sounders flying on board polar orbiting satellites. We used the sea ice concentration data to assess how far into the modeling domain the sea ice extended during each day of the simulation. Monthly sea ice concentrations for 6 months of 2002 are shown in Figure 2-2. We selected May 30, 2002 as the day when the sea ice option is turned off because most of the domain was free of sea ice by this time. October 13, 2002 was selected as the day when the sea ice is turned back on because sea ice with a concentration of 100% reached land in the north of the domain on that day. These days are admittedly arbitrary, but there is no consensus on the day of the year that is best for the switchover as the onset and break up of sea ice varies spatially and temporally.

MM5 has a POLAR option (Cassano et al. 2001) for use at high latitudes that improves the treatment of heat transfer through snow and ice surfaces. More levels are added in the MM5 soil model to improve the representation of heat transfer through ice sheets. The thermal diffusivity is changed for grid points containing snow, permanent ice or sea ice, and a sea ice surface type is added to the 13 surface types available in the standard version of MM5. The sea surface type allows for fractional coverage of sea ice at any ocean grid point, and surface fluxes are calculated separately for open water and sea ice portions of the grid cell. Fluxes are averaged before they are fed to the overlying atmosphere. The sea ice can range from 0.2 to 0.95 meters in thickness.

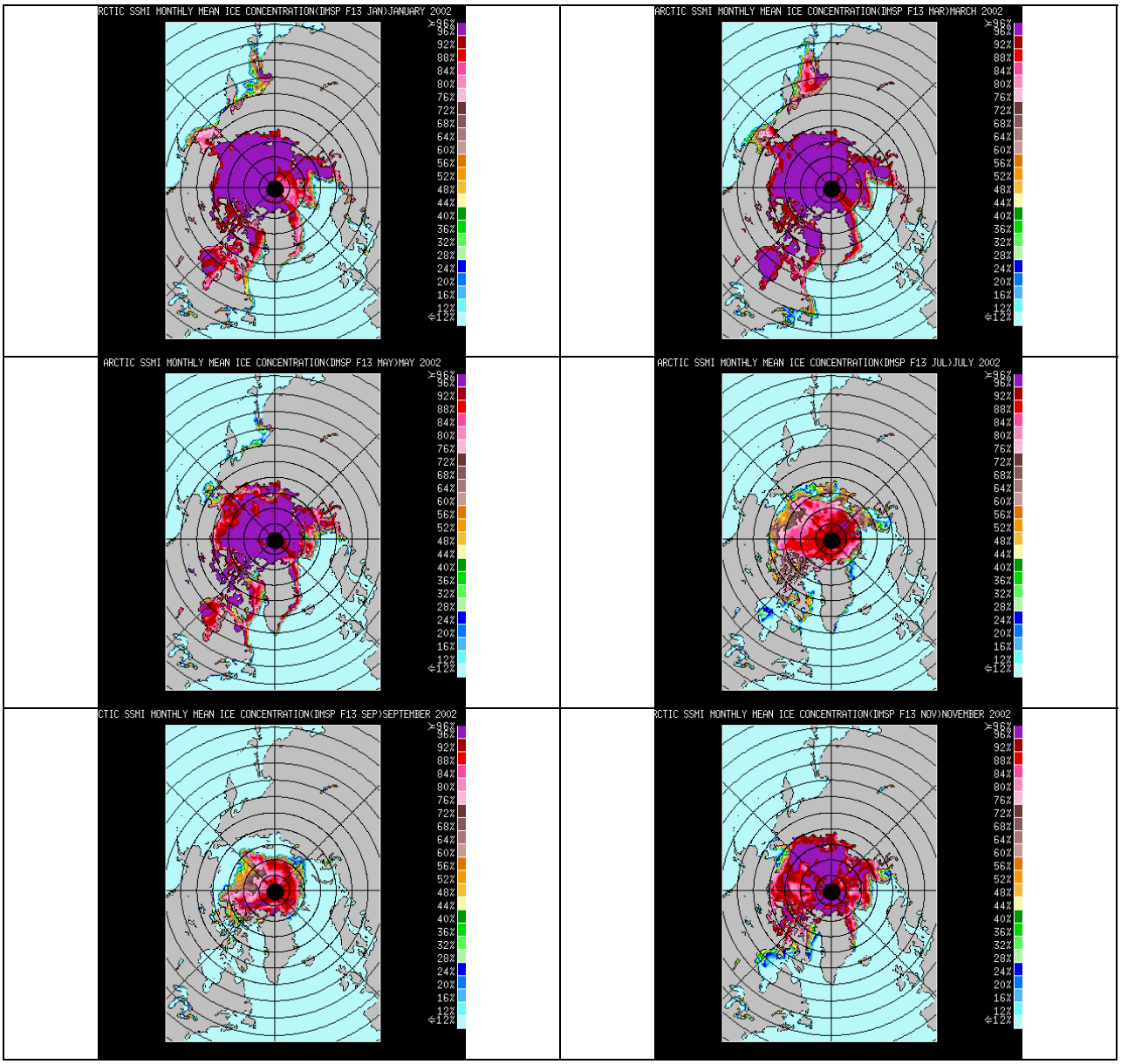

Figure 2-2. Monthly mean sea ice concentrations. January, March, May, July, September, November.

Turbulent fluxes between the surface and the atmosphere are parameterized using the 1.5 order turbulence closure parameterization from the NCEP ETA model. Thermal properties in the soil model for snow and ice are modified following Yen at al (1981). The number of substrate levels is increased from 6 to 8 with an increase in substrate depth from 0.47 to 1.91 meters.
The latent heat of sublimation is used for the calculation of the latent heat flux over ice surfaces, and ice saturation is assumed when calculating saturation mixing ratios over ice.

To treat stratiform clouds, we use the Reisner II cloud microphysics scheme (Reisner et al. 1998). Although this scheme is more computationally intensive than the "simple ice" option, the EPA recommends that a mixed phase ice scheme be employed in MM5 to drive aqueous chemistry and wet scavenging in CMAQ. This is because the simple ice approach treats all

condensed water forms as a single liquid variable, which when passed to CMAQ overstates the quantity of liquid cloud and precipitation water available for chemistry and removal. Furthermore, the most recent version of CMAQ includes separate contributions from precipitating ice (graupel). Although the initial Alaska visibility modeling will be performed using CALPUFF, subsequent air quality modeling of Alaska may be done with CMAQ so the Reisner II cloud microphysics scheme was selected to allow the use of CMAQ at a later date if desired. For cumulus convection, we select the Grell scheme, which has been used successfully by the UAF group. Cumulus convection was not expected to play a large role in the Alaska simulation during winter, but significant convection can occur in the summer, particularly in the Denali area. Convection in this region is driven largely by topographic/land surface forcings (Tilley 2004).

Prior modeling efforts in Alaska have mainly used the RRTM or CCM2 radiation schemes. They showed that RRTM performed better in some cases and that CCM2 did better in others, and there was no guide to determine *a priori* which would be the best choice for this application (Tilley, 2004). We tested three MM5 radiation schemes, CCM2, RRTM and CLOUD. The CLOUD radiative package was widely used before the advent of the RRTM scheme, and has a simpler treatment of the longwave absorption than RRTM, which uses the correlated-k method of calculating absorption coefficients. The shortwave treatments in CLOUD and RRTM are similar. We tested the CLOUD scheme in order to have a range of complexity of parameterization when evaluating the sensitivity of the Alaska simulation to the choice of radiation scheme. We ran MM5 for a 5-day period in July and a 5-day period in January to span the range of climatological conditions the model was likely to encounter in the annual 2002 run and examined the results on both the 15 km and 45 km domains. Based on the surface wind and temperature performance, the CCM2 scheme did not sufficiently improve MM5 performance to justify its added computational burden (~20%), so we selected the RRTM parameterization to be the radiation scheme for the 2002 annual period.

We performed a sensitivity test in which we looked at the choice of Land Surface Model (LSM) for the summer months. Recall that, in winter, we must use the 5-layer LSM in order to make the sea ice parameterization. In summer, however, we are free to select the best-performing LSM scheme for this application. The Pleim-Xu scheme has been shown to perform well over the continental U.S. (Olerud and Sims 2003; Kemball-Cook et al. 2004) and also allows use of the Pleim deposition scheme in subsequent CMAQ modeling; we therefore made a run (S4) using the Pleim-Xu scheme and the RRTM radiation scheme for the July time period. Overall, the Pleim-Xu scheme did not cause significant improvement over the other LSM schemes, so we elected to use the NOAH/ETA LSM/PBL combination.

Thus, in the winter, we use the sea ice option, the 5-layer LSM and the ETA PBL. During summer, however, we turn off the sea ice option, allowing us to choose a more detailed land surface model. The OSU land surface model has been shown to be effective in simulating the Alaskan summer when used with the ETA PBL (Tilley, 2004), and we use this configuration as our starting point. Note that although the LSM/PBL/sea ice/snow configuration changes in going from summer to winter, the rest of the physics options are held constant throughout the year. The MM5 physics options used for the winter and summer months are summarized in Tables 2-2 and 2-3, respectively.

Table 2-2. Physics options selected for the 2002 WRAP Winter Alaska MM5 simulation.

Physics Option	Parameterization
Cloud Microphysics	Reisner II
Cumulus Parameterization	Grell
Planetary Boundary Layer	ETA
Land Surface Model	5-Layer Model
Radiation	RRTM
Shallow Convection	None
Varying SST with time?	Yes
Sea Ice	Yes
Snow Cover	Simple Snow Model

Table 2-3. Physics options selected for the 2002 WRAP Summer Alaska MM5 simulation.

Physics Option	Parameterization
Cloud Microphysics	Reisner II
Cumulus Parameterization	Grell
Planetary Boundary Layer	ETA
Land Surface Model	OSU
Radiation	RRTM
Shallow Convection	None
Varying SST with time?	Yes
Sea Ice	No
Snow Cover	No

MM5 was configured to use its FDDA capabilities to nudge the model toward observed wind, temperature, and moisture fields on both 45 km and 15 km grids throughout the 2002 annual simulation. Analysis (or grid) nudging was performed at 3-hourly intervals both for the two-dimensional surface fields and for the three-dimensional fields aloft, excluding the boundary layer depth. Exclusion of the boundary layer in the FDDA process removes the potential for damping out resolved mesoscale forcings in the model that are important to boundary layer development and thus the vertical fluxes of momentum, heat, and moisture into the free atmosphere and to the surface. The dataset used for nudging is the NCAR/NCEP Reanalysis Project (NNRP) reanalysis. Available from NCAR, NNRP contains 6-hourly fields generated by a global data assimilation system. Note that the NNRP analysis fields were used instead of the usual Eta Data Assimilation System (EDAS) fields used in most U.S. MM5 applications because Alaska lies outside the EDAS domain. Analysis nudging coefficients are shown in Table 2-4. Two-dimensional surface nudging was done using NCAR/NCEP Reanalysis Project (NNRP) surface analyses. Surface nudging was enhanced via the "little_R" program using hourly NWS surface observations from NCAR dataset ds472. The network of observing stations used for nudging in the Alaska application is shown in Figure 2-3.

Table 2-4. FDDA analysis nudging coefficients (s^{-1}).

	45 km	15 km
Wind	2.5×10^{-4}	1.0×10^{-4}
Temperature	2.5×10^{-4}	1.0×10^{-4}
Water vapor	1.0×10^{-5}	1.0×10^{-5}

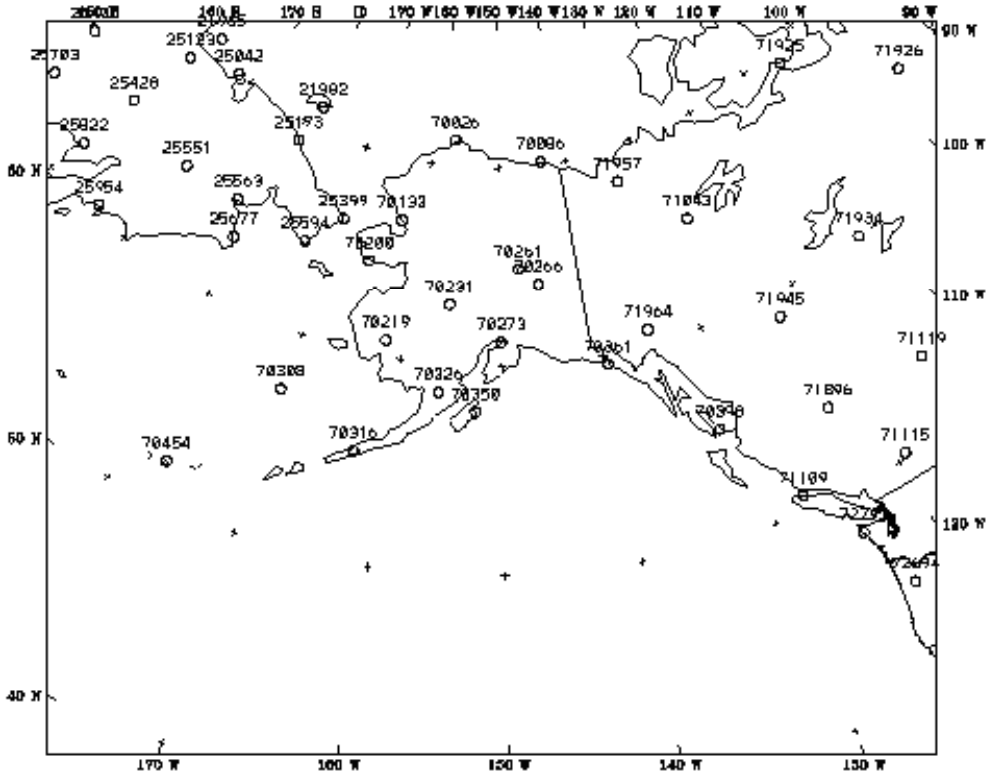

Figure 2-3. Stations contributing data in the 45 km modeling domain used for observational nudging.

Global topographic data at 10-minute (latitude/longitude) resolution was used to define terrain elevations on the 45-km grid; higher 5-minute resolution from the same dataset were used for the smaller 15-km domain. Land use distribution on the MM5 domains was defined from the 24-category USGS vegetation data with a resolution of 10 minutes.

Model Application

The 2002 annual simulation was made in sequential 5-day run segments, each with an initial spinup period of 12 hours that overlapped the last 12 hours of the preceding run (i.e., in 5 ½ day run segments). This was done so that the air quality model can be started at either 0Z or 12Z without including the MM5 re-initialization period. MM5 was re-initialized at the beginning of each 5-day period to reduce error propagation through the simulation. That is, each 5 ½ day run segment is independent of the previous segment. The 2002 annual simulation included the final two weeks of December 2001 to allow for sufficient spin-up time for photochemical/visibility applications with start dates at the beginning of January 2002. The model was run with 90 second and 30 second time steps on the 45 km and 15 km grids, respectively.

3.0 EVALUATION METHODOLOGY FOR THE ALASKA 2002 ANNUAL RUN

The goal of this evaluation is to determine whether the meteorological fields generated by the 45/ 15 km 2002 MM5 Alaska simulation are sufficiently accurate to use as inputs to CALPUFF for visibility modeling. If errors in the meteorological fields are too large, CALPUFF's ability to replicate regional pollutant levels over the entire base year will be severely hampered and the predicted air quality and visibility impacts from future year growth and controls will be highly questionable. To provide a reasonable meteorological characterization to the dispersion/visibility model, MM5 must represent with some fidelity the:

- Large-scale weather patterns (i.e., synoptic patterns depicted in the 850-300 mb height fields), as these are key forcings for mesoscale circulations;
- Mesoscale and regional wind, temperature, PBL height, humidity, and cloud/precipitation patterns;
- Mesoscale circulations such as sea breezes and mountain/drainage circulations;
- Diurnal cycles in PBL depth, temperature, and humidity.

For visibility applications, the moisture and condensate fields are particularly important as they significantly impact PM chemical formation, removal, and light scattering efficiency. In addition, cloud and precipitation fields are a good measure of the integrated performance of the model since these are model-derived quantities and are not nudged to observations. Because of the model's coarse resolution of 45 km/15 km, the present run cannot be expected to faithfully simulate the high frequency pattern or variability of the convective precipitation, but should reproduce the synoptic-scale precipitation and cloud patterns.

In this study, the operational performance assessment entailed a comparison of the predicted meteorological fields to available surface and aloft observed meteorological data that are collected, analyzed, and disseminated by the National Weather Service, NCEP, and NCAR. The performance evaluation was carried out both graphically and statistically to assess model performance for winds, temperatures, humidity, and the placement, intensity, and evolution of key weather phenomena.

3.1 SURFACE STATISTICAL EVALUATION

Johnson (2003) provides a synopsis of the challenges associated with undertaking an objective and meaningful performance evaluation of meteorological models. Climatic variability, complex mesoscale phenomena, stochastic variability, and scientific limitations contribute to unique performance issues in each meteorological modeling exercise, thereby forcing modelers to take a subjective approach to model performance evaluation. Objective statistics that offer a quantitative model assessment exist, but implementation of the metrics is subjective. For example, defining the area over which domain-averaged metrics are calculated is a subjective decision. In general, metrics averaged over large modeling domains are avoided, as errors can

cancel one another, rendering the average meaningless. Conversely, splitting the modeling domain into small analysis sub-domains can make sample sizes too small to be representative.

For the surface evaluation, we use a standard set of statistical measures that are detailed below. These metrics are calculated on hourly and daily time frames for wind speed, wind direction, temperature, and humidity at the surface. While no strict criteria establishing acceptable model performance exist, general guidelines have been developed by Emery et al. (2001) and are described later.

Mean Observation (M_o): calculated from all sites with valid data within a given analysis region and for a given time period (hourly or daily):

$$M_o = \frac{1}{IJ}\sum_{j=1}^{J}\sum_{i=1}^{I} O_j^i$$

where O^i_j is the individual observed quantity at site i and time j, and the summations are over all sites (I) and over time periods (J).

Mean Prediction (M_p): calculated from simulation results that are interpolated to each observation point used to calculate the mean observation (hourly or daily):

$$M_p = \frac{1}{IJ}\sum_{j=1}^{J}\sum_{i=1}^{I} P_j^i$$

where P^i_j is the individual predicted quantity at site i and time j. Note that mean observed and predicted winds are vector-averaged (for east-west component u and north-south component v), from which the mean wind speed and mean resultant direction are derived.

Least Square Regression: performed to fit the prediction set to a linear model that describes the observation set for all sites with valid data within a given analysis region and for a given time period (daily or episode). The y-intercept a and slope b of the resulting straight line fit are calculated to describe the regressed prediction for each observation:

$$\hat{P}_j^i = a + bO_j^i$$

The goal is for a 1:1 slope and a "0" y-intercept (no net bias over the entire range of observations), and a regression coefficient of 1 (a perfect regression). The slope and intercept facilitate the calculation of several error and skill statistics described below.

Bias Error (B): calculated as the mean difference in prediction-observation pairings with valid data within a given analysis region and for a given time period (hourly or daily):

$$B = \frac{1}{IJ}\sum_{j=1}^{J}\sum_{i=1}^{I}\left(P_j^i - O_j^i\right)$$

Gross Error (E): calculated as the mean *absolute* difference in prediction-observation pairings

$$E = \frac{1}{IJ}\sum_{j=1}^{J}\sum_{i=1}^{I}\left|P_j^i - O_j^i\right|$$

with valid data within a given analysis region and for a given time period (hourly or daily): Note that the bias and gross error for winds are calculated from the predicted-observed residuals in speed and direction (not from vector components u and v). The direction error for a given prediction-observation pairing is limited to range from 0 to ±180°.

Root Mean Square Error (RMSE): calculated as the square root of the mean squared difference in prediction-observation pairings with valid data within a given analysis region and for a given time period (hourly or daily):

$$RMSE = \left[\frac{1}{IJ}\sum_{j=1}^{J}\sum_{i=1}^{I}\left(P_j^i - O_j^i\right)^2\right]^{1/2}$$

The RMSE, as with the gross error, is a good overall measure of model performance. However, since large errors are weighted heavily (due to squaring), large errors in a small subregion may produce a large RMSE even though the errors may be small and quite acceptable elsewhere.

Systematic Root Mean Square Error ($RMSE_S$): calculated as the square root of the mean squared difference in regressed prediction-observation pairings within a given analysis region and for a given time period (hourly or daily):

$$RMSE_S = \left[\frac{1}{IJ}\sum_{j=1}^{J}\sum_{i=1}^{I}\left(\hat{P}_j^i - O_j^i\right)^2\right]^{1/2}$$

where the regressed prediction is estimated for each observation from the least square fit described above. The $RMSE_S$ estimates the model's linear (or systematic) error; hence, the better the regression between predictions and observations, the smaller the systematic error.

Unsystematic Root Mean Square Error ($RMSE_U$): calculated as the square root of the mean squared difference in prediction-regressed prediction pairings within a given analysis region and for a given time period (hourly or daily):

$$RMSE_U = \left[\frac{1}{IJ}\sum_{j=1}^{J}\sum_{i=1}^{I}\left(P_j^i - \hat{P}_j^i\right)^2\right]^{1/2}$$

The unsystematic difference is a measure of how much of the discrepancy between estimates and observations is due to random processes or influences outside the legitimate range of the model.

A "good" model will provide low values of the RMSE, explaining most of the variation in the observations. The systematic error should approach zero and the unsystematic error should approach RMSE since:

$$RMSE^2 = RMSE_S^2 + RMSE_U^2$$

It is important that RMSE, $RMSE_S$, and $RMSE_U$ are all analyzed. For example, if only RMSE is estimated (and it appears acceptable) it could consist largely of the systematic component. This error might be removed through improvements in the model inputs or use of more appropriate options, thereby reducing the error transferred to the photochemical model. On the other hand, if the RMSE consists largely of the unsystematic component, this indicates that further error reduction may require model refinement (new algorithms, higher resolution grids, etc.), or that the phenomena to be replicated cannot be fully addressed by the model. It also provides error bars that may be used with the inputs in subsequent sensitivity analyses.

Index of Agreement (IOA): calculated following the approach of Willmont (1981). This metric condenses all the differences between model estimates and observations within a given

$$IOA = 1 - \left[\frac{IJ \cdot RMSE^2}{\sum_{j=1}^{J} \sum_{i=1}^{I} \left| P_j^i - M_o \right| + \left| O_j^i - M_o \right|} \right]$$

analysis region and for a given time period (hourly and daily) into one statistical quantity. It is the ratio of the total RMSE to the sum of two differences - between each prediction and the observed mean, and each observation and the observed mean:

Viewed from another perspective, the index of agreement is a measure of the match between the departure of each prediction from the observed mean and the departure of each observation from the observed mean. Thus, the correspondence between predicted and observed values across the domain at a given time may be quantified in a single metric and displayed as a time series. The index of agreement has a theoretical range of 0 to 1, the latter score suggesting perfect agreement.

Most of statistics used to evaluate meteorological model performance are given in absolute terms (e.g., wind speed error in m/s), rather than in relative terms (percent error) as is commonly shown for air quality assessments. The major reason for this is that a very different significance is associated with a given relative error for different meteorological parameters. For example, a 10% error for wind speed measured at 10 m/s is an absolute error of 1 m/s, a minor error. Yet a 10% error for temperature at 300° K is an absolute error of 30° K, a ridiculously large error. On the other hand, pollutant concentration errors of 10% at 1 ppb or 10 ppm carry similar significance.

3.2 THE METSTAT ANALYSIS PACKAGE

ENVIRON has developed a statistical analysis software package to calculate and graphically present the statistics described above. The package is comprised of a single Fortran program (METSTAT) to generate observation-prediction pairings and to calculate the statistics, and a Microsoft Excel macro (METSTAT.XLS) that plots the results.

The Fortran program reads MM5 output prediction files and surface observational data files. The program reads either MM5 observation FDDA input files directly, or observation data in an ASCII format. The program then spatially and temporally pairs MM5 predictions with observations for a user-defined time and space window. Since the surface layer in MM5 is usually rather thick relative to the heights at which the observational data were recorded, the METSTAT program also includes a micro-meteorological module that scales mid-layer predicted winds to 10 m heights, and mid-layer predicted temperatures to 2 m heights, using common stability-dependent similarity relationships. The horizontal analysis range can be given for an entire MM5 grid, by an LCP or polar stereographic coordinate box, or as a list of specific site identifiers (such as WBAN or AIRS numbers), as labeled on the observational file. This allows for an evaluation at a single site, a subset of specific sites (e.g., those along a coastline that would be difficult to select by defining an LCP box) or over an entire regional domain.

The program then proceeds to calculate the statistics described above for each hour and for each day of the time window. The following parameters are considered:

Wind Speed, Temperature, Humidity:
- Mean Observed
- Mean Predicted
- Bias
- Gross Error
- RMSE
- RMSES
- RMSEU
- IOA

Wind Direction:
- Mean Observed
- Mean Predicted
- Bias
- Gross Error

The RMSE and IOA have not been typically used to quantify error for wind direction, and thus are not calculated by the program.

Separate ASCII files containing the hourly and daily statistics are generated, formatted specifically to facilitate import into the Excel macro. The Excel macro is used to plot the data. The hourly statistics are plotted as time series, to show the diurnal variation of model performance. The daily statistics are plotted as bar charts to show daily performance over an episode. The macro also allows the daily results from multiple MM5 runs to be plotted together to ease the inter-comparison of performance.

3.3 STATISTICAL BENCHMARKS

Emery et al. (2001) have derived a set of daily performance "benchmarks" for typical meteorological model performance. These standards were based upon the evaluation of over 30 MM5 and RAMS meteorological simulations in support of air quality applications performed in the last decade, as reported by Tesche et al. (2001). The purpose of these benchmarks was not

necessarily to give a passing or failing grade to any one particular meteorological model application, but rather to put its results into the proper context. For example, expectations for meteorological model performance for the U.S. west coast might not be as high as for a flatter domain located over the Midwest. The key to the benchmarks is to understand how poor or good the results are relative to the universe of other model applications run for various areas of the U.S.

The statistical performance benchmarks are given in Table 3-1.

Table 3-1. Statistical benchmarks for evaluating meteorological model performance.

	Wind Speed	Wind Direction	Temperature	Humidity
RMSE	≤ 2 m/s			
Mean Bias	≤ ±0.5 m/s	≤ ±10°	≤ ±0.5 K	≤ ±1 g/kg
Gross Error		≤ 30°	≤ 2 K	≤ 2 g/kg
Index of Agreement	≤ 0.6		≤ 0.8	≤ 0.6

Note that the meteorological modeling performance benchmarks are based on historical model performance for applications in the lower 48 states. Given the shorter history and level of applications and harsher conditions, one would not expect the model to perform as well in Alaska as the continental U.S. Thus, the performance benchmarks are a particularly stringent test for meteorological modeling of Alaska.

3.4 SURFACE STATISTICAL ANALYSIS FOR ALASKA

The statistical evaluation of MM5 surface fields was performed using NCAR dataset ds472, which contains hourly observations of the commonly measured variables from airports in the U.S. and Canada. The locations of ds472 observing sites furnishing data used in this analysis are shown in Figure 3-1. Dataset variables include temperature, dew point, wind speed/direction and gusts, cloud cover fraction and cloud base for multiple cloud layers, visual range, precipitation rates and snow cover, and a descriptive weather code. The key data of interest were extracted for the various sub-domains, and processed into the appropriate formats for METSTAT.

As discussed earlier, some care must be taken in selecting an area for averaging. The problem with evaluating statistics is that the more data pairings that are summarized in a given metric, the better the statistics generally look, and so calculating a single set of statistics for a very large area (e.g., the entire 45 km domain) would not yield significant insight into model performance. Therefore, a balance must be struck between taking a large enough area to create a representative sample and choosing such a large area as to smear out the signal of interest. Since the Class I areas that are the focus of the CALPUFF modeling all lie within the 15 km domain, we will perform the METSTAT evaluation on the 15 km domain only.

The Alaska 15 km domain was divided into four subdomains based on topography and similarity of meteorological regime. The subdomains are shown in Figure 3-2. The NE and SE subdomains contain most of the highest terrain in the 15 km domain. For each subdomain, METSTAT was used to calculate hourly and daily statistical measures, and these were compared against model performance benchmarks developed by Emery et al. (2001) as summarized in

Table 3-1. The surface meteorological evaluation of the 2002 annual 45/15 km MM5 simulation of Alaska is presented in Section 4.

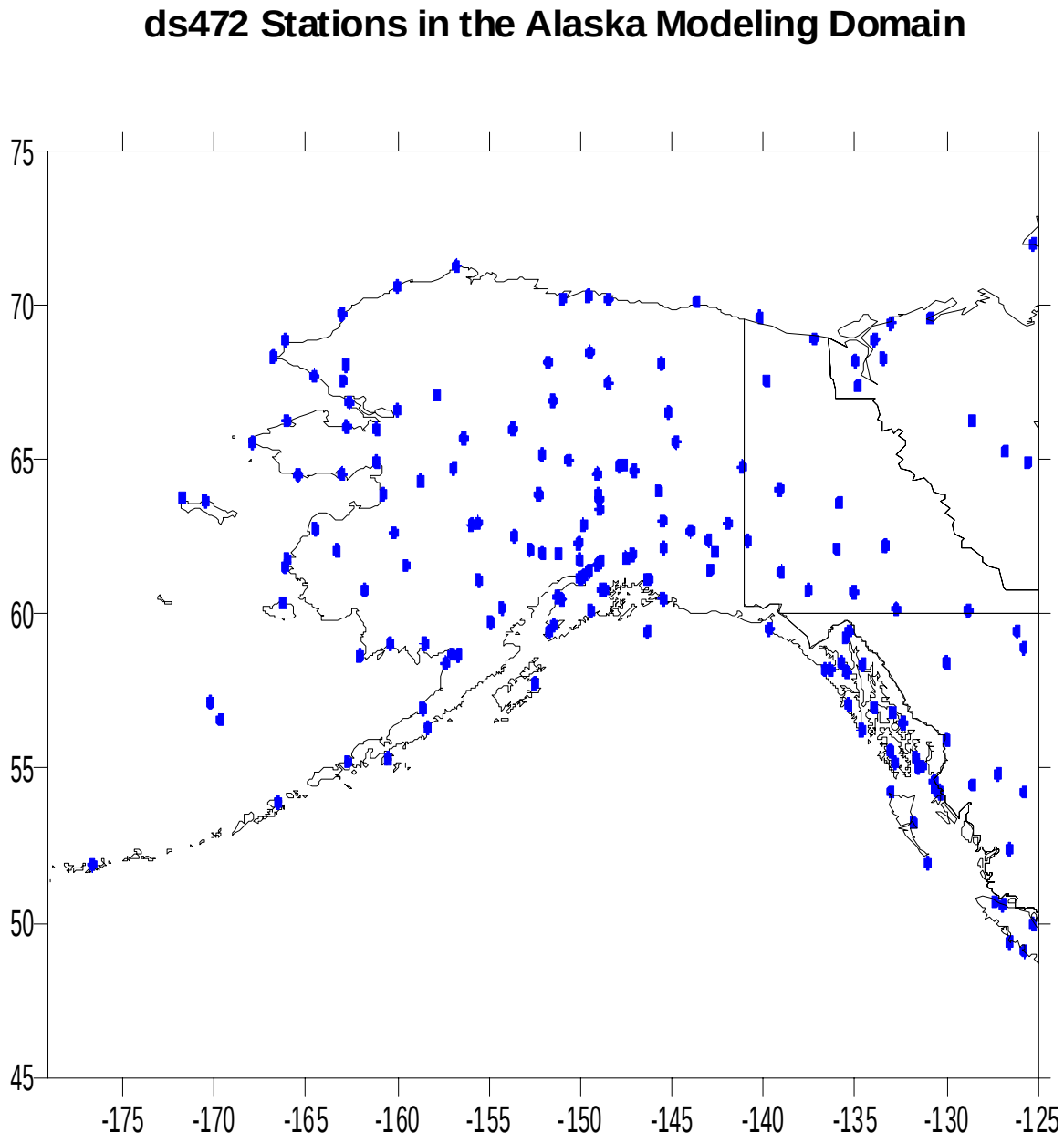

Figure 3-1. ds472 stations in the Alaska modeling domain.

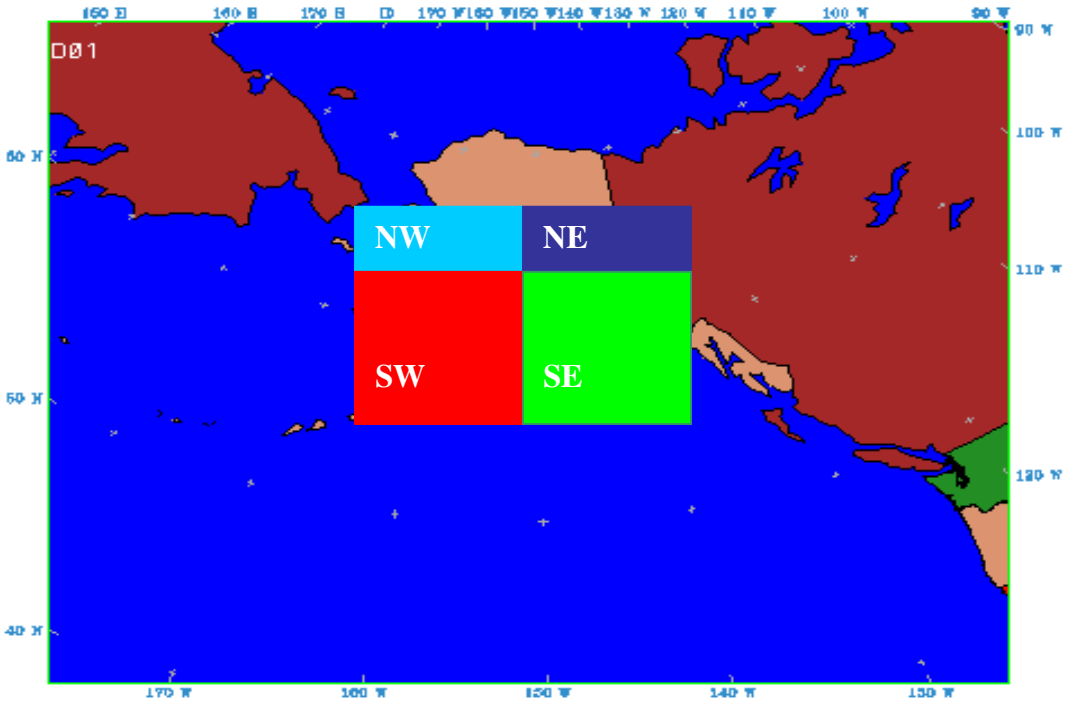

Figure 3-2. Four METSTAT subdomains (SE, SW, NW and NE) for the Alaska 2002 MM5 performance evaluation.

3.5 PRECIPITATION EVALUATION

In order to evaluate the precipitation fields in the Alaska 2002 MM5 application, we examined the annual cycle in the monthly rainfall totals in the MM5 run and compared them to observed monthly rainfall totals. For each month, we developed a field of observed total precipitation over the Alaska grid. The observed precipitation amounts were generated using the CMAP (Climate Prediction Center Merged Analysis of Precipitation) gridded precipitation amount dataset (Xie and Arkin, 1997). This data set is available from the National Weather Service's Climate Prediction Center at:

http://www.cpc.ncep.noaa.gov/products/precip/realtime/retro.html.

The CMAP dataset has global coverage, although it is gridded at a low resolution of 2.5°x 2.5° (~275 km). Because of the coarse resolution of the observations, we evaluated only the 45 km grid model run's precipitation. The evaluation of the 2002 MM5 precipitation estimates over Alaska is presented in Section 5.

3.6 UPPER AIR EVALUATION

Because of the regional nature of the haze problem, and the fact that most pollutant transport of interest occurs above the surface, evaluation of the MM5 upper air meteorological fields assumes particular importance in this study. Analysis of MM5 tropospheric output fields is made more difficult by the spatial and temporal resolution of the upper air sounding network, which is sparse

in time and space compared with the surface observing network. Radiosonde measurements are usually taken twice each day by an observing network of approximately 15 stations in Alaska. Upper air plotting capabilities have been developed by the Iowa Department of Natural Resources (RAOBPLOT) to compare sounding data at individual sites and times to MM5 predicted soundings. This allows for a site-by-site comparison of wind, temperature, and humidity profiles, and also provides the user the capability to diagnose and evaluate the heights, strengths, and depths of key stability regimes (e.g., boundary layer depths, inversion heights) from observational soundings and MM5 predictions. The observed soundings are derived from the Forecast Systems Laboratory (FSL)/ National Climatic Data Center (NCDC) Dataset.

As with the surface evaluation, we focus on performance in the 15 km grid. To assess whether MM5 is simulating the vertical structure of the atmosphere with reasonable accuracy in the 15 km run, we compared model temperature and dew point soundings with those from the available radiosonde stations. The stations used in our analysis were distributed among the four subdomains used in the surface evaluation, and a subset of those are shown in Figure 3-4. Additional stations were used in the initial stages of the upper air analysis, but are not mentioned in Section 6, and are omitted from Figure 3-4 for the sake of clarity.

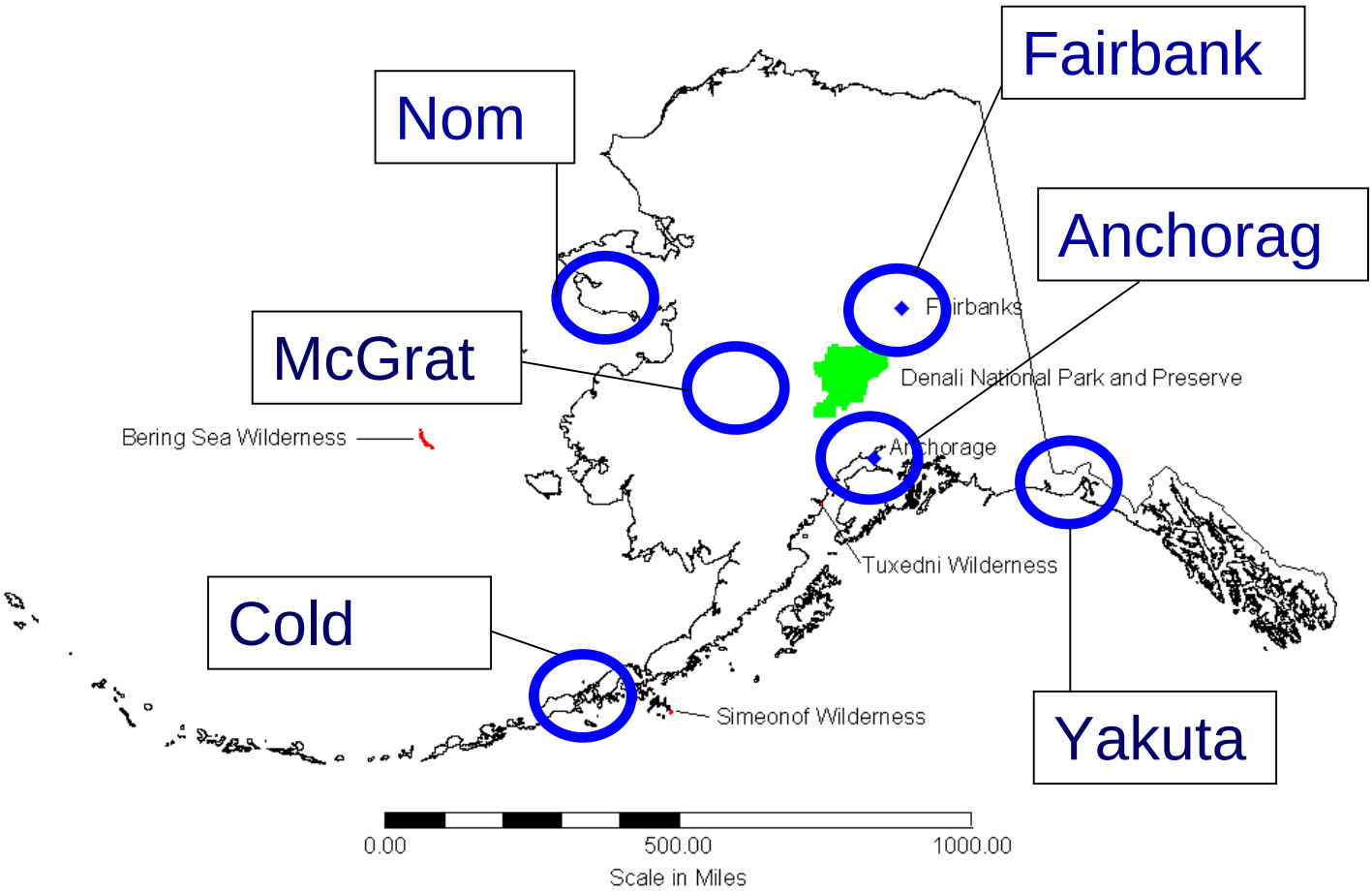

Figure 3-4. Radiosonde Stations Used in Alaska Upper Air Analysis of 15 km Domain (See Section 6).

4.0 SURFACE EVALUATION OF THE 2002 ALASKA RUN

In Section 4, we evaluate the surface performance of the Alaska 2002 MM5 run using METSTAT and surface observations from the ds472 database (see Figure 3-1).

4.1 SUBDOMAIN SURFACE FIELD METSTAT EVALUATION

The starting point for the analysis of the 2002 MM5 run was an assessment of the surface statistics for wind, temperature, and humidity using METSTAT. We focused on the 15 km domain surface statistics because this domain contains the Class I areas of primary interest for the visibility modeling effort. As described in Section 3, the 15 km domain was divided into four subdomains (Figure 3-2), and each subdomain was evaluated month-by-month to isolate differences in the model's performance over the course of the year in that region. For the purpose of organizing the analysis, we will show "soccer plots" on which are displayed average performance statistics for each run over each subdomain for a particular month. The subdomains abbreviations used in the discussion below are: NW for northwest, SW for southwest, NE for northeast, and SE for southeast. Soccer plots plot two performance statistics and compare them against a boxed goal of performance benchmarks.

Soccer plots are shown for wind speed RMSE versus wind direction error, temperature bias versus temperature error, and humidity bias versus humidity error. In each plot, a solid blue line indicates the benchmark. A data point that falls inside the box represents a model run that meets the performance benchmark. Perfect model performance is indicated by a data point at (0,0). The closer a data point is to the origin, the better the model's performance. It should be re-emphasized that the benchmarks are not used as an acceptance/rejection criteria of the MM5 model simulation. Rather, they put the MM5 model performance into perspective and allow the identification of potential problems in the MM5 fields.

In addition to the benchmark this is plotted as a boxed goal in the soccer plots, we also show the performance envelope for the WRAP 2002 annual MM5 simulation for the western subdomains (subdomains 1 through 4 in Figure 4-1). In the WRAP 2002 annual MM5 run, Kemball-Cook et al. (2004) noted significant performance differences between the eastern and western U.S., some of which likely stem from the more mountainous western terrain. For example, a mountain region whose topography is not well resolved by the model will likely have larger wind direction errors at the surface than a flatter domain. WRAP subdomains 1-4 include the mountainous terrain of the Rockies and Sierra Nevada, and provide a better performance comparison than many of the urban-scale ozone simulations in (Tesche 2001) that may not have included significant topography in the modeled region. The red envelope in the Alaska soccer plots shows the outer bound within which the WRAP subdomains were located on the WRAP runs soccer plots.

Soccer plots were generated for each month of the 2002 Alaska run, and it was found that the model performance had a strong dependence on season. To emphasize this, we show a seasonal summary soccer plot for summer (June July and August), another for winter (November, December, January and February), and a third soccer plot for the spring and fall months

(September, October, March, April, and May). These temporal divisions are arbitrary and were made based on model surface performance alone.

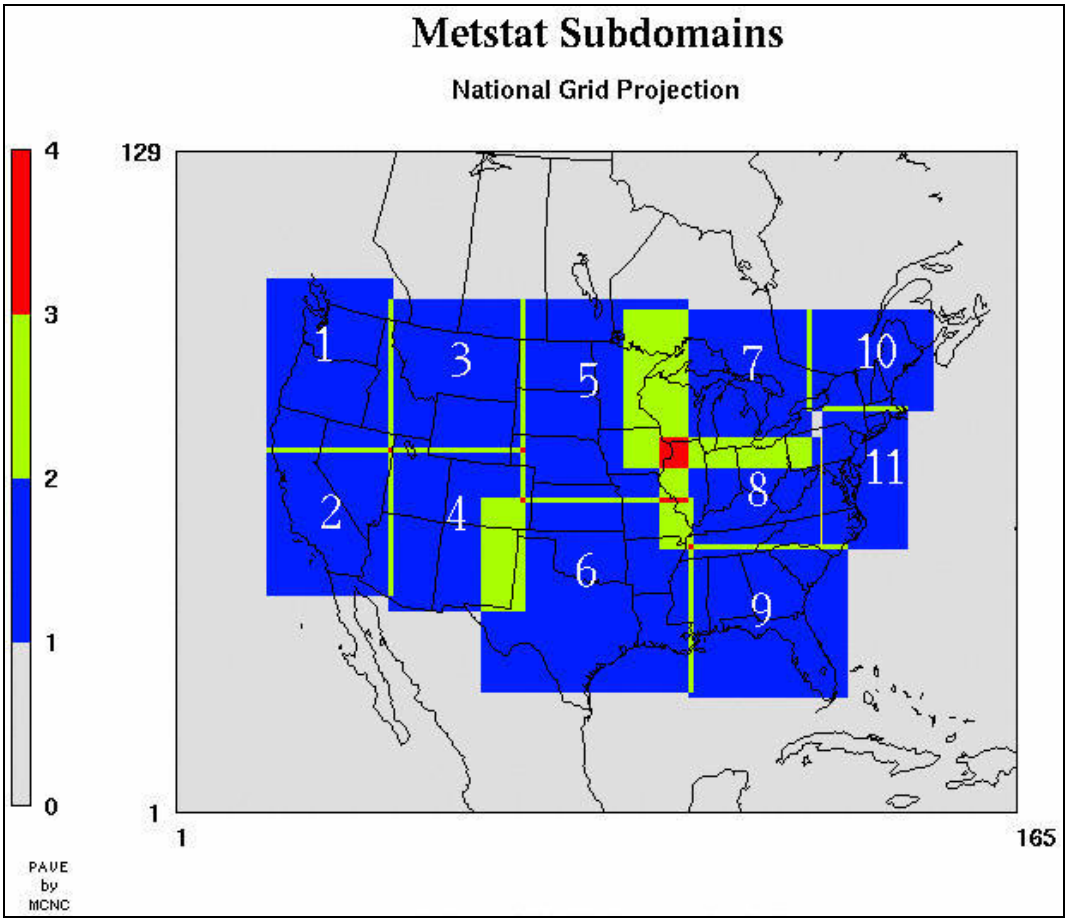

Figure 4-1. METSTAT subdomains for the WRAP 2002 MM5 performance evaluation.

Winter Temperature Soccer plots

Figure 4-2a shows the wind soccer plot for the winter months November, December, January, and February. Performance is stratified by region, with the SW and NW subdomains falling within the benchmark for wind direction error and NE and SE falling outside. The SE and NE subdomains are the most mountainous of the four, and it is reasonable that the wind direction will be less accurate there, as the topography is not as well resolved as in lower-lying regions of Alaska, especially using the coarse 15 km grid resolution. The SE, NE, and NW subdomains were comparable in wind speed RMSE, and the SW subdomain performed slightly worse. For all four months, all subdomains lie within the WRAP western U.S. performance envelope. In determining wind performance, the subdomain location was more important than the month.

Figure 4-2b shows the temperature soccer plot for the winter months. All subdomains fall outside the performance benchmark for temperature error for all four months. For bias, most subdomains fall outside the benchmark. The NE subdomain has a warm bias (except in November, when it has a small cold bias), but the other three subdomains have a cold bias. The

SW subdomain had the best performance in terms of error, and SE had the smallest bias. Overall, performance was best in the SW domain. Although all subdomains fell outside the benchmark, only the SE subdomain (the most mountainous of the four) falls outside the WRAP performance envelope.

Figure 4-2c shows the humidity soccer plot for the winter months. There is not much difference in performance among subdomains, with all subdomains showing a small wet bias. There is a slight improvement in performance as winter progresses from November to February. Note that one reason for the good humidity performance is that the absolute humidity is very low during the cold, dry Alaskan winter. The benchmarks were calibrated based on urban air quality simulations performed over the U.S. mainland during summer, and are based on regions with higher humidity. Therefore, the benchmarks are not a particularly stringent test for humidity performance in winter in Alaska.

We show two month-long sets of observed and modeled time series to illustrate winter performance. The January NW hourly temperature time series (Figure 4-3) is typical of winter MM5 performance, and shows reasonable agreement throughout the month, albeit with a slight cold bias. Note the absence of a diurnal temperature cycle due to the lack of insolation in the middle of Alaskan winter. For NW (Figure 4-4), the humidity time series shows a wet bias, which may in part explain the cold bias. Having excess water (frozen or liquid) at the surface affects the partitioning of surface energy, diverting an excess of energy to latent rather than sensible heating. The general trend follows the observations, but with an offset that dwindles as the month progresses. The wind speed time series (Figure 4-5) shows a consistent low wind speed bias and the wind direction time series (Figure 4-6) shows good agreement, with a small positive wind direction bias.

Next, we examine the February time series for the NE domain. Performance in this subdomain was problematic for MM5. Figures 4-7 and 4-8 show the modeled and observed wind speed and direction time series. The wind speed has a consistent negative bias, and the wind direction has an overall positive bias. During the period from 2/14-2/22, there are a series of large changes in wind direction that are not well simulated by MM5. The temperature and humidity time series (Figures 4-9 and 4-10, respectively) also show significant errors during this time. There is a wet bias in the humidity and an overall warm bias that arises because MM5 simulates the peak temperature of each day but not the diurnal cycle in temperature that appears in the observations. MM5 is unable to capture the diurnal cycle in temperature or humidity during the month of February. The observations show a pronounced diurnal cycle, but the MM5 temperature and humidity time series do not develop a diurnal cycle until approximately February 20. The warm bias shown on the soccer plot is primarily caused by the lack of a nighttime drop in the surface temperature. The wet bias in the humidity soccer plot for February is apparent in Figure 4-10.

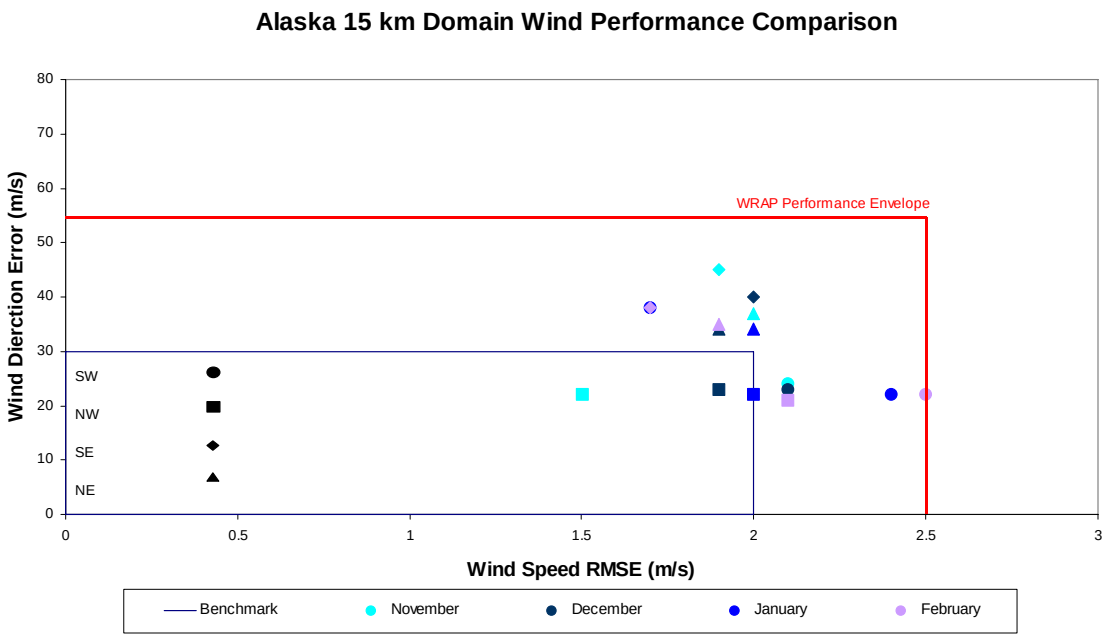

Figure 4-2a. Winter wind soccer plot for four Alaska subregions.

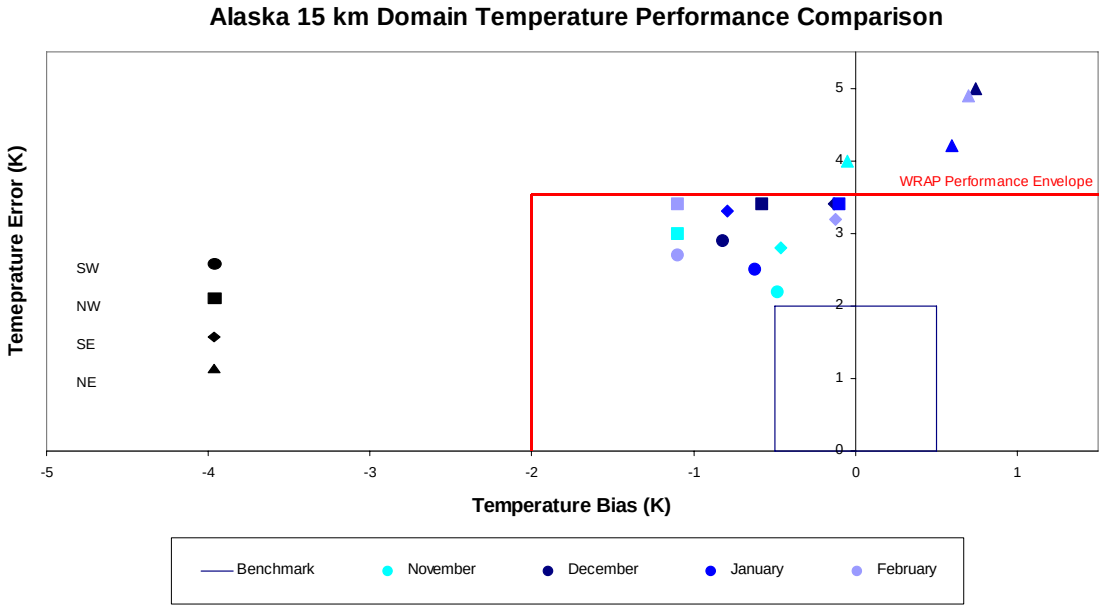

Figure 4-2b. Winter temperature soccer plot for four Alaska subregions.

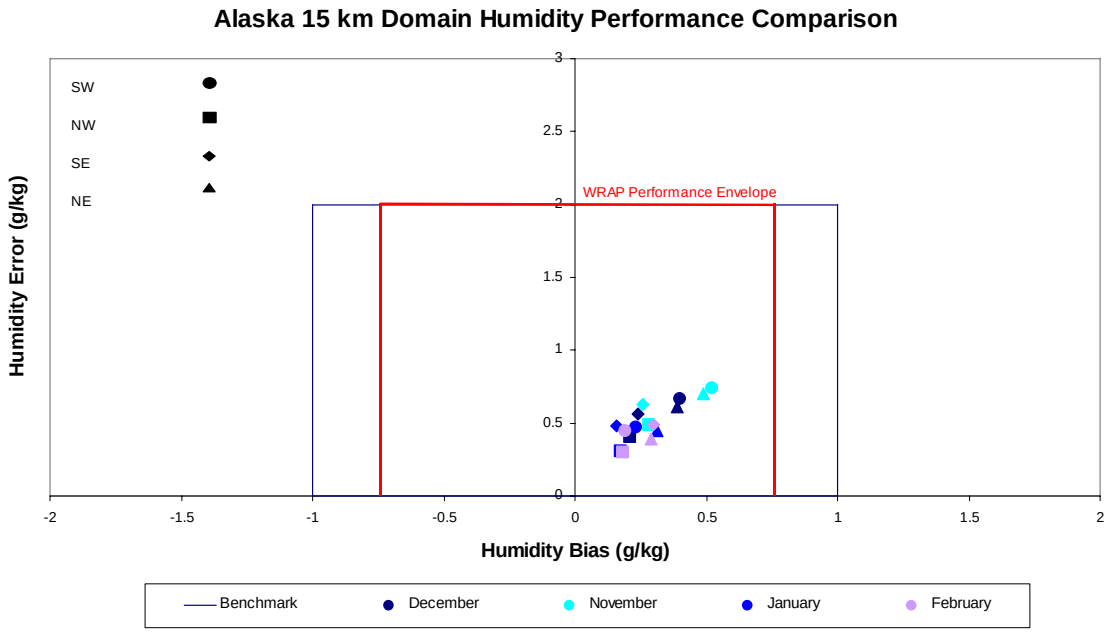

Figure 4-2c. Winter humidity soccer plot for four Alaska subregions.

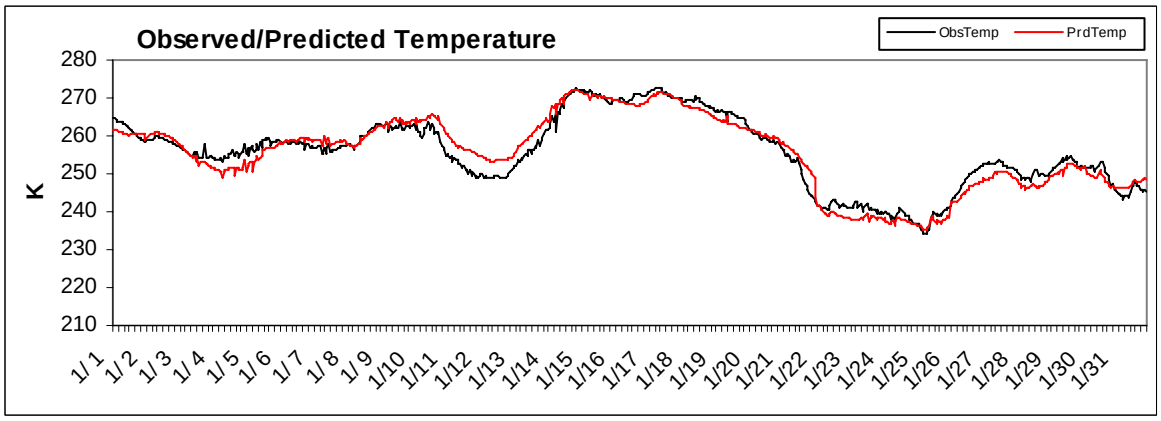

Figure 4-3. January NW Alaska subregion temperature hourly time series.

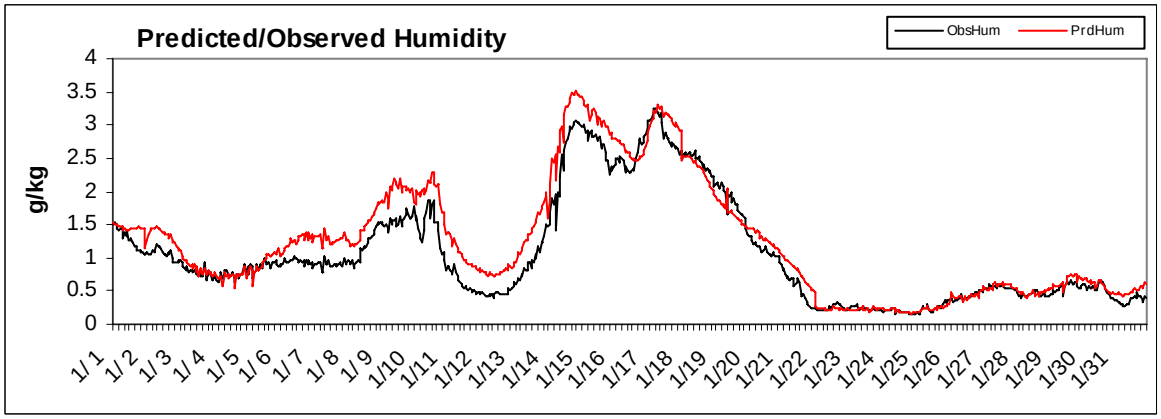

Figure 4-4. January NW Alaska subregion humidity hourly time series.

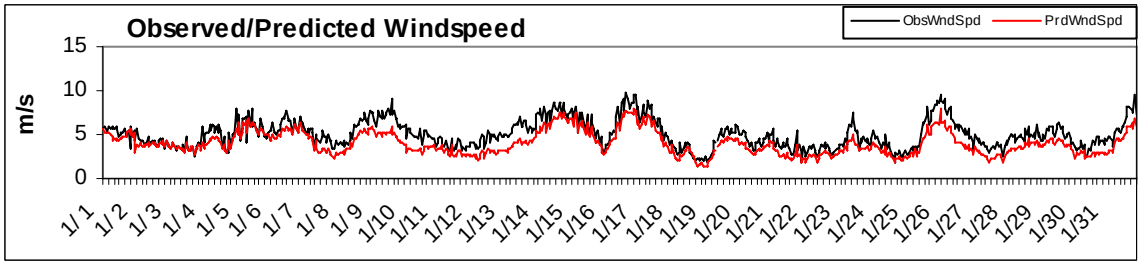

Figure 4-5. January NW Alaska subregion wind speed hourly time series.

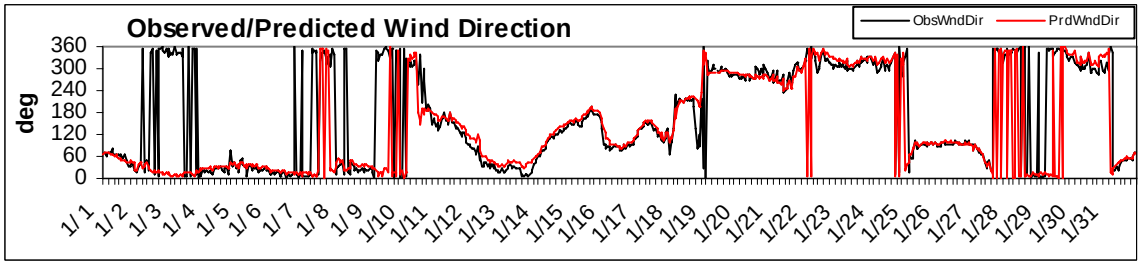

Figure 4-6. January NW Alaska subregion wind eirection hourly times series.

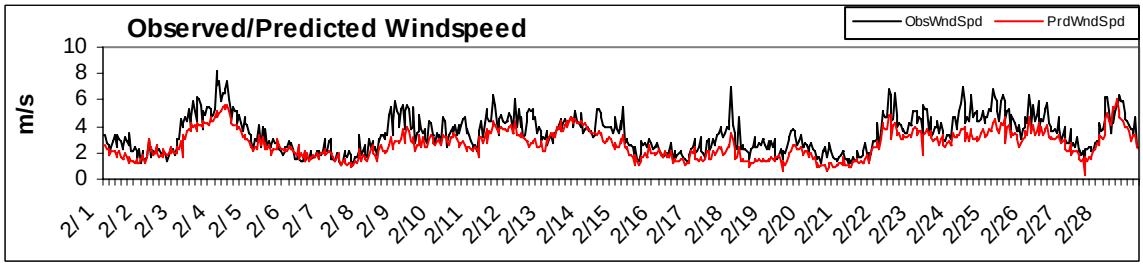

Figure 4-7. February NE Alaska subregion wind speed hourly time series.

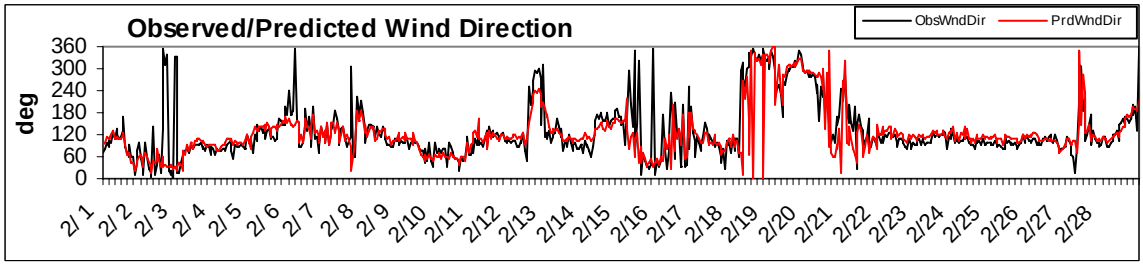

Figure 4-8. February NE Alaska subregion wind direction hourly time series.

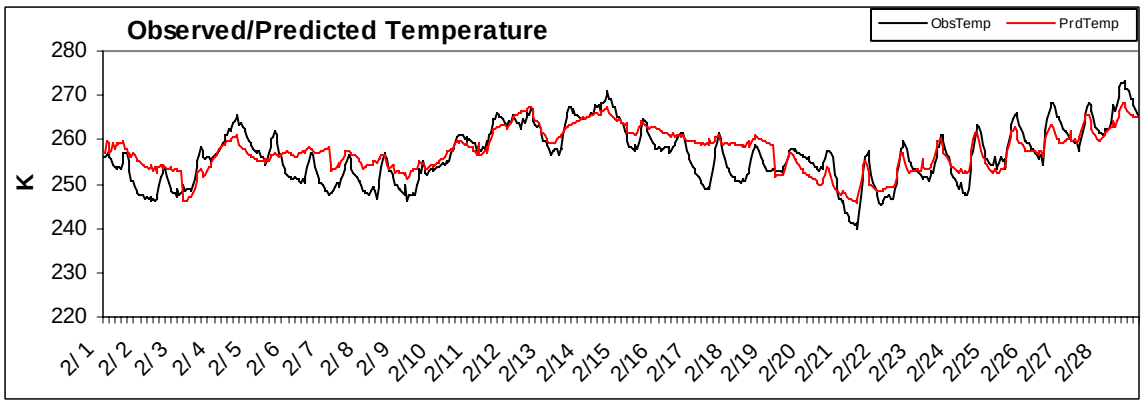

Figure 4-9. February NE Alaska subregion temperature hourly time series.

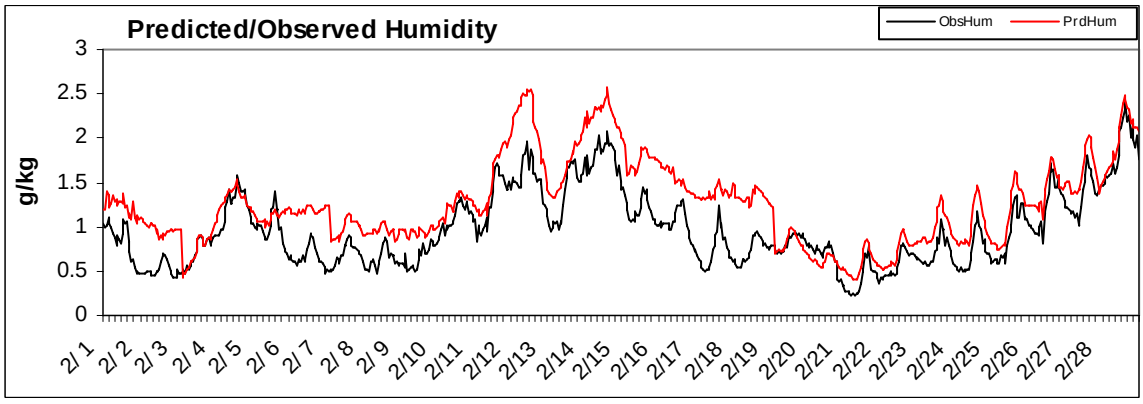

Figure 4-10. February NE Alaska subregion humidity hourly time series.

The wind soccer plot for the summer months is shown in Figure 4-11a. In the summer, overall performance improved relative to winter, with general reductions in both the wind direction error and the wind speed RMSE. As in winter, the NE and SE subdomains had larger wind direction errors than the less mountainous NW and SW subdomains. The summer wind performance falls within the benchmark for the NW and SW subdomains, and just outside of it for the NE and SE subdomains. All subdomains for all months fall well within the WRAP performance envelope, showing that surface wind is well simulated in summer.

The temperature soccer plot for the summer months is shown in Figure 4-11b. There is a pronounced cold bias during July and August that is strongest in the SE subdomain. In June, the SE and NE subdomains have a cold bias, while the SW and NW subdomains have a warm bias. Compared to winter, the summer temperature error was generally lower. This may be due to the more pronounced diurnal cycle or because of the use of the more detailed land surface model in summer. Performance in the NW and SW subdomains was better than in the SE or NE subdomains. This is reasonable given the lower terrain of NW and SW, which also showed the best temperature performance of all subdomains in winter. SE had the largest bias during July and August. Figure 4-11c shows the time series for the SE subdomain for July. The daily temperature maximum is fairly well predicted, but the daily minimum is too low. This is a different source of cold bias than we saw above for the winter (Figure 4-3). Although all subdomains and months fell outside the performance benchmark during summer, they were all within the WRAP performance envelope except for July and August for the SE subdomain.

Figure 4-11d shows the humidity soccer plot for the summer months. There is a general wet bias, which is strongest during the month of June. The wet bias is most pronounced in the NW and NE subdomains. The wet bias in summer is larger than in winter, with the NE and NW subdomains lying outside the benchmark, and NE outside the WRAP performance envelope in June. This is due in part to the higher summer humidity. It may also be due to the presence of sea ice and/or snow lingering in the northern part of the 15 km domain into June. During the summer months, the POLAR option and the sea ice are turned off, and this may lead to errors in surface fluxes in areas that remain covered in ice or snow.

Figure 4-12a shows the wind soccer plot for the spring and fall months. The division by geographic region is striking. The SE subdomain lies outside the benchmark for wind direction error for all months. Except for the September NE subdomain, all other subdomains lie within the benchmark for wind direction error. All of the months for a particular subdomain tend to lie in a group. Overall, NW is the best performing subdomain; SE has the largest wind direction error, and SW has the largest wind speed RMSE. Within each subdomain, October tended to be the worst-performing month (3 out of 4 subdomains) in spring and fall. This is when the POLAR option transition occurred and also when the atmosphere's lower boundary condition is changing rapidly due to the formation of sea ice.

Figure 4-12b shows the temperature soccer plot for the fall and spring months. This figure shows a strong cold bias during these months. The bias is most pronounced in the SE and NE subdomains, and during the months of May, April, and March. The SW and NW subdomains fared best, generally falling within the WRAP performance envelope. The months with the worst performance are March, April, and May. The Fall/Spring transition seasons have a larger cold bias than the summer and winter seasons. This suggests that the timing of the switch on/off of the POLAR option may be problematic. It is difficult to determine when to perform this

switch over as the sea ice creeps southward or retreats northward. At any given time, there will be inevitably be parts of the domain for which the POLAR configuration is appropriate, and parts for which it is not. For instance, in Figure 2-2, part of the domain has sea ice in March, and part does not. Part of the domain will have snow cover, and part will not.

Figure 4-12c shows the humidity soccer plot for the spring and fall months. All subdomains for all months show a wet bias except SE in September. In summary, for spring and fall, nearly all subdomains show a wet bias and all show a cold bias. The cold, wet bias is particularly extreme in March and May, and we now turn our attention to these two months.

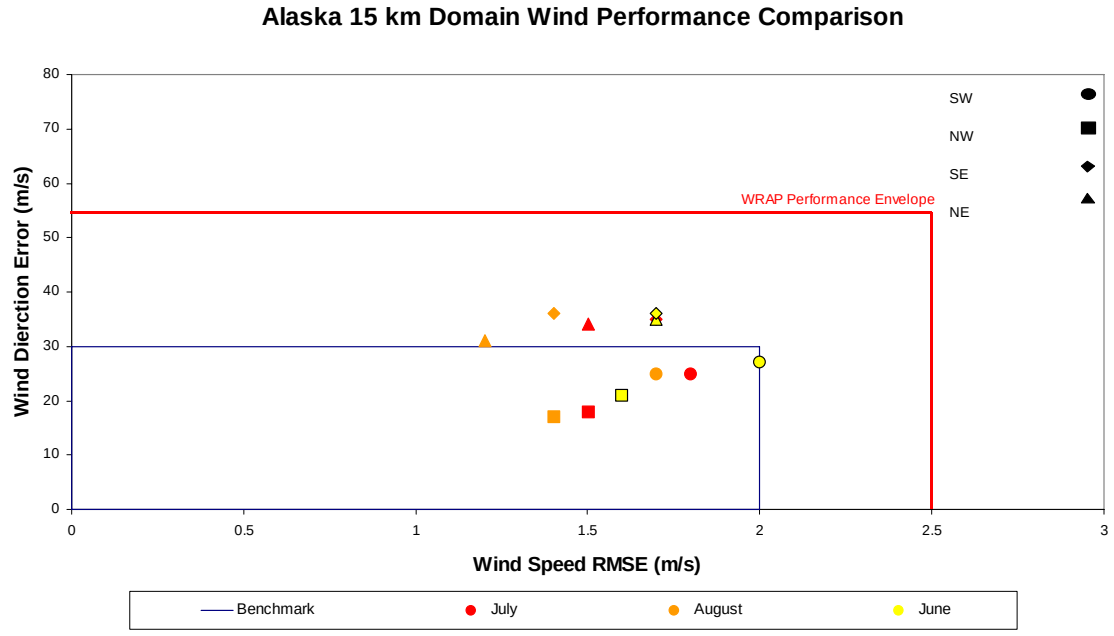

Figure 4-11a. Summer wind soccer plot for four Alaska subregions.

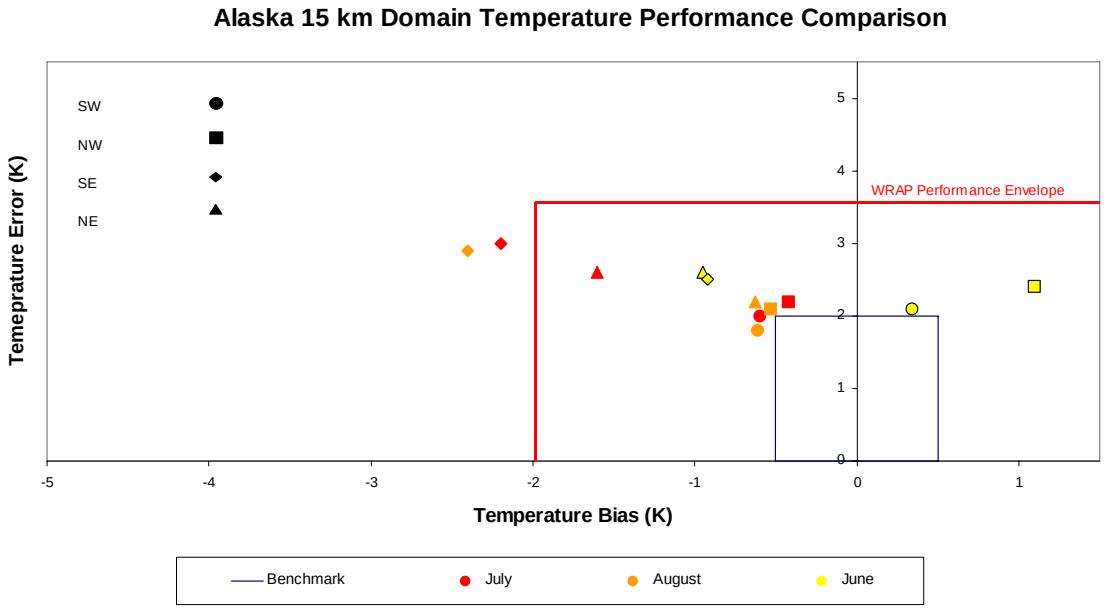

Figure 4-11b. Summer temperature soccer plot for four Alaska subregions.

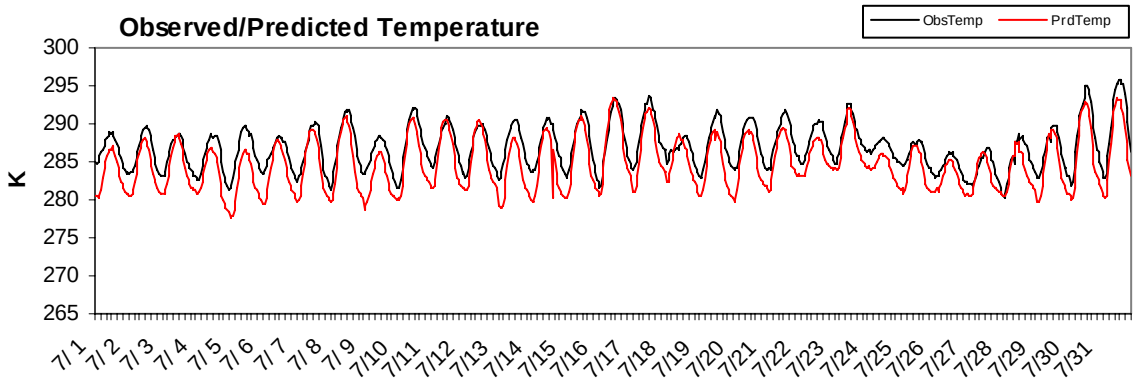

Figure 4-11c. July SE Alaska subregion temperature hourly time series.

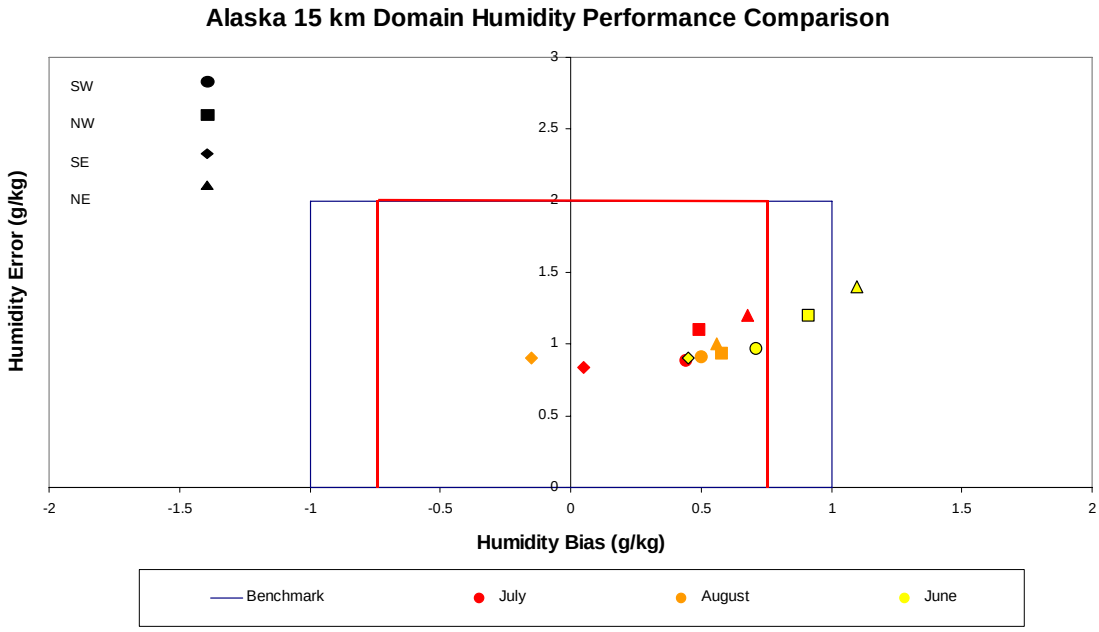

Figure 4-11d. Summer humidity soccer plot for four Alaska subregions.

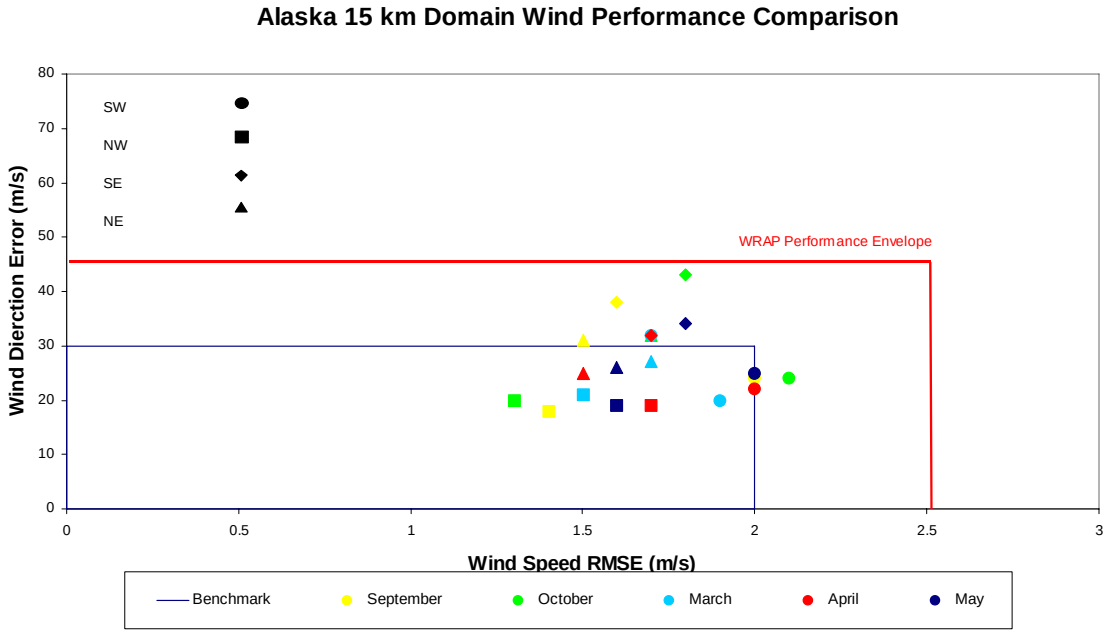

Figure 4-12a. Spring/Fall wind soccer plot for four Alaska subregions.

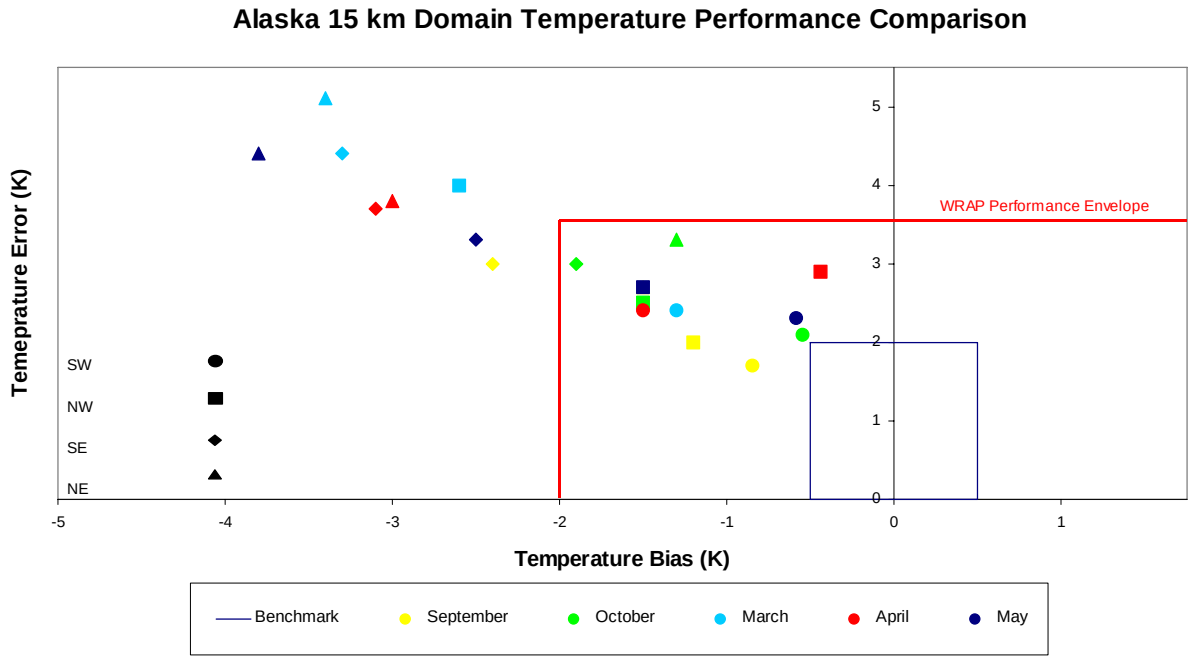

Figure 4-12b. Spring/Fall temperature soccer plot for four Alaska subregions.

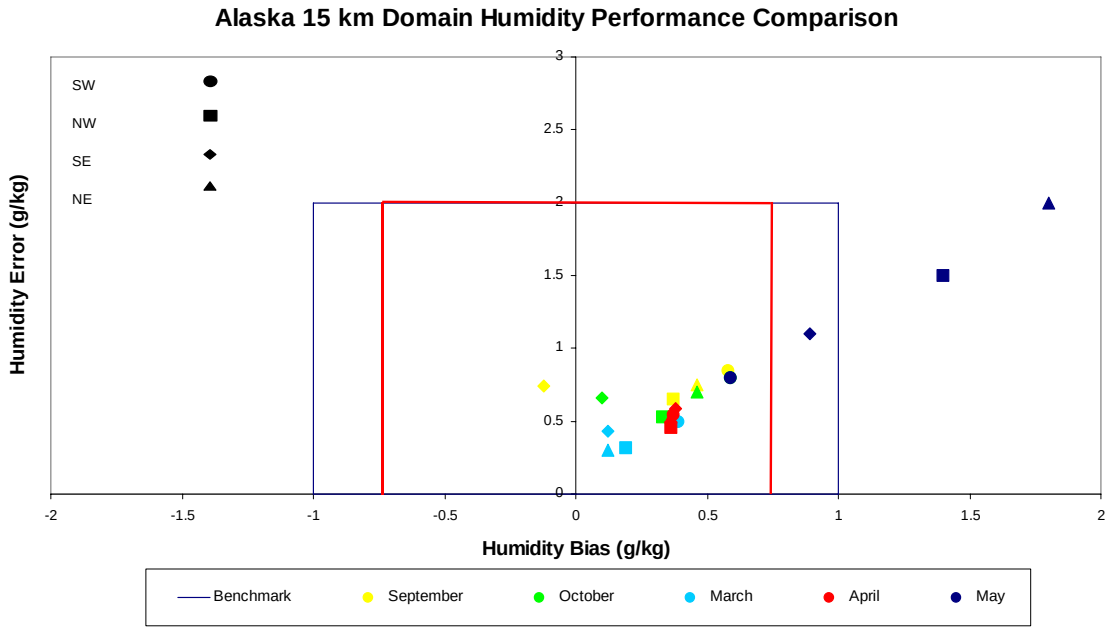

Figure 4-12c. Spring/Fall humidity soccer plot for four Alaska subregions.

Figure 4-13 shows the hourly time series for temperature for March for the NE subdomain. Throughout the course of the month, the model consistently underestimates the daily maximum temperature. This problem is the primary cause of the cold bias, and is particularly evident during the 3/21-3/26 time period. The wind direction shows a large error near these times (Figure 4-14). Figure 4-15 shows the corresponding time series for humidity.

May is the other month with outlying subdomains on the fall/spring temperature soccer plot. Throughout the course of the month, the model consistently underestimates the daily maximum temperature. This problem is likely related to the cold bias, and is particularly evident during the 5/17-5/28 time period. The model shows a steady increase in humidity superimposed on the diurnal cycle from 5/11 to 5/26. This increase does not exist in the observations. The diurnal cycle in humidity is too pronounced in the model run, and there are sudden large decreases in humidity at the same time as the sudden drops in temperature. The cause of these temperature/humidity excursions is unclear, and there is no corresponding signal in the wind time series. The combination of a spurious moistening trend and a diurnal cycle in humidity that is too strong may be the cause of the cold bias in temperature. When the ground is unrealistically wet, energy that should go into sensible heating of the surface is instead diverted into evaporation of the excess moisture, and the temperature is kept artificially low. An important question for further study is why the amplitude of the diurnal cycle in humidity is too large. This behavior is seen in April and May (see, for example, Figures 4-17 and 4-18), but not in other seasons. Inspection of the corresponding wind direction and wind speed time series (Figures 4-19 and 4-20) does not show a consistent bias that might explain excessive moistening through mishandling of advection. The POLAR option remains on until May 30, and it is

possible that May would be better simulated without the POLAR option; this would allow the use of the better performing OSU LSM.

In fall, temperature performance was better than in spring, and the spurious diurnal cycle in humidity was absent. All subdomains fell within the humidity performance benchmark. The worst performing subdomain for temperature in fall was the SE subdomain in October and September.

Figure 4-21 shows the SE temperature time series for September. There is a consistent cold bias, with the entire modeled time series translated downward from the observed time series. The MM5 diurnal cycle is weaker than the observed diurnal cycle, with maxima uniformly too low. The humidity time series (Figure 4-22) does not show a corresponding bias, and instead shows a reasonable simulation of the observed time series. Therefore, the temperature bias is not correlated with a bias in the humidity. Neither the wind speed nor the wind direction time series (Figures 4-23a and 4-23b) offer much insight into the source of the cold bias.

During the first half of October, the temperature time series (Figure 4-24) shows a consistent cold bias that is similar to that seen in September (Figure 4-21). The diurnal temperature cycle is somewhat weaker than observed, but the model captures much of the variation in the observations, albeit with a cold bias. During the second half of the month, however, the modeled variability is much smaller than the observed variability. Although the modeled and observed means are similar, the model misses the diurnal cycle. This mid-month change in the character of the modeled time series is likely due to the switch on of the POLAR option. The humidity time series shows a similar change in behavior with the switch to the POLAR configuration. After the POLAR option is switched on, the modeled low frequency variability is more or less correct but it misses much of power at the high frequencies (~1 day or less). There is no signal in the humidity (i.e. a wet bias) that correlated well enough with the temperature time series to explain the cold bias, and this is different from what happened in the spring. The reason for the fall temperature bias is unclear.

We now examine the timing of the switch to the POLAR option. Figures 4-28 through 4-31 show the temperature time series for the SE domain for September, October, November and December. In September and the first half of October, the model does a reasonable job of simulating the observed variability, although there is a pronounced cold bias. After the switch to the POLAR configuration, the modeled variability decreases markedly. The signal of the modeled diurnal cycle in temperature is strongly damped, although a diurnal cycle still exists in the observations. As we move from October to December, the observed diurnal cycle becomes weaker as the daily peak in the intensity of solar radiation diminishes, and the modeled and observed temperature time series come into closer agreement. This can be seen on the soccer plot Figure 4-32, which shows how the SE subdomain temperature performance varies over the course of 2002.

In terms of temperature bias, MM5 performs best in SE during winter, when the POLAR option is on and is most clearly applicable over the entire domain. Performance deteriorates suddenly in March, and remains poor through May. There is then a general improvement in performance over the course of the year as summer passes and winter returns.

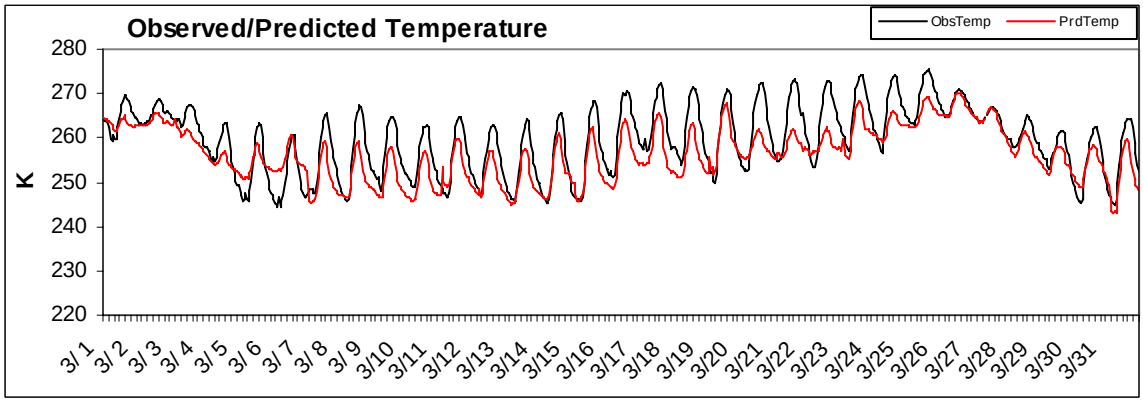

Figure 4-13. NE Alaska subregion March temperature hourly time series.

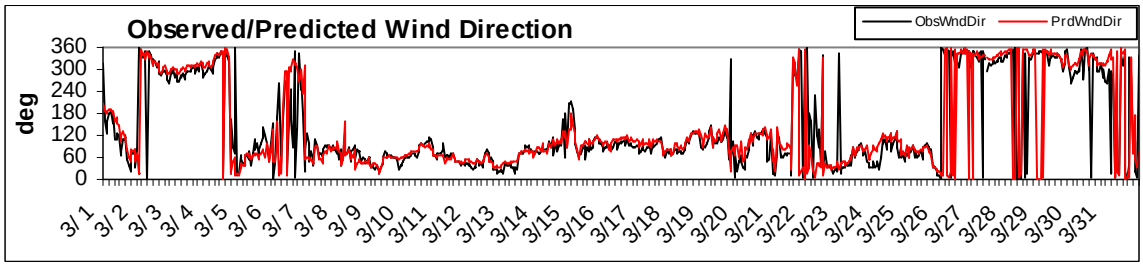

Figure 4-14. NE Alaska subregion March wind direction hourly time sSeries.

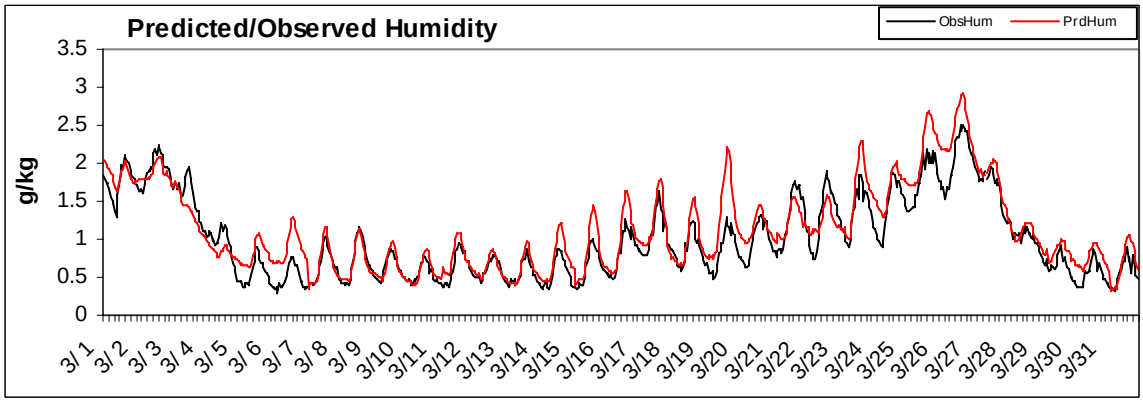

Figure 4-15. NE Alaska subregion March humidity hourly time series.

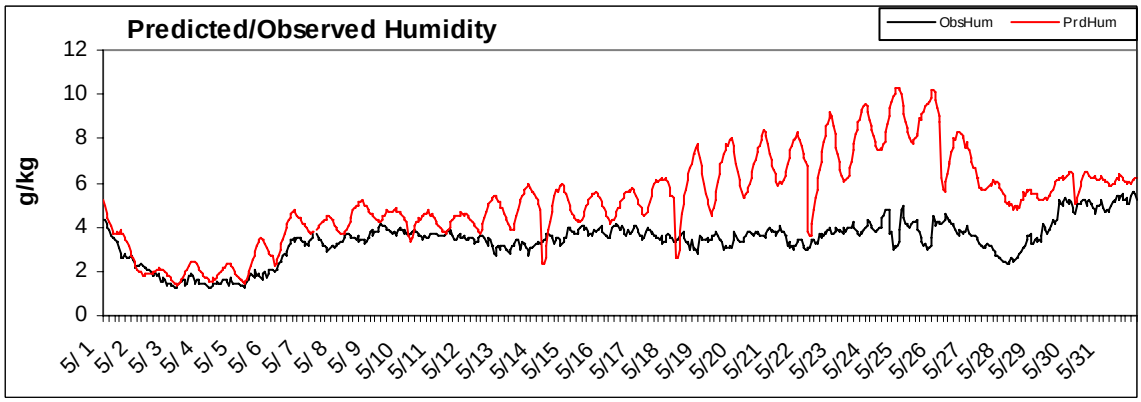

Figure 4-16. NE Alaska subregion May temperature hourly time series.

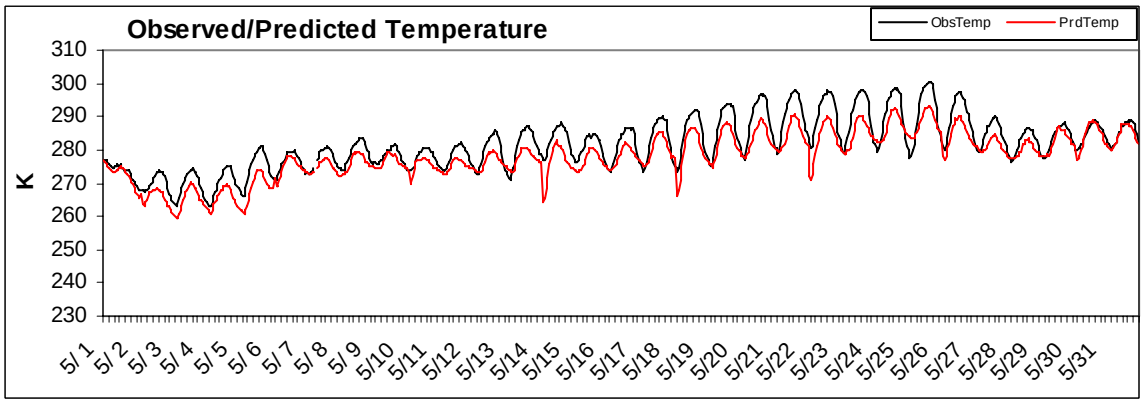

Figure 4-17. NE Alaska subregion May humidity hourly time series.

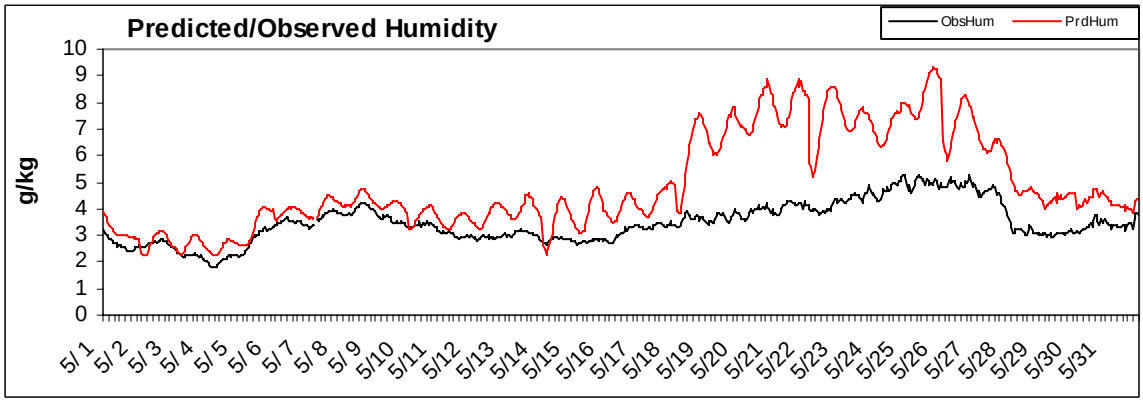

Figure 4-18. NW Alaska subregion May humidity hourly time series.

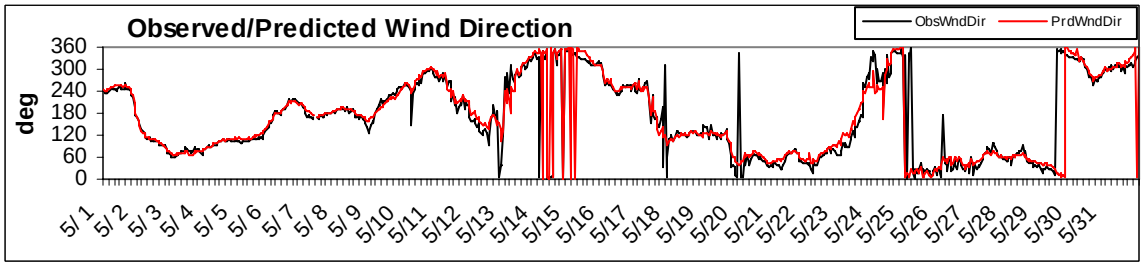

Figure 4-19. NW Alaska subregion May wind direction hourly time series.

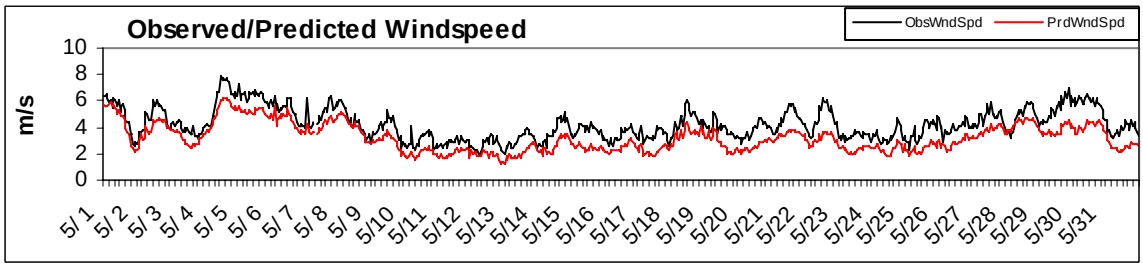

Figure 4-20. NW Alaska subregion May wind speed hourly time series.

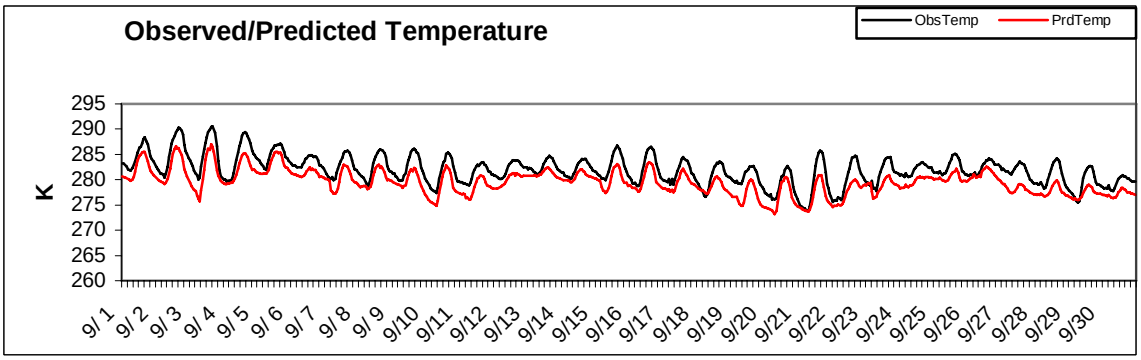

Figure 4-21. SE Alaska subregion September temperature hourly time series.

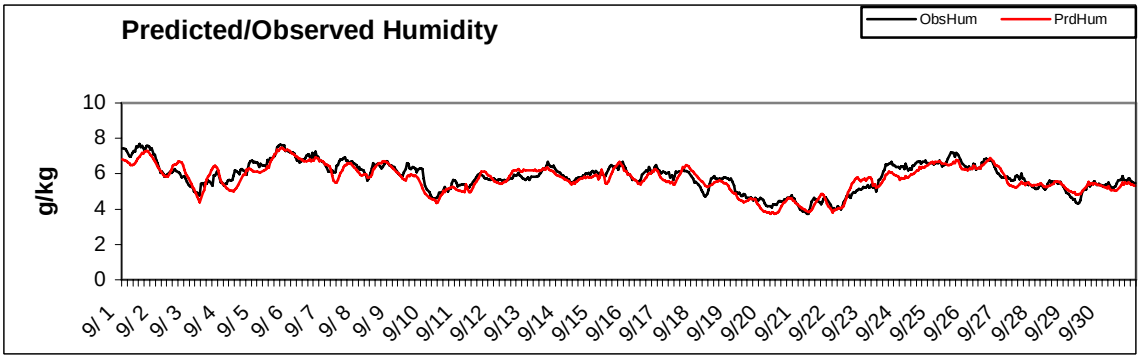

Figure 4-22. SE Alaska subregion September humidity hourly time series.

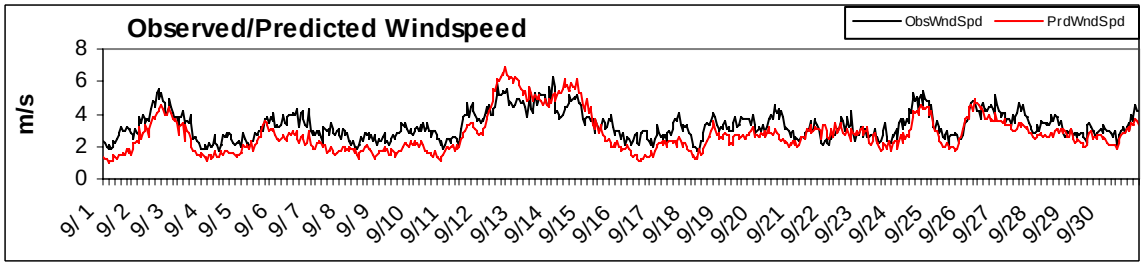

Figure 4-23a. SE Alaska subregion September wind speed hourly time series.

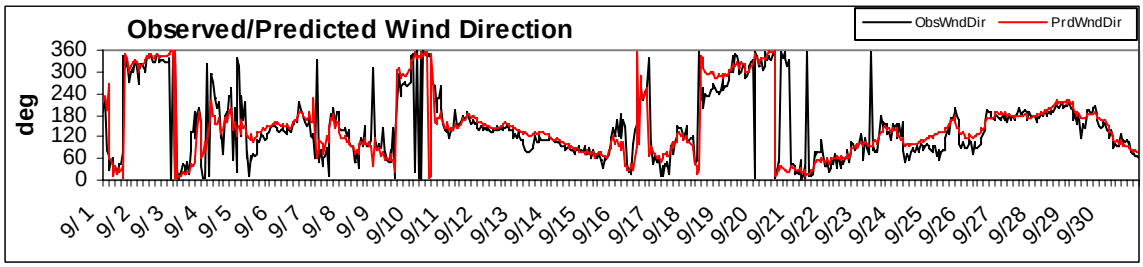

Figure 4-23b. SE Alaska subregion September wind direction hourly time series.

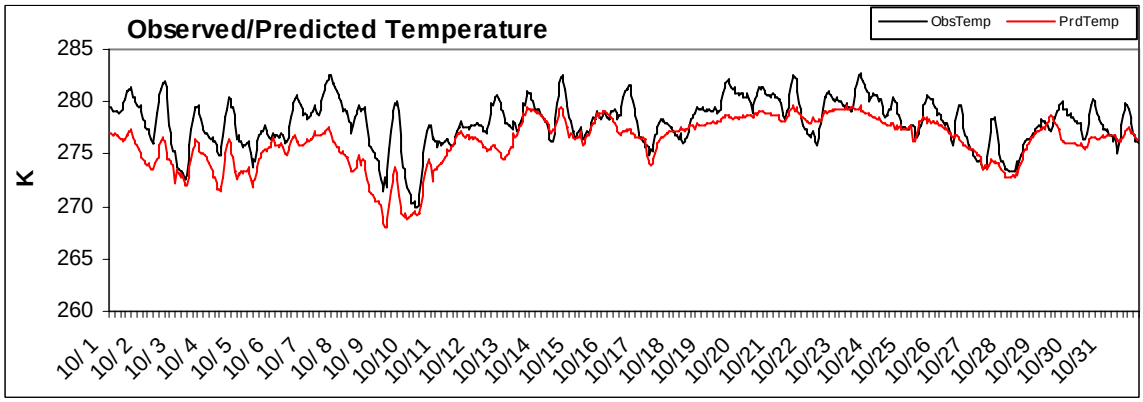

Figure 4-24. SE Alaska subregion October temperature hourly time series.

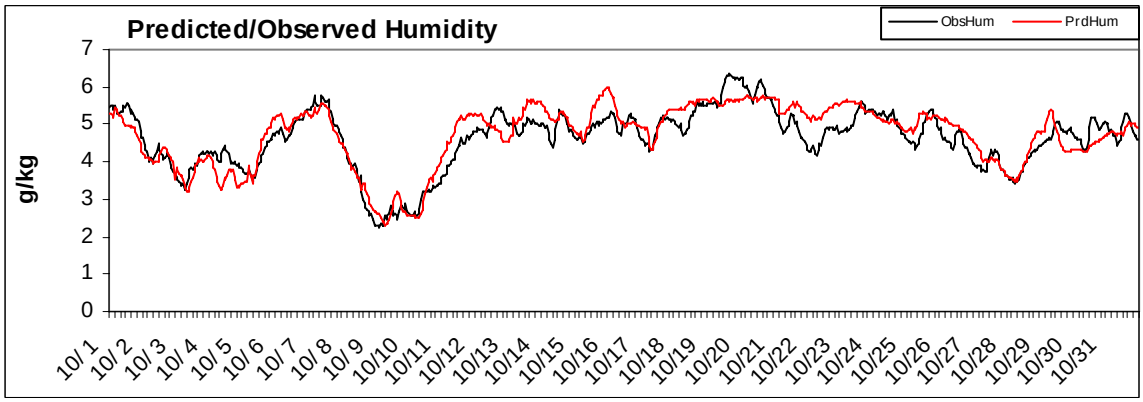

Figure 4-25. SE Alaska subregion October humidity hourly time series.

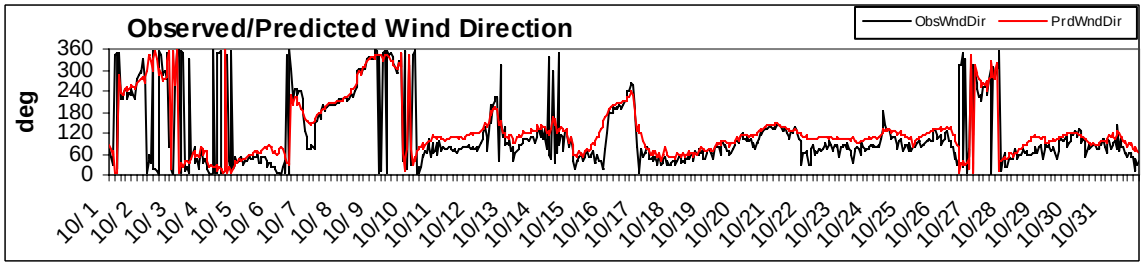

Figure 4-26. SE Alaska subregion October wind direction hourly time series.

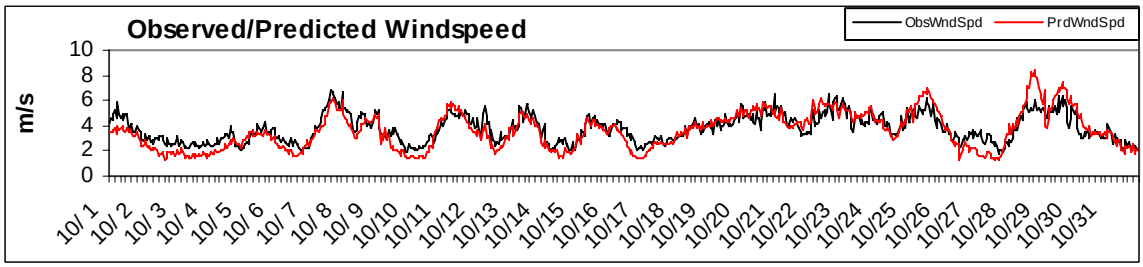

Figure 4-27. SE Alaska subregion October wind speed hourly time series.

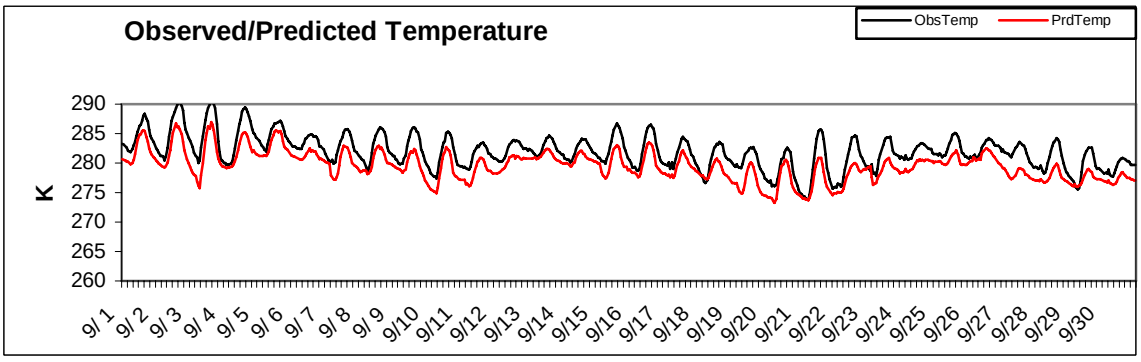

Figure 4-28. SE Alaska subregion September temperature hourly time series.

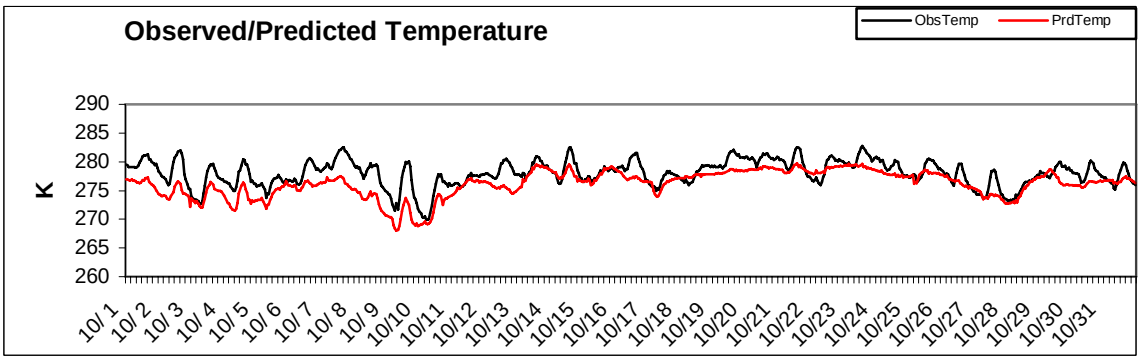

Figure 4-29. SE Alaska subregion October temperature hourly time series.

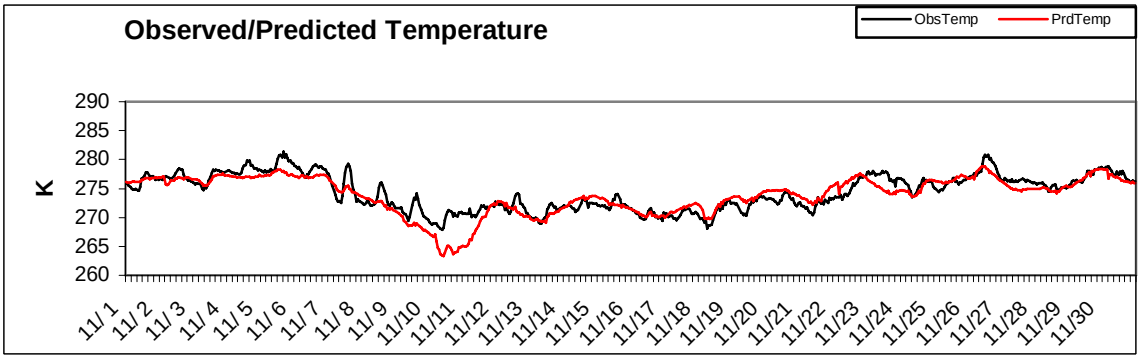

Figure 4-30. SE Alaska subregion November temperature hourly time series.

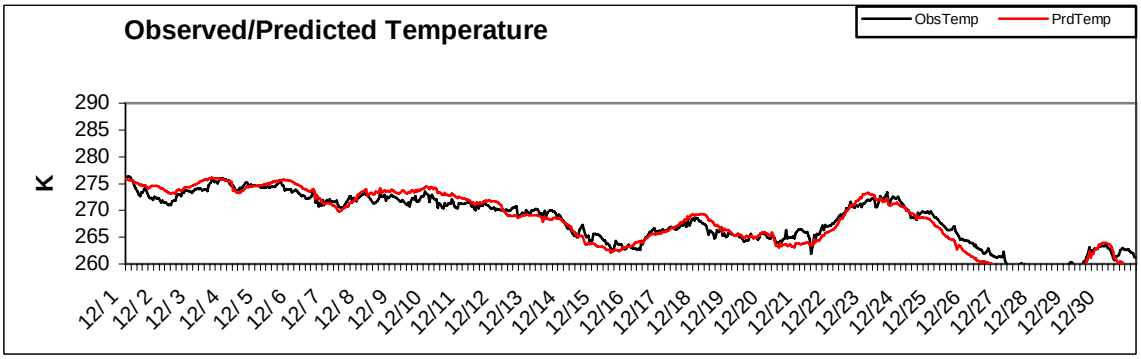

Figure 4-31. SE Alaska subregion December temperature hourly time series.

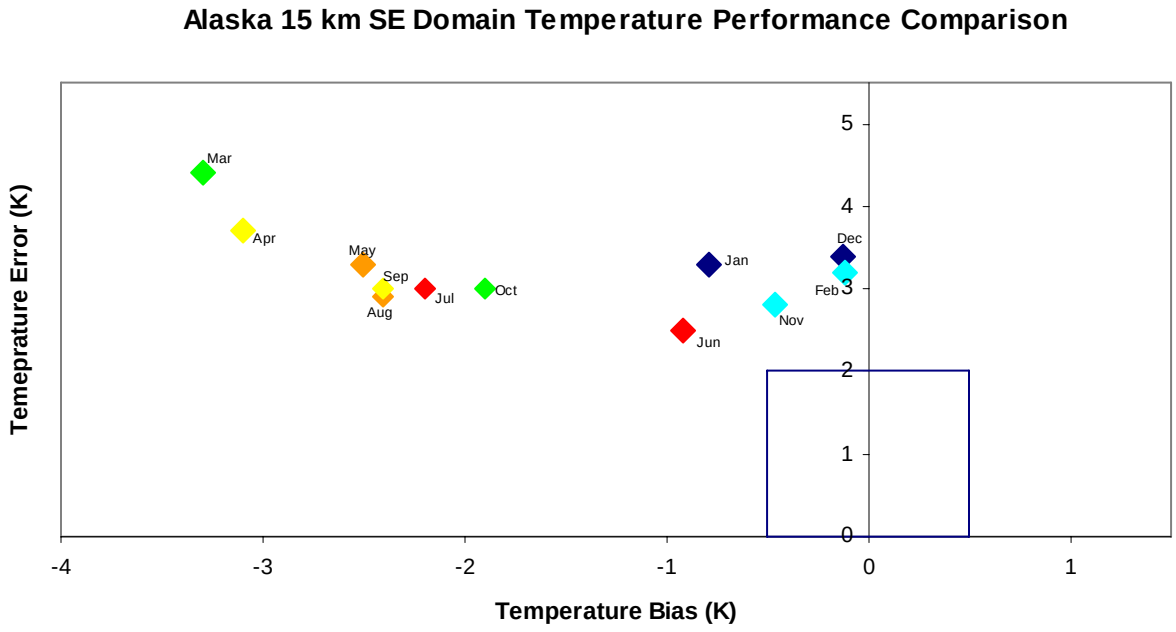

Figure 4-32. Temperature soccer plot for SE Alaska subregion subdomain.

Summary of the Annual Cycle in MM5 Surface Performance

- Overall, MM5 performance was reasonably good given the challenges of modeling Alaska.
- For surface wind, the Alaska 15 km run was within the performance envelope of the WRAP 2002 36 km Annual Run western continental U.S. subdomains.
- For surface winds, the more mountainous subdomains NE and SE had a larger wind direction error (generally outside the benchmark) than the NW and SW subdomains (generally within the benchmark) throughout the annual cycle.
- Examination of wind speed time series showed a consistent low wind speed bias similar to what was seen in the WRAP 2002 36 km Annual Run western U.S. subdomains.
- For surface winds, the best performance occurred during summer.
- For temperature and humidity, the best surface performance came during the winter months of November-February.
- The temperature bias was smallest during the winter months, but the temperature error was smallest during the summer months. The larger winter error is related to MM5's difficulty in reproducing the small amplitude of the observed diurnal cycle. In summer, when a more detailed land surface model is used, and the diurnal cycle of insolation has a larger amplitude, the modeled temperature time series tracked the observed time series more closely and the temperature error was generally smaller than in winter.
- Surface performance showed a general cold, wet bias, which was most pronounced during spring and fall.
- Fall performance was better than spring performance.
- A spurious diurnal cycle in humidity appeared in spring, and may be related to the large cold biases seen during March-May.
- Transition seasons of fall and spring were most difficult for MM5 to simulate and this may be related to the changing lower boundary condition, and the timing of the switch over to the POLAR configuration.

5.0 PRECIPITATION EVALUATION FOR THE ALASKA 2002 ANNUAL RUN

In this section, we evaluate the precipitation fields in the Alaska 2002 MM5 run. We examine the annual cycle in the monthly precipitation totals on the MM5 45 km grid and compare them to observed monthly precipitation totals. The observed precipitation rates were generated using the CMAP (Climate Prediction Center Merged Analysis of Precipitation) gridded precipitation amount dataset. This data set is available from the National Weather Service's Climate Prediction Center at:

http://www.cdc.noaa.gov/cdc/ data.cmap.html.

The CMAP dataset (Xie and Arkin, 1997) has global coverage, and is gridded at a resolution of 2.5°x 2.5° (~275 km). There are some regions of missing data near the North Pole, and these are left blank in Figures 5-1 and 5-2. Higher resolution data sets covering the Alaska domain were not readily available for the 2002 time period. Because the observed precipitation is gridded at a relatively low resolution, we limit our analysis to the 45 km domain. The 15 km domain will likely show finer structure in the precipitation fields related to the topography, but the observations cannot resolve these fine-scale features. A comparison of monthly precipitation amounts on the 45 and 15 km grids (not shown), showed that, for resolved and convective precipitation, the patterns were similar but the 15 km maxima were more intense. One possible reason for this is the more accurate treatment of orography at 15 km. The height of the tallest mountain in the 15 km domain is 3048 m when viewed at a resolution of 15 km. When seen on the 45 km grid, the height of this peak drops to 2783 m, or a loss of nearly 10% of the height of the mountain.

Based on the results of the surface performance, we will divide the analysis into winter (November, December, January, and February), summer (June, July, August) and spring (March, April, May) and fall (September, October).

Winter

The observations for the November-February time period (Figures 5-1 and 5-2) show that, during winter, the most intense precipitation feature in the modeling domain is the maximum associated with the deep Aleutian low centered southeast of the Aleutian Islands and out of the modeled region. The Pacific high is weak and lies far south of the domain during the winter months. Another precipitation maximum lies along the west coast of North America. The winter rainfall along the southern coast of Alaska reaches a maximum in November/December and then tapers off during January/February.

Meanwhile, in northern and central Alaska, there is relatively little precipitation compared to the southern coast. There are several reasons for this. First, the air is cold and dry. The surface flow at the coast in winter is southwesterly along that section of the North American coast that is getting a large amount of rainfall because it is at the eastern end of the Aleutian Low. Most of Alaska is north of this circulation from the Aleutian low and experiences general northeasterly flow during the December-January-February period. Therefore, cold, dry Arctic air is transported there in contract to the moist warm marine air that arrives at the coast. The Aleutian low is too far south of central Alaska and the storm track steers most of the systems south. In

addition, the mountain ranges that line the southeastern coast of Alaska produce orographic rainfall, depleting moisture from air heading inland.

During the winter months, MM5 does a good job of simulating the evolution and intensity of the precipitation field. It simulates the maxima along the coast of western North America and the southeastern coast of Alaska. The coastal precipitation maxima in MM5 extends further west into the Pacific than in the observations in November and December, but the overall shape is generally well-predicted and the accuracy of the observed precipitation over the ocean is questionable. MM5 shows a relative minimum over the Aleutian Islands and to their northwest, as is seen in the observations. It also captures the relative maximum extending northward into the Bering Strait during December. The maxima are more intense in the model output than in the observations but this may be an artifact of the coarser resolution of the observations (~275 km) than the model (45 lm).

One performance problem during the winter is that the precipitation over the Alaskan interior (where the 15 km domain is located) is consistently over predicted, even allowing for the different resolutions of observations and model predictions. This likely contributes to the overstated wet bias seen in the winter months in the METSTAT surface performance statistics (Figure 4-2c). The SW subdomain appears to be particularly wet in December, and this is reflected in the soccer plot (Figure 4-2c). It is difficult tell whether precipitation in the SE subdomain is over-predicted because orographic effects likely play a key role here and whether the different resolutions of observations and model predictions confound the issue. By February, MM5's over prediction of precipitation over the Alaskan interior is not as severe. This is reflected in the surface humidity statistics, as Figure 4-2c shows that February humidity performance represented an improvement over that of the November-January period.

Summer

During the summer, the Aleutian low dissipates, and the Pacific High strengthens and moves northward. This has a dramatic effect on the rainfall in the 45 km domain. The rainfall along the southern coast of Alaska and the western coast of North America diminishes markedly, reaching a minimum in intensity in July. The interior of Alaska gets most of its precipitation during the summer. During the summer, the northern half of the 45 km domain lies in a low-level convergence zone, with southerly flow over the southern 2/3 of the domain and northerly flow to its north (Peixoto and Oort 1992). Figure 5-5 shows a convergence zone in the NCEP-NCAR Reanalysis as well, one thin band across Alaska right collocated with the band of precipitation in the MM5 output fields as well as the observations.

During the summer months, MM5 does a good job of reproducing the observed precipitation pattern. In June, it locates the precipitation maximum over Alaska in the southeast, correctly places the precipitation minimum in northwestern Alaska, and models the transition between these two regions. The maxima and minima in precipitation are more intense in the MM5 fields than in the observed fields. The different resolutions of the modeled and observed fields is particularly important here, as the maximum in the rainfall lies over the mountains and is convective.

MM5's performance over land was generally better than performance over the ocean. In July, for example, the overall shape of the precipitation field over the ocean is not well-simulated.

MM5 predicts a maximum in the Gulf of Alaska (northwest of Seattle) that does not exist in the observations. Most of the MM5 precipitation over the ocean in July is coming from the convective component. It is not clear why this should be the case. In, fact, as we move from July to December, the convective component of precipitation becomes larger (not shown).

Spring

In March, the most noticeable feature of the MM5 precipitation field is the over prediction of precipitation in the interior of Alaska. In particular, the area corresponding to the 15 km SW subdomain is receiving too much precipitation. This fact is reflected in the METSTAT statistics and the soccer plot (Figure 4-12c). Modeled precipitation is too intense over Siberia.

In April, as in March, there is too much precipitation falling over the interior of Alaska. The smaller scale of the features in the precipitation field over the interior of Alaska suggests that these may be associated with convective rainfall, which would not be well resolved by the CMAP data. Even accounting for this effect, however, it appears that MM5 is generating too much precipitation over the 15 km domain.

The situation in May is similar to that of April. The overall pattern is well reproduced. The 45 km simulation shows the signature of convective rainfall in the SE subdomain. But the two subdomains that show the biggest wet bias (NE, NW) in the METSTAT soccer plot (Figure 4-11d), are not impressive in terms of rainfall over prediction. It is possible that something other than the precipitation bias may be causing the wet bias in the surface humidity in May. Further tests, possibly regarding the characterization of the land surface, may be in order. The POLAR option switches off on May 30.

Fall

Over the Alaskan interior, precipitation pattern is approximately correct when the different resolutions are taken into account, but the intensity is much greater in the MM5 field. MM5 reproduces the maximum along the western coast of North America, and has a minimum just east of the Alaska/Canada border. The rainfall maximum along the southern Alaskan appears in the MM5 field, as does the minimum in the region where the Pacific High is located. The basic shape of the precipitation field over the ocean is well-simulated. As October arrives there is further improvement in the accuracy of the precipitation field with the onset of winter (similar to the surface performance). The Aleutian low gains strength and precipitation intensifies over the ocean in both observations and the MM5 fields. The MM5 precipitation field is too intense over the Aleutian chain. This should correspond to an over prediction of surface humidity in the SW subdomain, and in Figure 4-12c, we do see a wet bias. There is also too much precipitation in central Alaska.

We may expect that the transition between seasons, which we treat by necessity with some level of arbitrariness, to be the most difficult for the model to handle. We have selected one parameterization set for summer, and a second set for winter, so the transitions between the two regimes may be expected to be the hardest for the model to handle accurately.

Summary

Summary of the Annual Cycle of Comparison of Observed and Modeled Precipitation;

- MM5 tends to overestimate precipitation over the Alaska 15 km domain, and this is reflected in the wet bias in the surface performance statistics.

- In May, however, the large positive humidity bias cannot be easily explained by an excess of precipitation in the northern subdomains, and further investigation is required to determine whether the POLAR option should be turned off earlier than May 30.

- Precipitation in the model not as coastally trapped along North America's west coast as in the observations. This represents a large error, considering the low resolution of the observations.

- MM5 overestimates precipitation off the coast of the northwestern U.S.

- The partitioning of MM5 rainfall into its convective and non-convective components bears further investigation. The model generates a great deal of convective rainfall in situations where one might not expect convection to occur (i.e. over the cold north Pacific Ocean).

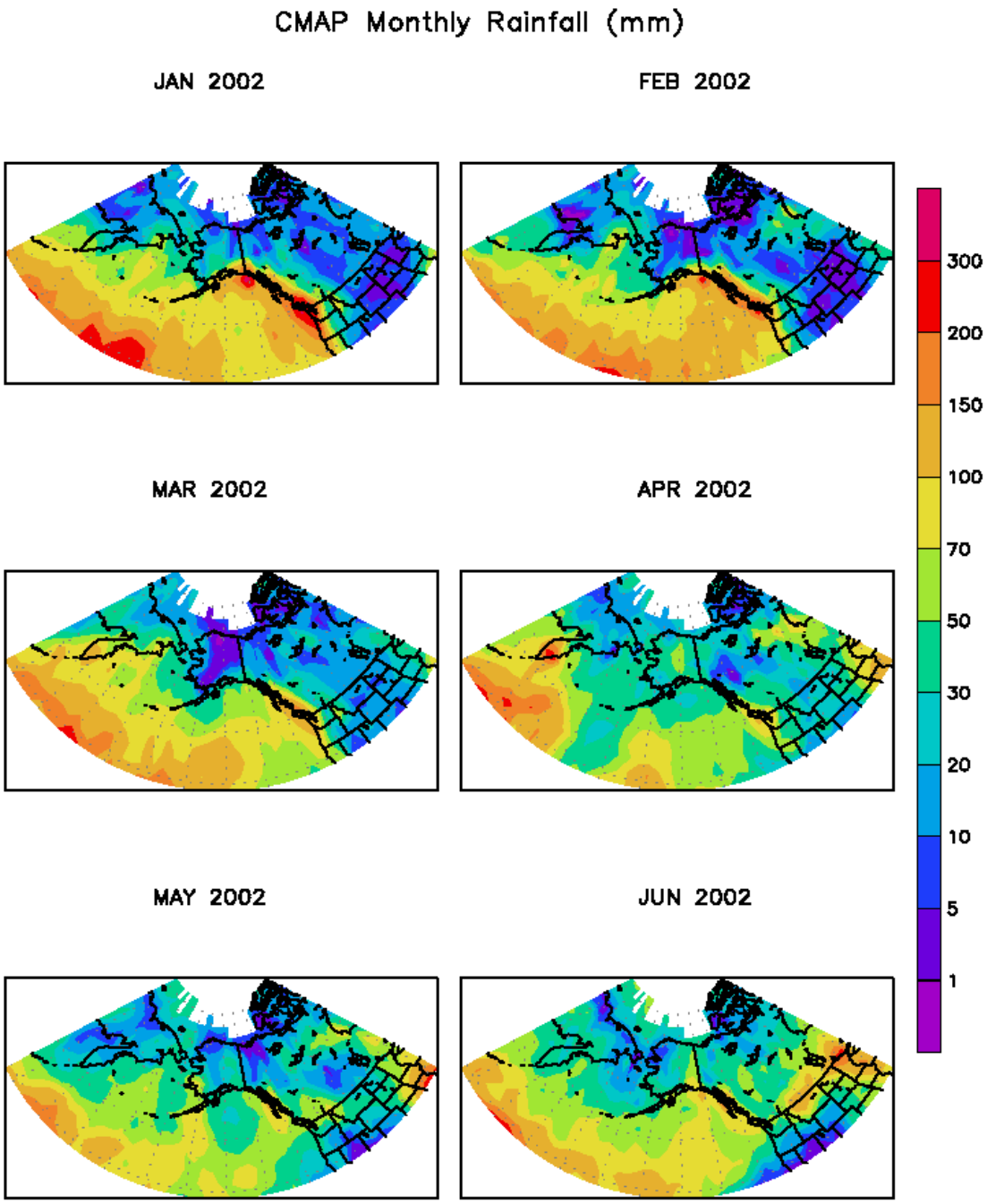

Figure 5-1. CMAP observed precipitation for January-June 2002 (mm).

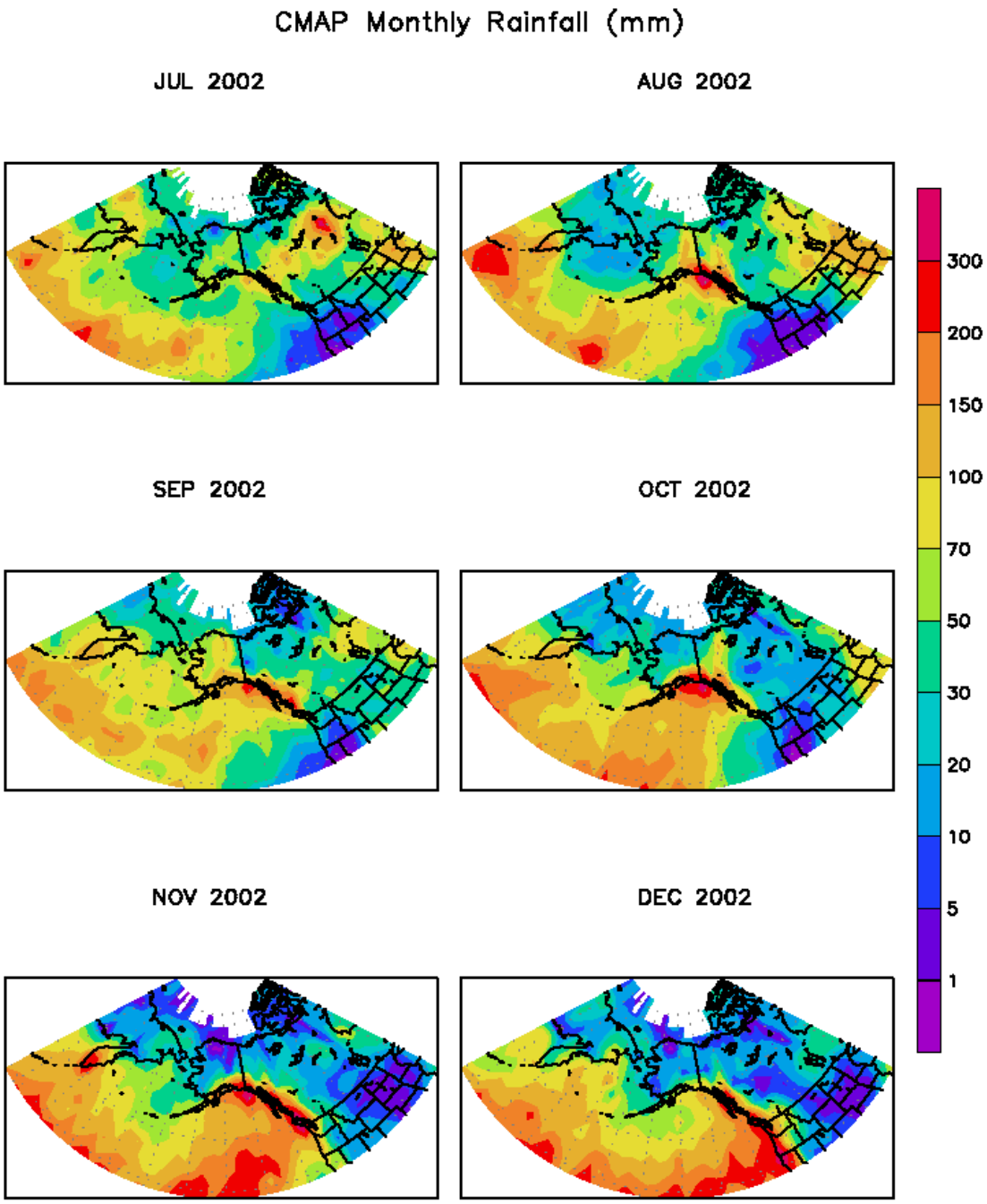

Figure 5-2. CMAP observed precipitation for July-December 2002 (mm).

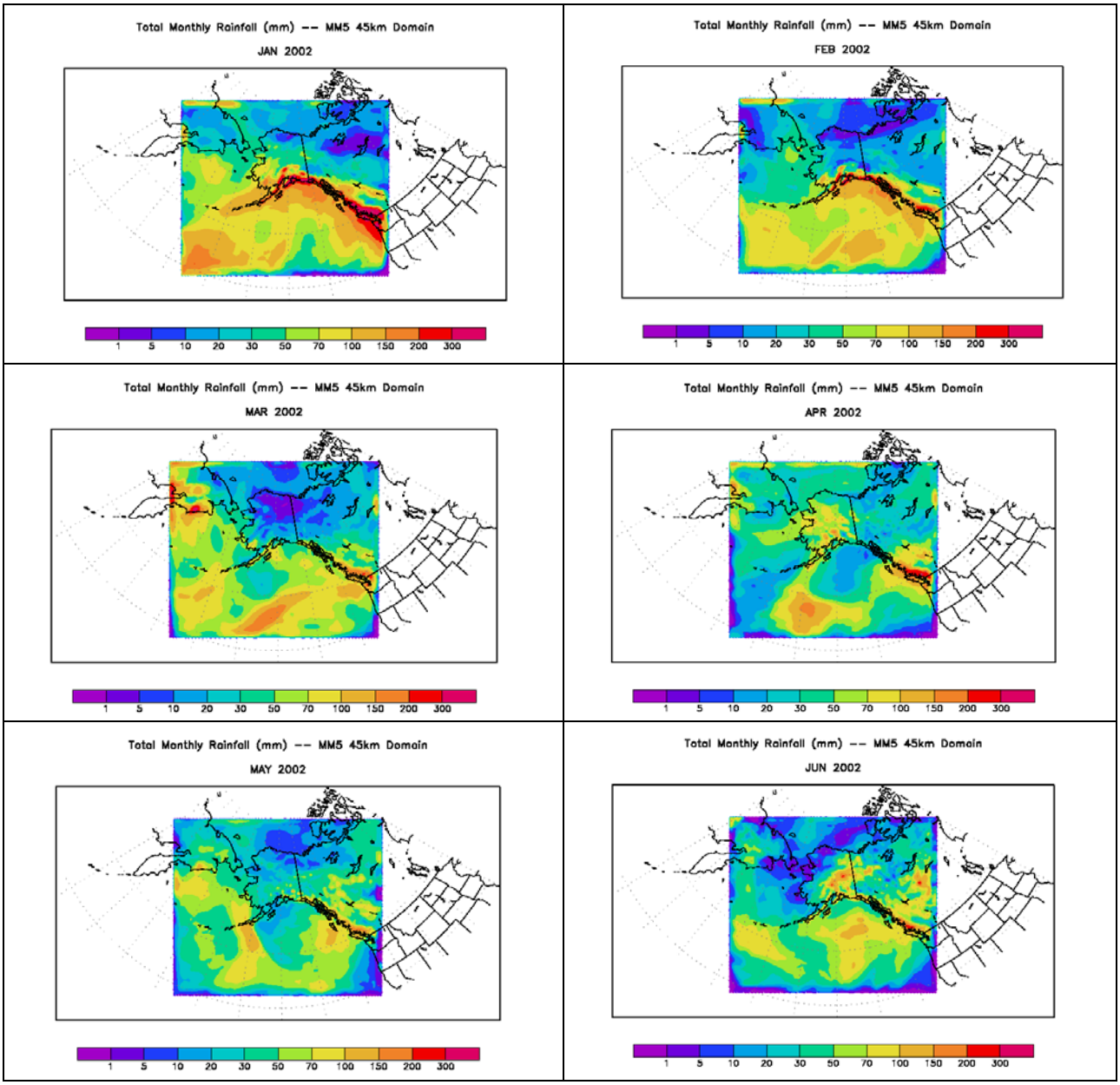

Figure 5-3. MM5 estimated precipitation for January-June 2002 (mm).

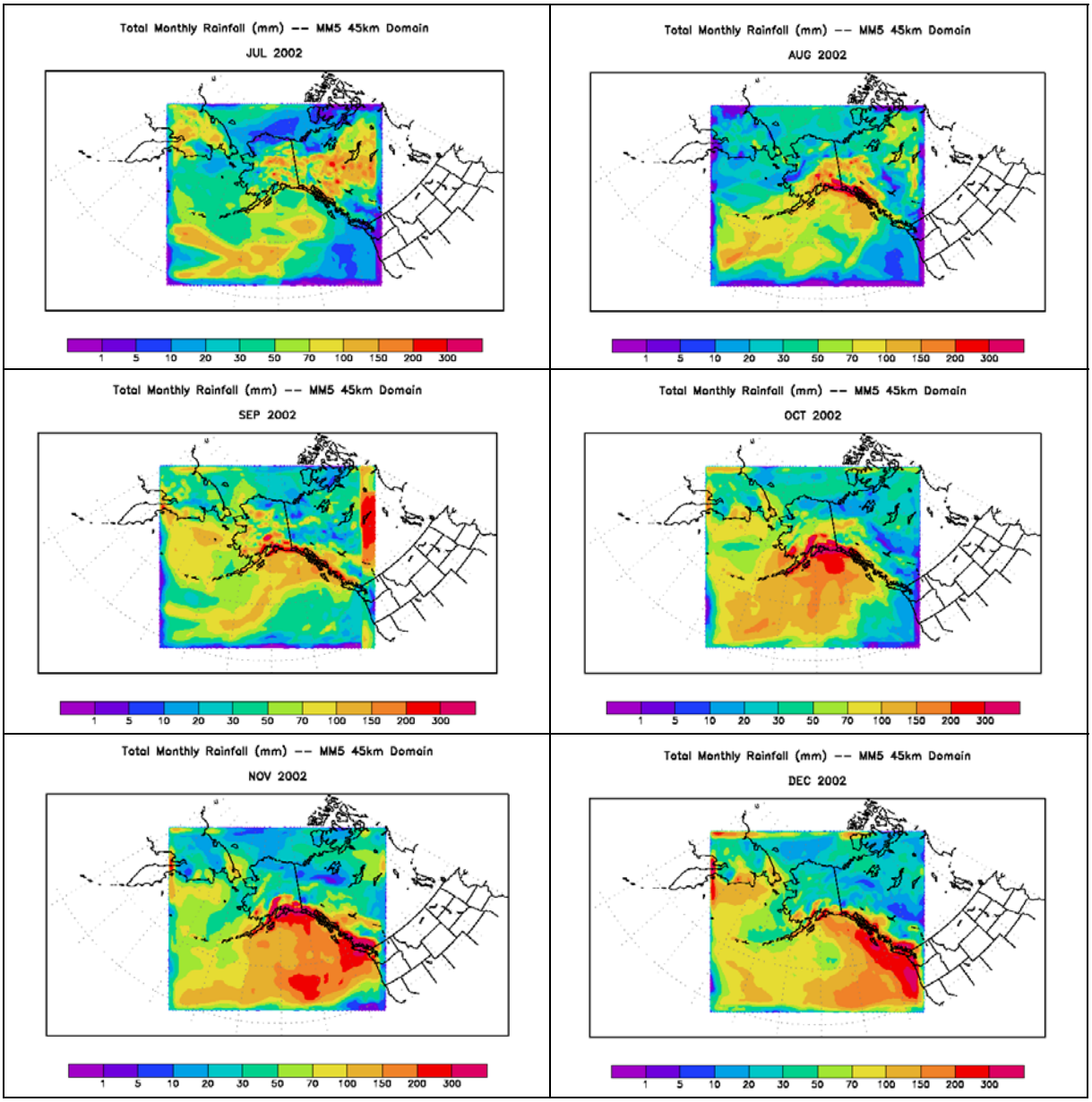

Figure 5-4. MM5 estimated precipitation for July-December 2002 (mm).

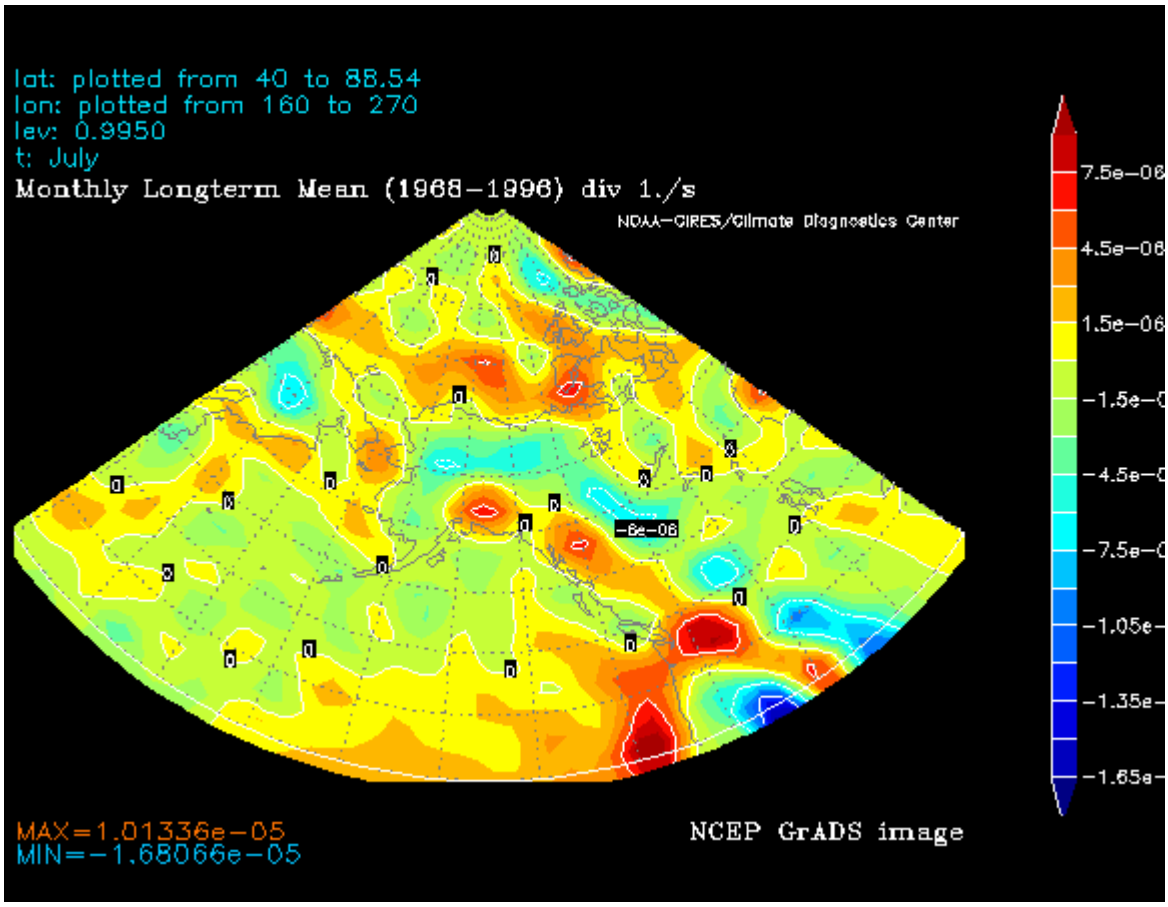

Figure 5-5. NCEP-NCAR Reanalysis July Monthly Mean Divergence Field.

6.0 UPPER AIR EVALUATION

To assess whether MM5 is simulating the vertical structure of the atmosphere with reasonable accuracy in the Alaska annual run, we compared model temperature and dew point soundings with those from a limited number of radiosonde stations shown in Figure 3-4.

The analysis of radiosonde soundings for all stations in the 15 km domain over the entire annual run is labor intensive, thus we organized the upper air analysis as follows: first, we looked at a large number of soundings for July, December, September and May in order to gain a qualitative understanding of the model's performance strengths and deficiencies. Next, we focused on time periods for which the surface or precipitation analysis indicated that the model performance was problematic. In this section, we will use the observed and modeled soundings to try to understand why the model had performance difficulties at the surface or with precipitation discussed in Sections 4 and 5. As we go through these soundings, we will discuss features of the plots shown that were noted in the more general analysis of the July, December, September and May soundings. Note that 12Z is 3 am Alaskan Standard Time (AST), and 00Z is 3 pm AST on the previous day.

We begin with the winter surface performance issues. Figure 4-2b showed a warm bias in the NE subdomain for the months of December, January, and February. This is in marked contrast to the cold bias seen in most months for all four subdomains. We turn to the upper air soundings to see why this might be. Figure 4-9 suggested that a reason for the warm bias was the lack of a sufficiently strong diurnal cycle during the first 20 days of February in the MM5 time series. During this time period, the model tracks the daily maximum temperature reasonably well, but fails to capture the daily minimum.

Figure 6-1 shows the February 18, 3 am sounding for the Fairbanks station, which lies in the NE subdomain. The observed temperature and dew point soundings are shown in black, and the corresponding MM5 soundings are shown in red. The temperature sounding lies to the right of the dew point sounding. The modeled and observed winds are shown on the right hand edge of the figure. The most striking feature of the observed sounding is the large near-surface temperature inversion. It is night in mid-winter, and this temperature profile shows that there is strong radiative cooling of the surface. The observations show that the atmosphere is saturated through a 50 mb layer near the surface, with drier air above. MM5 produces an inversion near the surface, but it is not as strong as the observed inversion. The observed temperature at the surface is –25° C, while MM5 predicts a surface temperature of about –12° C. The type of sounding, in which observations showed a strong inversion near the surface and MM5 's inversion was too weak, which was a very common feature of the MM5 predictions during December, January, and February at Fairbanks. Failure to simulate the strength of the surface inversion may explain the warm bias at the surface during the winter months in the NE subdomain.

Throughout the depth of the troposphere, MM5 remains closer to saturation than the observed atmosphere. This was a feature common to many of the soundings in the 2002 annual run. Another feature of this plot common to many MM5 soundings throughout the year is the mismatch between the observed and modeled surface pressure. This may be in part an artifact introduced by the coarse resolution of the model. If the modeled terrain is smoothing out the terrain, this will introduce a bias into the surface pressure field. Also, since the surface pressure

is a measure of the integrated mass of the air column, if the modeled atmosphere is too cold, MM5 predicts a denser atmosphere than is observed and should then over predict the surface pressure, as we see here.

Finally, there are significant differences between the observed and modeled wind speed and direction. At 950 mb, for example, the observed wind is from the southwest, while the modeled wind is from the northeast. Note that the METSTAT statistics, which are an average over a large area, do not suggest the existence of such a severe bias in the wind direction. Figure 4-8, the wind direction time series for NE for February, does not show a large wind direction error on February 18. Figure 4-2a shows that NE lies outside the benchmark for wind direction error in February, but is still within the WRAP performance envelope. The wind direction improves somewhat further aloft, but there is a consistent low wind speed bias up to about 200 mb. This is surprising in a model run which is nudged to an analysis above the boundary layer. The poor wind performance may certainly explain the lack of low-level inversion in MM5. Another reason is that MM5 predicts water vapor in the atmosphere than exists in the observed atmosphere. This additional moisture will trap outgoing infrared radiation and warm the lower atmosphere and the surface in MM5. The drier observed atmosphere traps less outgoing radiation, permitting a larger cooling to space and greater cooling at the surface.

METSTAT showed a wet bias at the surface for all subdomains for all winter months. This sounding is neither dry enough nor cold enough near the surface, and is too close to saturation, indicating that the problem with the excessive moisture is not limited to the surface. It is unclear what caused this excessive moistening of the troposphere in MM5.

During our METSTAT analysis of the surface meteorological model performance, we noted that during the winter months, all subdomains except NE had a cold bias at the surface, and that all subdomains had a wet bias. We look now at a sounding from the NW subdomain. The model performance in NW during the winter was within the benchmark for wind speed and direction for November-January and was outside the benchmark but within the WRAP performance envelope for all winter months for temperature. This was a subdomain where the model did relatively well during winter.

Figure 6-2 shows the observed and modeled soundings for December 9 at 3 am AST for Nome, which lies in the NW subdomain. This sounding has a slight inversion at the surface, but the inversion is not as strong as that seen in Figure 6-1. The model has a very small cold bias at the surface, and the surface pressure too large, but not as far off as in the Figure 6-1. The modeled temperature has an inversion that is reasonably close to what it should be. The temperature profile is too cold, and the dew point temperature is generally too warm from the surface up to 400 mb. MM5, then, is predicting a troposphere that is too cold and too close to saturation. Notice that the atmosphere has a relatively dry layer centered at approximately 500 mb. MM5 does not simulate this dry layer. Failure to predict a dry layer in the mid-troposphere was a common feature of the soundings throughout the year. In Figure 6-2, the wind speeds are too low in the upper troposphere and also have a consistent directional bias in the lowest 100 mb of the atmosphere. This is an example of reasonably good performance, albeit with MM5's chronic tendency to come too close to saturation throughout the depth of the troposphere. This excessive moistening is a likely explanation for the model's tendency to overestimate precipitation throughout the 15 km domain.

Figure 6-3 shows a sounding that highlights some of the typical winter performance problems noted above. The soundings are for 3 am AST, December 7, 2002 for Yakutat, which is in the SE subdomain of the 15 km domain (see Figure 3-4). The observed sounding has an inversion in the 1000-900 mb layer, is subadiabatic between 950 mb and 700 mb, and follows the moist adiabat up to the tropopause just above 300 mb. This type of sounding was seen frequently during the upper air analysis of this run. The modeled behavior shown here is fairly typical of MM5's simulation of this type of observed sounding. The modeled surface temperature is too cold, but the model does have the inversion and the overlying subadiabatic layer. Overall in this sounding, the model simulates the lapse rate and the separation between the dew point and temperature profiles, but has a cold bias from the surface up to 400 mb. The model makes a direction error in the winds in the layer under 900 mb, which may explain the difference between observed and modeled soundings there. Above 900 mb, the modeled winds are generally blowing in the right direction, except in the 300-200 mb layer, but have a low wind speed bias.

Figure 6-4 shows another winter sounding for Cold Bay, which is in the SW subdomain (Figure 3-4). The overall cold bias throughout the depth of the troposphere is also apparent in this sounding. There is a warm bias at the surface, and a mismatch between the observed and modeled surface pressure. In this case, unlike that shown in Figure 6-3, MM5 does find the appropriate level of saturation through most of the troposphere, although the model misses the drier layers between 700 mb and 500 mb. What is striking about this sounding is the error in the wind speed and direction. For instance, in the relatively dry 700-500 mb layer, the modeled wind direction has an error of nearly 90 degrees. This suggests that at least part of the reason MM5 does not simulate the temperature profiles properly in this layer is that the wind is blowing from the wrong direction, and possibly advecting air with different properties into the Cold Bay region. Although the model solution is being nudged toward the analysis wind fields, there are significant errors in the 700-200 mb layer. It is possible that this is due to the relatively coarse resolution of the analysis. The nudging coefficients used here are generally employed in conjunction with the higher resolution EDAS analysis fields. Since we are using the lower resolution NNRP analysis here, it is possible that the nudging coefficients should be increased.

We turn now to the months of March and May, during which the largest surface performance problems occurred. March and May had very large cold biases and May had a large wet bias at the surface. MM5's surface humidity performance was furthest outside the benchmark, especially in the NE domain. We therefore choose the Fairbanks station, which lies in that subdomain, and look at the upper air performance there on days when the wet bias in the surface statistics was strong. Figure 6-5 shows the 3 pm AST sounding for March 7, 2002. The observations show a relatively dry sounding with an inversion near the surface, a subadiabatic layer from approximately 1000 mb to 800 mb, where there is another deeper inversion extending up to 600 mb. The dew point temperature profile is reasonably accurate from the surface up until about 800 mb, when the observed profile becomes drier and the model profile does not. This causes a wet bias from about 800 mb up to the tropopause. The modeled wind speeds are low in the layer from 900-300 mb but the wind direction is close to observations.

Although the modeled winds from the surface up to 900 mb are reasonably accurate, the temperature is nearly 10 degrees too low and the dew point temperature is too high. Note that there is only a small mismatch with the surface pressure. MM5 predicts a substantial inversion while the observations show a very shallow inversion right at the surface, with a nearly adiabatic layer right above. MM5 appears to be cooling the surface excessively. It is possible that there is ice or snow on the surface in the modeled atmosphere where none existed in the real world. It is

difficult to say whether this is the case because observed ice and snow fields for 2002 were not readily available.
This type of excessive surface cooling in the model was common in March and May in multiple subdomains. Figure 6-6 through 6-8 shows a similar situation for three different times during the March and May periods. Figure 6-6 is for Anchorage in the SE subdomain for May 18 at 3 pm AST. Figures 6-7 shows a sounding from May 15 at 3 pm AST for McGrath and Figure 6-8 is a similar sounding from Fairbanks (NE subdomain) for May 25 at 3 pm AST. All three soundings show good performance above the boundary layer, and suffer from the strong cold bias at the surface as discussed above. The Fairbanks sounding is particularly interesting because it is warm at the surface at 27° C. This sounding is similar to those for deep convecting boundary layers commonly seen in summer over the continental U.S. Here, the model performs well above 950 mb, but the surface temperature is far too low and dew point is too high. Again, this good performance aloft coupled with poor performance near the surface suggests a problem with MM5's characterization of the surface energy flux, and may be explained by an error in the snow or ice cover.

Moving now to summer, we will look at a sounding for Fairbanks (Figure 6-10) as an example of a typical sounding for stations in the SE showing a cold bias at the surface during the summer months (Figure 4-12b). This MM5 sounding shows a cold bias at the surface, as well as an inversion that does not appear in the observed profile, and a surface pressure mismatch with the observations. Although the low level winds are not poorly simulated, the model is too cold between 1025 and 900 mb and too warm between 900 and 850 mb. Above the inversion, from about 600 mb upward, the model does a good job of simulating the observed temperature profile. It misses most of the excursions about the mean dew point profiles; this suggests that the model is failing to simulate the complex cloud decks present on this day. This type of dew point profile, in which the modeled profile was in some sense simulated the mean of the observed profile but missed a lot of the variability, was quite common.

A summary of the upper air performance in the 2002 Alaska MM5 run on the 15 km domain can be summarized as follows:

- Surface biases seen in the upper air soundings are consistent with the results of the METSTAT analysis of the surface meteorological model performance.

- The upper air results show that the most common cause of the large surface cold bias seen in the spring surface results was due to anomalous surface cooling, even when the overlying sounding was well-simulated. This may be related to mischaracterization of the surface. The timing of these errors is such that they occur in the transition times when snow and sea ice are advancing or retreating, which suggests that it may be difficult for MM5 to properly simulate the changing atmospheric lower boundary condition.

- Mismatches between the observed and modeled surface pressure were common. This phenomenon was also noted in the analysis of the 2002 WRAP annual run (Kemball-Cook et al. 2005).

- The modeled troposphere is frequently closer to saturation than the observed atmosphere. This is likely to be the cause of the excess precipitation found over the 15 km domain.

- Wind direction and speed errors were very common in the lower atmosphere, and were surprisingly prevalent above the boundary layer, where the model is nudged to an analysis.

- The nudging coefficients may need to be increased when the NNRP reanalysis is used as the observational analysis.

- The MM5 dew point temperature profile frequently misses sharp excursions in the observed profile. While this may be due in part to the limited model resolution, particularly in the upper layers, it is also likely due to errors in characterizing the complex multiple cloud decks common in Alaska.

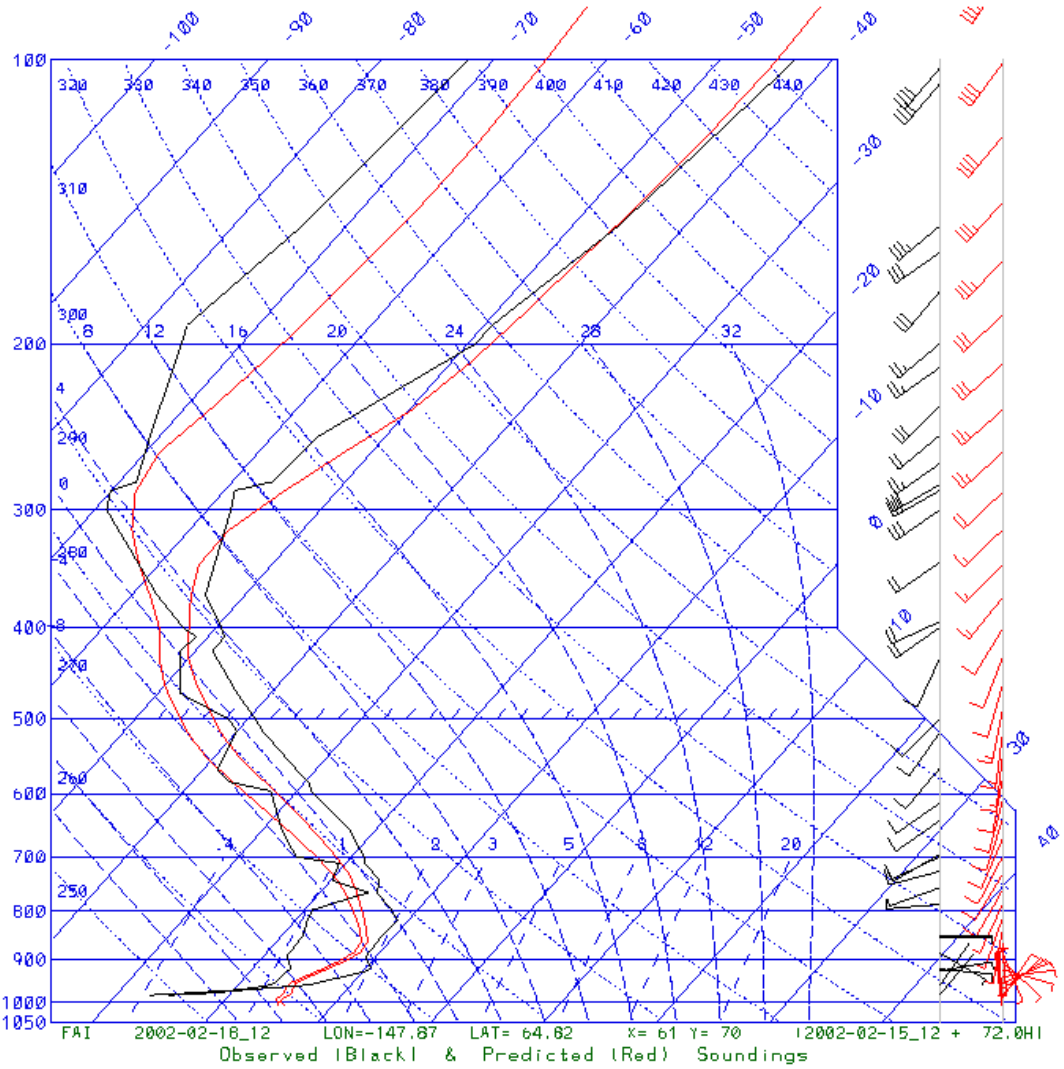

Figure 6-1. Observed and MM5 Soundings for Fairbanks for February 18 at 3 am LST.

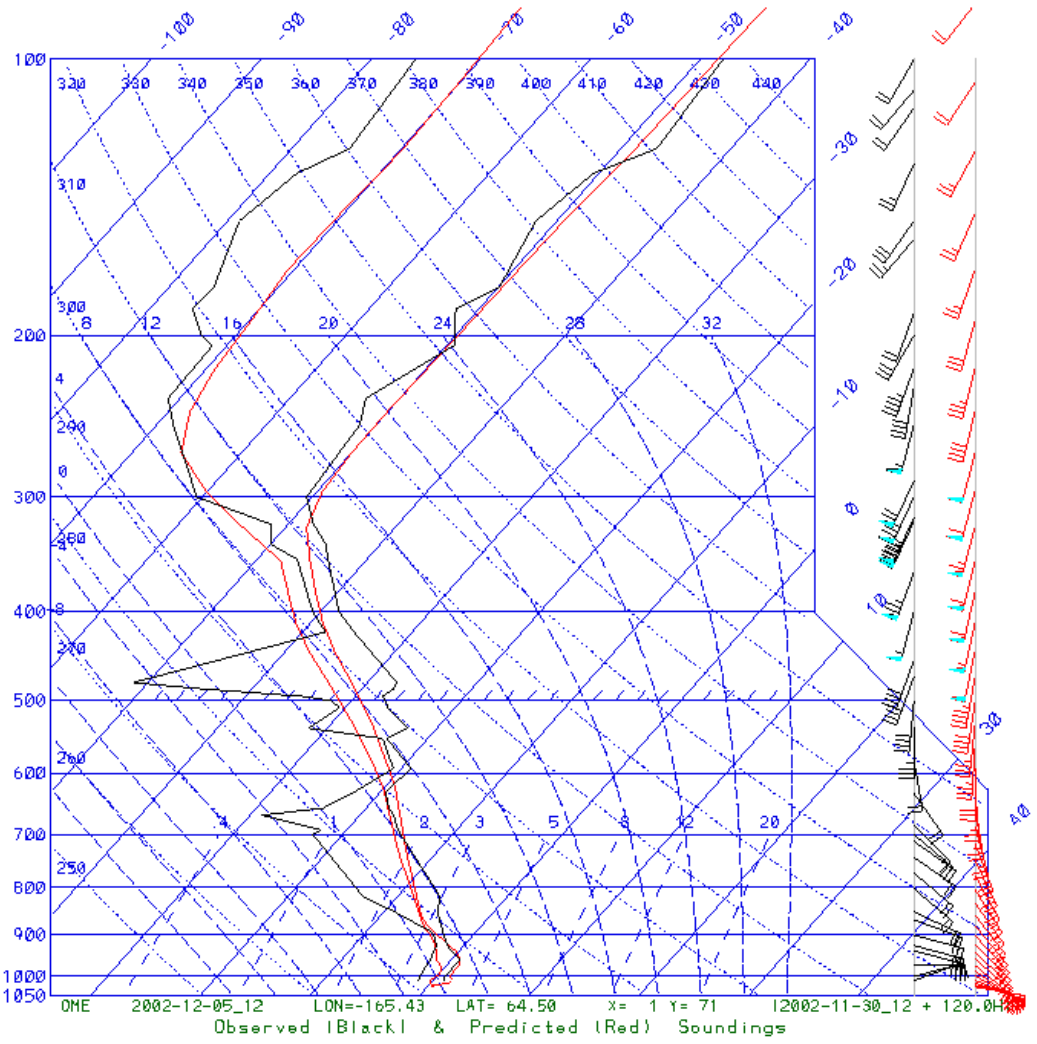

Figure 6-2. Observed and MM5 Soundings for Nome for December 5 at 3 am LST.

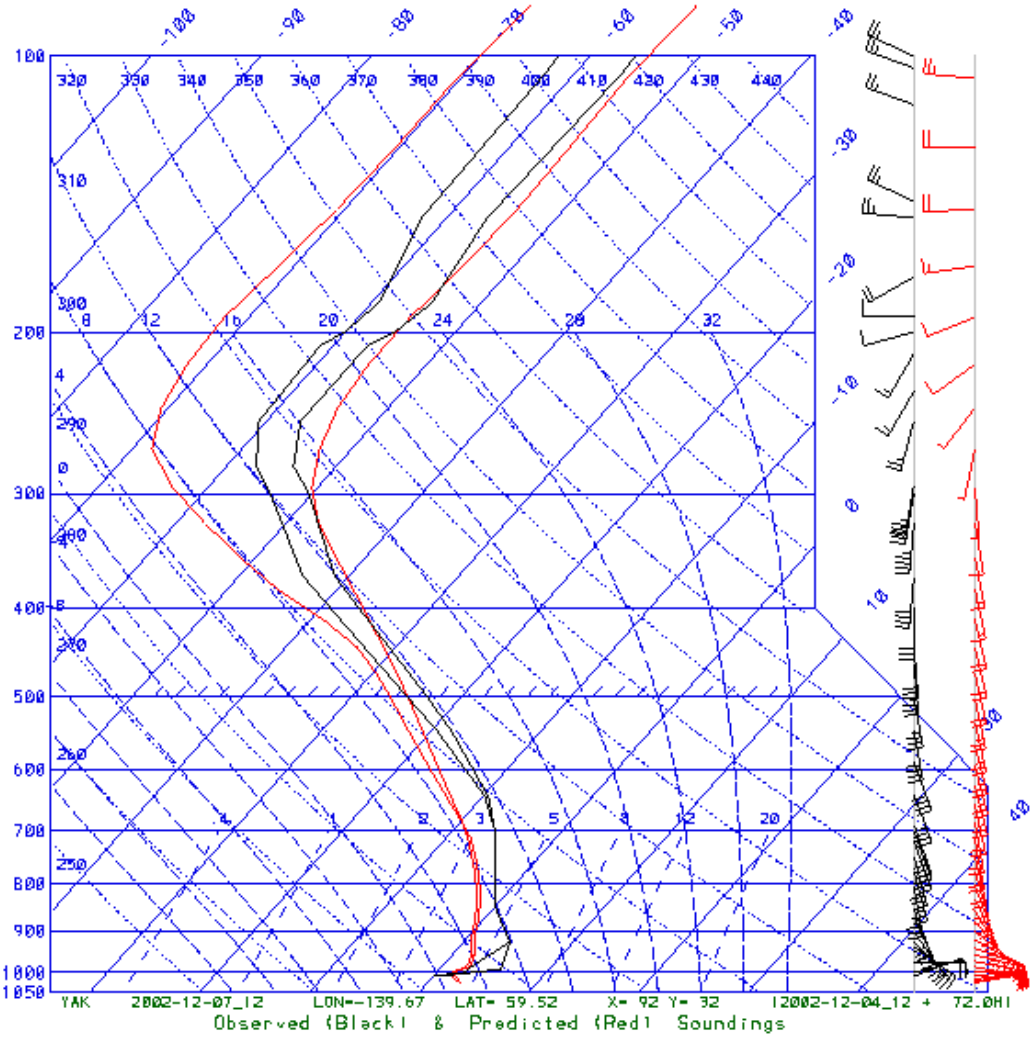

Figure 6-3. Observed and MM5 Soundings for Yakutat for December 7 at 3 am LST.

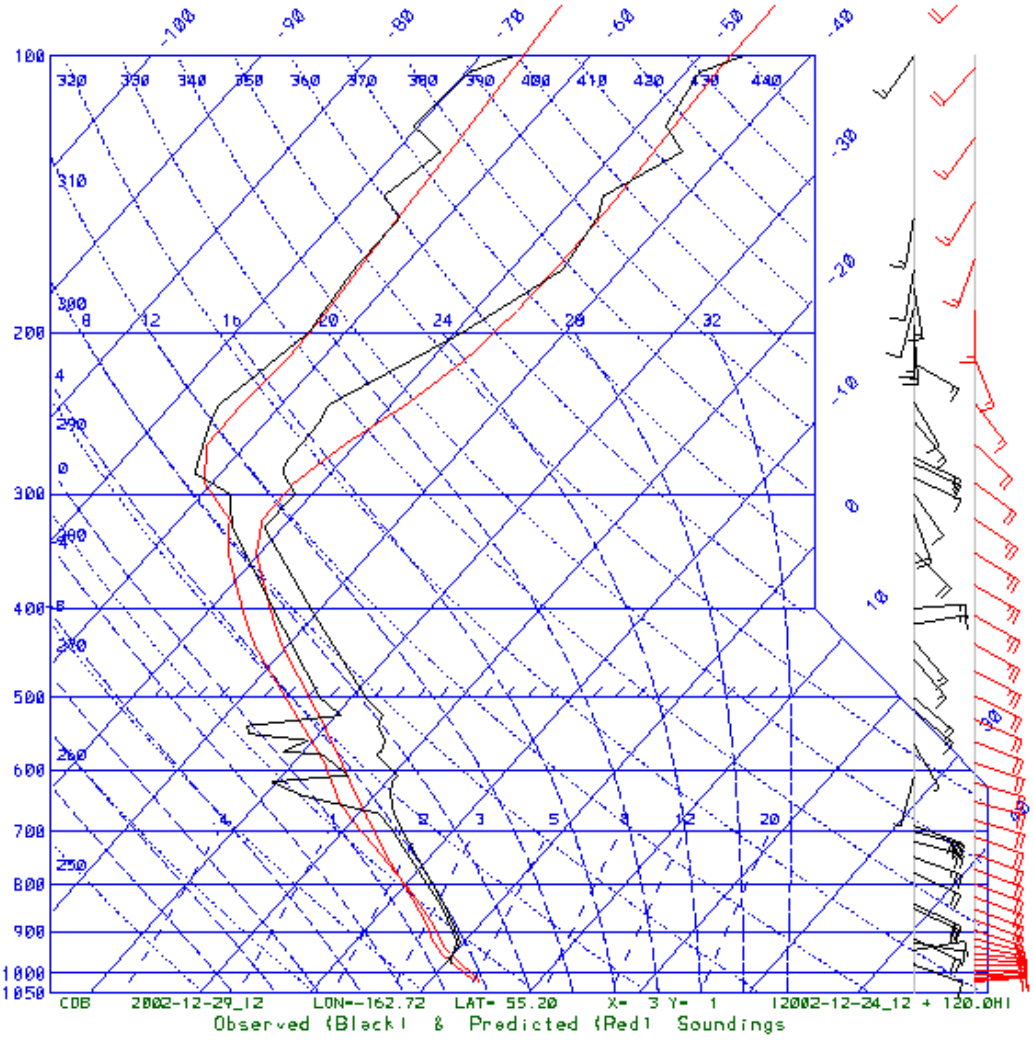

Figure 6-4. Observed and MM5 Soundings for Cold Bay for December 29 at 3 am LST.

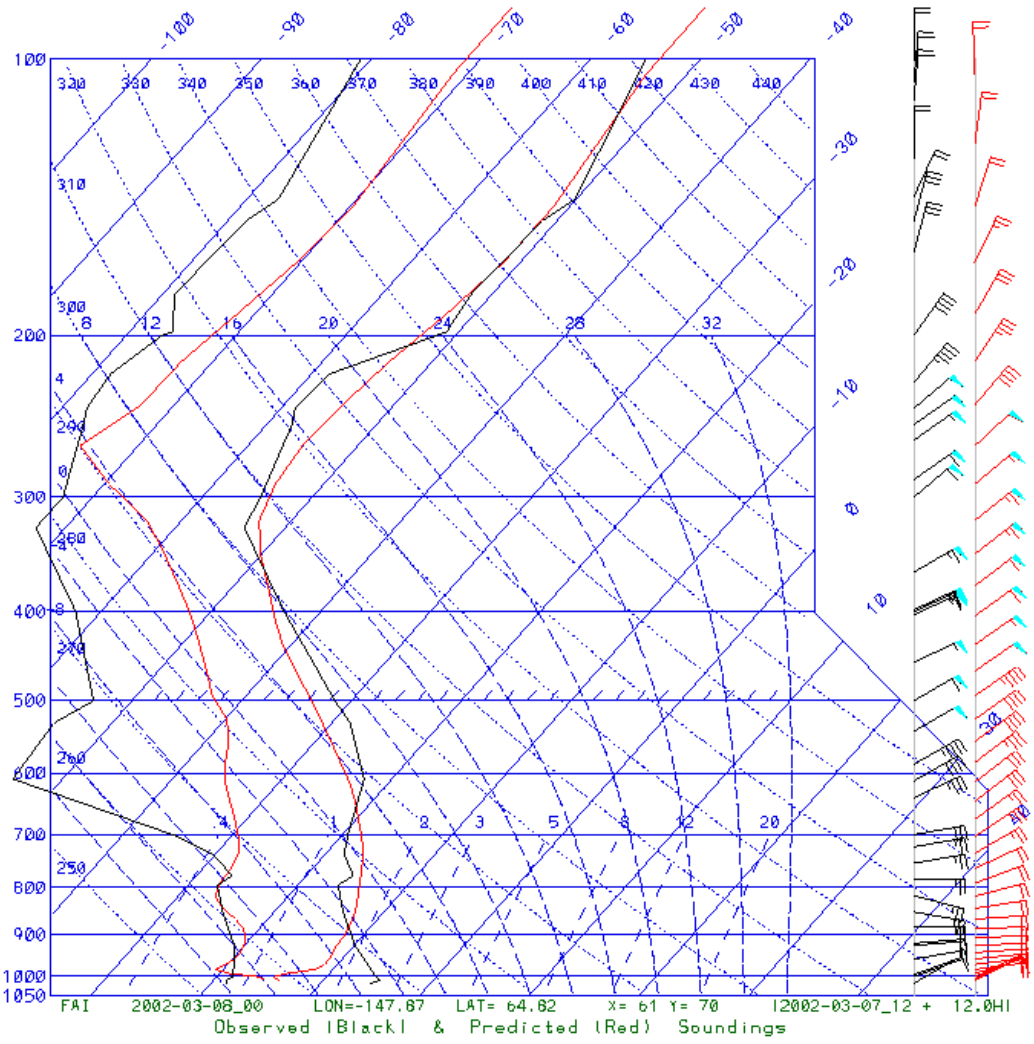

Figure 6-5. Observed and MM5 Soundings for Fairbanks for March 8 at 0Z.

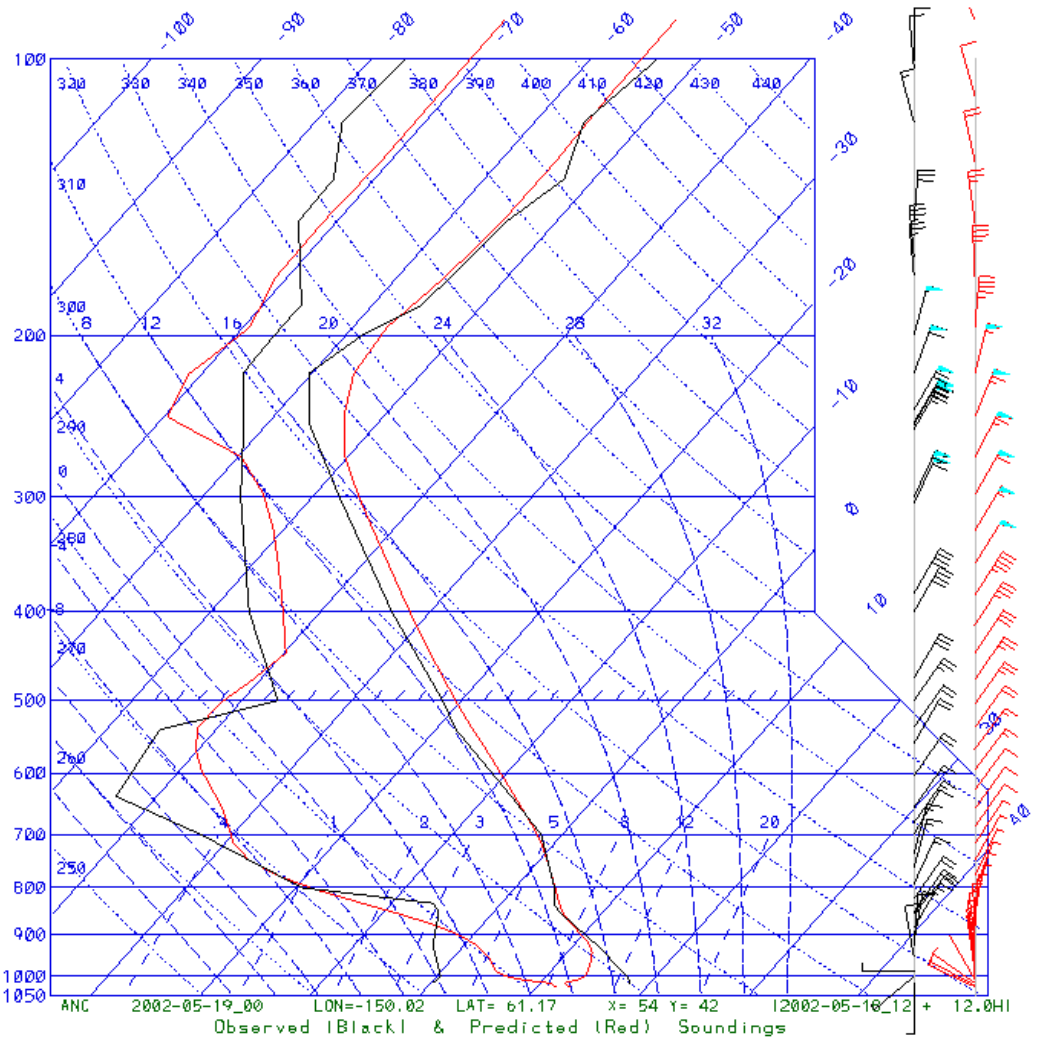

Figure 6-6. Observed and MM5 Soundings for Anchorage for May 19 at 0Z.

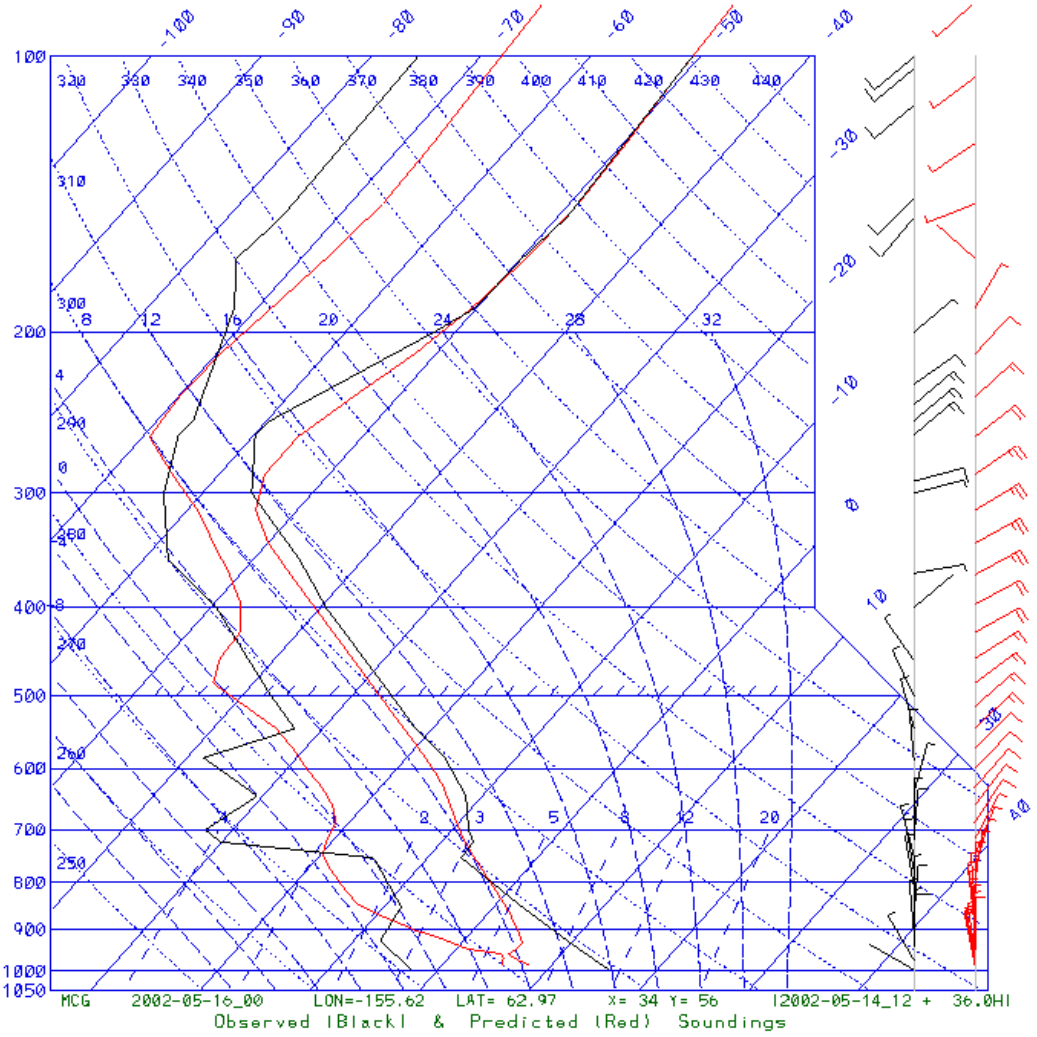

Figure 6-7. Observed and MM5 Soundings for McGrath for May 16 at 0Z.

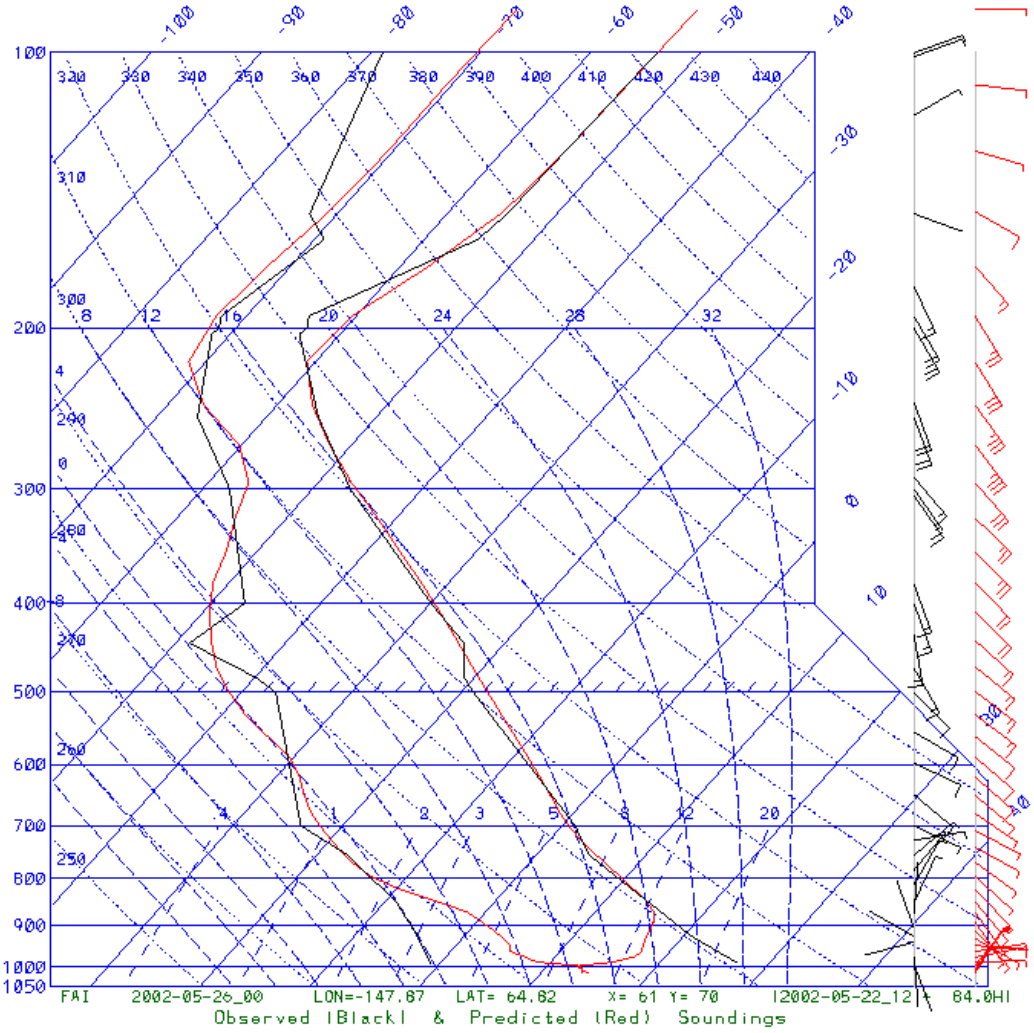

Figure 6-8. Observed and MM5 Soundings for Fairbanks for May 26 at 0Z.

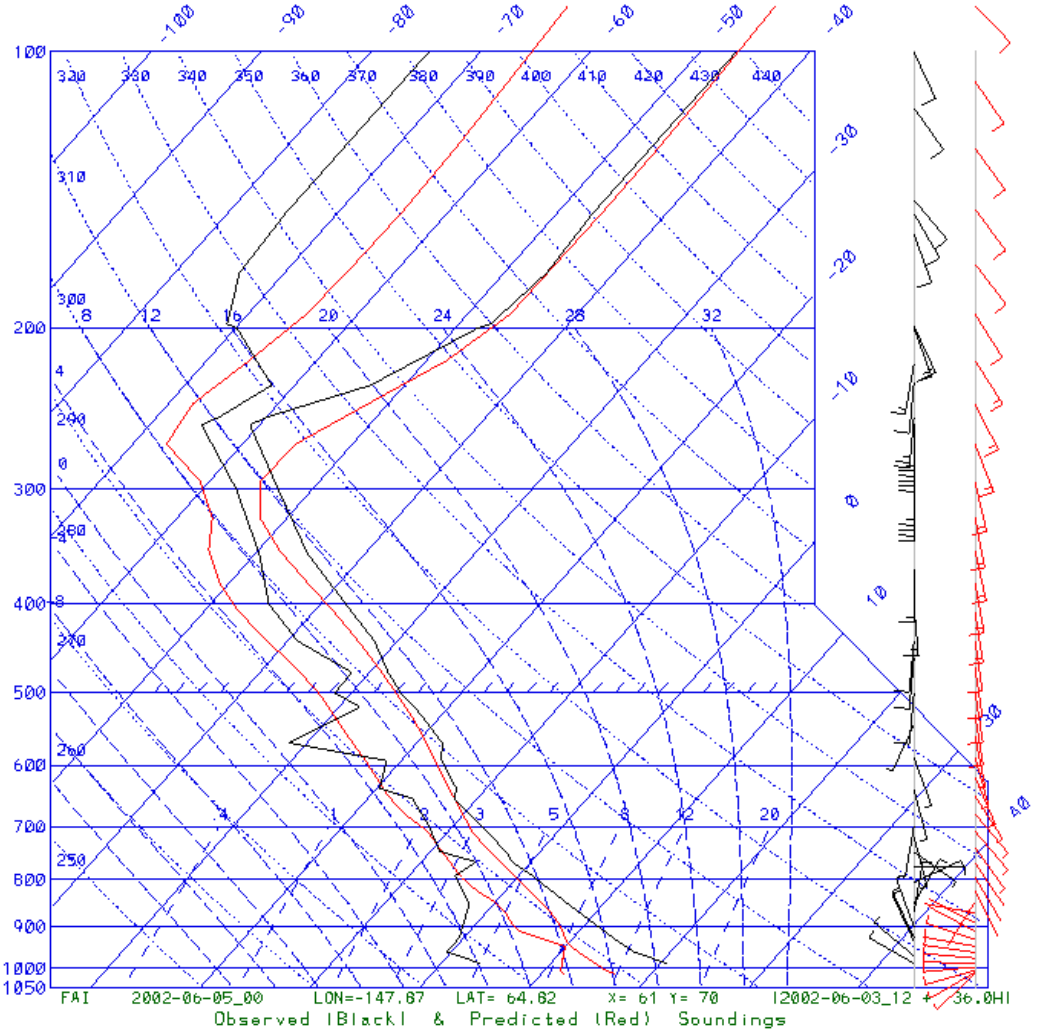

Figure 6-9. Observed and MM5 Soundings for Fairbanks for June 5 at 0Z.

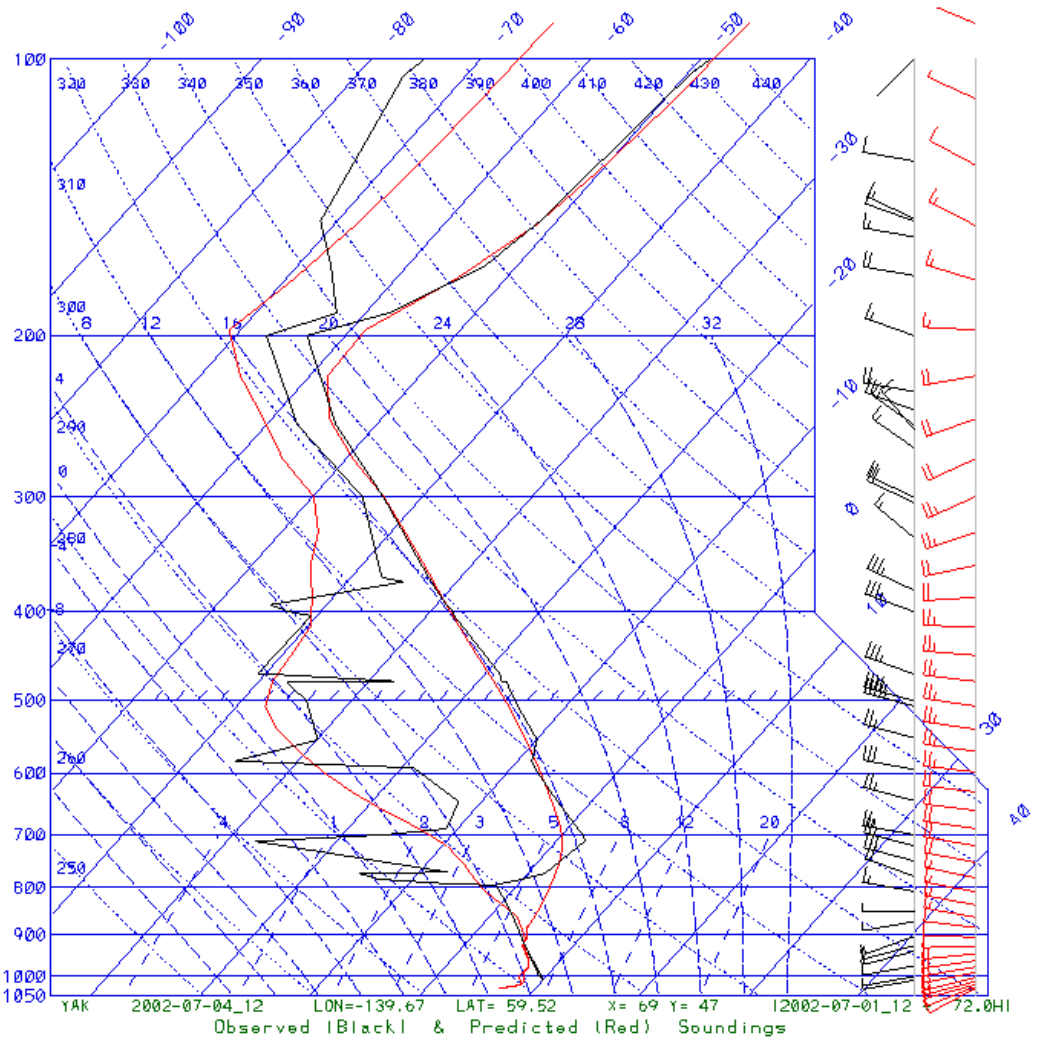

Figure 6-10. Observed and MM5 Soundings for Yakutat for July 4 at 12Z.

7.0 SUMMARY AND CONCLUSIONS

Overall, we obtained reasonable MM5 performance given the challenges of modeling Alaska. For most subdomains and most months, the surface performance of the Alaska 15 km run was comparable to that of WRAP 2002 36 km annual run for the western continental U.S. subdomains. A significant exception is the surface performance during May, when temperature and humidity lay far outside the WRAP envelope as well as the performance benchmarks. March and April also had large cold biases. It is possible that the timing of the switch on and off of the POLAR option caused difficulty for the model, and further investigation of the timing of the switch to the more accurate summer land surface model may be warranted. However, it is also possible that errors in characterization of the surface are inevitable given the 15 km resolution of the fine grid.

For temperature and humidity, the best surface performance came during the winter months of November-February. Surface performance showed a general cold, wet bias, which was most pronounced during spring and fall. Fall performance was better than spring performance. A spurious diurnal cycle in humidity appeared in spring, and may be related to the large cold biases seen during March-May. The cause of this spurious diurnal cycle is not clear. The transition seasons of fall and spring were the most difficult for MM5 to simulate and this may be related to the changing lower boundary condition, and the timing of the switch over to or from the POLAR configuration.

Examination of wind speed time series showed a consistent low wind speed bias similar to what was seen in the WRAP 2002 36 km annual run western U.S. subdomains. For surface winds, best performance during summer. In general, the model performed better in the subdomains that were less mountainous. For surface winds, the more mountainous subdomains NE and SE had a larger wind direction error (generally outside the benchmark) than the NW and SW subdomains (generally within the benchmark) throughout the annual cycle. The upper air soundings often showed significant errors in both wind direction and speed at low levels.

MM5 tends to overestimate precipitation over the Alaska 15 km domain, and this is reflected in the wet bias in the surface performance statistics. This may be related to the model's tendency to stay too close to saturation through the depth of the troposphere. In May, however, the large positive humidity bias at the surface cannot be easily explained by an excess of precipitation in the northern subdomains.

In spite of these performance difficulties, this MM5 run performed well enough in the context of other MM5 runs for visibility modeling efforts over complex terrain that the meteorological fields should be acceptable use as input fields for CALPUFF modeling of Alaska.

8.0 REFERENCES

Cassano, J., T. Parrish, and J. King. 2001. Evaluation of turbulent surface flux parameterizations for the stable surface layer over Halley, Antarctica. *Mon Wea. Rev.* **129**, 26-46.

Curry, J. and Coauthors. 2001. FIRE Arctic clouds experiment. *Bull. Am. Met. Soc*. **81**, 5-29.

Dudhia, J. 1993. A non-hydrostatic version of the Penn State/NCAR Mesoscale Model: validation tests and simulation of an Atlantic cyclone and cold front. *Mon. Wea. Rev.* **121**, pp.1493-1513.

Emery, C.A., E. Tai, and G. Yarwood. 2001. Enhanced Meteorological Modeling and Performance Evaluation for Two Texas Ozone Episodes. Prepared for the Texas Natural Resource Conservation Commission, by ENVIRON International Corporation, Novato, CA.

Grell, G.A., J. Dudhia, and D.R. Stauffer. 1994. A description of the Fifth Generation Penn State/NCAR Mesoscale Model (MM5). NCAR Technical Note, NCAR TN-398-STR, 138 pp.

Johnson, M. 2003. Meteorological modeling protocol: IDNR Annual MM5 Application. Prepared for the Iowa Department of Natural Resources Air Quality Bureau.

Kemball-Cook, S., Y. Jia, C. Emery, and R. Morris. 2004. 2002 annual MM5 simulation to support WRAP CMAQ visibility modeling for the section 308 SIP/TIP. Prepared for The Western Regional Air Partnership.

Mahrt, L. 1998. Stratified atmospheric boundary layers and the breakdown of models. *Theor. Comput. Fluid Dyn*., **11**, 263-279.

Olerud, D. and A. Sims. 2003. MM5 Sensitivity modeling in support of VISTAS (Visibility Improvement-State and Tribal Association) (DRAFT). Prepared for Mike Abraczinskas of the VISTAS Technical Analysis Workgroup by Baron Advanced Meteorological Systems, LLC.

Pleim, J.E. and J.S. Chang. 1992. A non-local closure model for vertical mixing in the convective boundary layer. *Atmos. Env*., **26A**, pp. 965-981.

Reisner, J.R., R.M. Rasmussen, and R.T. Bruintjes. 1998. Explicit forcing of supercooled liquid water in winter storms using the MM5 mesoscale model. *Quart. J. Roy. Met. Soc.*, **124B**, pp. 1071-1107.

Stauffer, D.R. and N.L. Seaman. 1990. Use of four-dimensional data assimilation in a limited-area mesoscale model. Part I: experiments with synoptic data. *Mon. Wea. Rev*. **118,** pp.1250-1277.

Stauffer, D.R. and N.L. Seaman. 1991. Use of four-dimensional data assimilation in a limited-area mesoscale model. Part II: effects of data assimilation within the planetary boundary layer. *Mon. Wea. Rev*., **118,** pp.734-754.

Tesche, T. 1994. Evaluation Procedures for Regional Emissions, Meteorological, and Photochemical Models. Presented at the 86th Annual Meeting of the Air and Waste Management Association, 14-18 June, Denver, CO.

Tesche, T., D. McNally, C. Emery, and E. Tai. 2001. Evaluation of the MM5 Modeling Over the Midwestern U.S. for Three 8-hour Oxidant Episodes. Prepared for the Kansas City Ozone Technical Workgroup, by Alpine Geophysics, LLC, Ft. Write, KY, and ENVIRON International Corp., Novato, CA.

Tilley, J. 2004. Personal communication.

Xie, P. and P. Arkin. A 17-year monthly analysis based on gauge observations, satellite estimates, and numerical model predictions. *Bull. Am. Met. Soc*. **78**, 2539-2559.

Xiu, A. and J.E. Pleim. 2000. Development of a land surface model. Part I: application in a mesoscale meteorology model. *J. App. Met.*, **40**, pp. 192-209.